JYVÄSKYLÄ STUDIES IN COMPUTING
238

Younes Abdi Mahmoudaliloo

Cooperative Spectrum Sensing Schemes for Future Dynamic Spectrum Access Infrastructures

JYVÄSKYLÄN YLIOPISTO

JYVÄSKYLÄ STUDIES IN COMPUTING 238

Younes Abdi Mahmoudaliloo

Cooperative Spectrum Sensing Schemes for Future Dynamic Spectrum Access Infrastructures

Esitetään Jyväskylän yliopiston informaatioteknologian tiedekunnan suostumuksella
julkisesti tarkastettavaksi yliopiston Agora-rakennuksen auditoriossa 3
kesäkuun 7. päivänä 2016 kello 12.

Academic dissertation to be publicly discussed, by permission of
the Faculty of Information Technology of the University of Jyväskylä,
in building Agora, auditorium 3, on June 7, 2016 at 12 o'clock noon.

UNIVERSITY OF JYVÄSKYLÄ

JYVÄSKYLÄ 2016

Cooperative Spectrum Sensing Schemes for Future Dynamic Spectrum Access Infrastructures

JYVÄSKYLÄ STUDIES IN COMPUTING 238

Younes Abdi Mahmoudaliloo

Cooperative Spectrum Sensing Schemes for Future Dynamic Spectrum Access Infrastructures

UNIVERSITY OF JYVÄSKYLÄ

JYVÄSKYLÄ 2016

Editors
Timo Männikkö
Department of Mathematical Information Technology, University of Jyväskylä
Pekka Olsbo, Ville Korkiakangas
Publishing Unit, University Library of Jyväskylä

URN:ISBN:978-951-39-6654-6
ISBN 978-951-39-6654-6 (PDF)

ISBN 978-951-39-6653-9 (nid.)
ISSN 1456-5390

Jyväskylä University Printing House, Jyväskylä 2016

ABSTRACT

Abdi Mahmoudaliloo, Younes
Cooperative Spectrum Sensing Schemes for Future Dynamic Spectrum Access Infrastructures
Jyväskylä: University of Jyväskylä, 2016, 66 p.(+included articles)
(Jyväskylä Studies in Computing
ISSN 1456-5390; **238**)
ISBN 978-951-39-6653-9 (nid.)
ISBN 978-951-39-6654-6 (PDF)
Finnish summary
Diss.

In cognitive radios (CRs), the information obtained from the surrounding radio environment is often an essential material for creating knowledge about the available resources and to apply that knowledge towards realizing reliable and efficient wireless communications. Consequently, since the spectrum sensing functionality in CRs provides information about the availability of the radio spectrum, which is considered as one of the most valuable communication resources, developing better spectrum sensing techniques is of critical importance and directly affects the performance of CR networks (CRNs) in many different aspects.

In this dissertation, better spectrum sensing schemes for CRNs are developed through considering a diverse collection of different processes and parameters involved. In particular, the research focus is on the so-called centralized cooperative spectrum sensing in which the sensing CR nodes send their local sensing outcomes to a so-called fusion center where the global decision about the availability of the spectrum is constructed. All the major phases in this cooperation are taken into account, including, the local sensing, reporting, and decision/data fusion processes. Accordingly, several important tradeoffs in designing these different phases are identified and formulated as standard optimization problems and their impact on the overall detection performance is thoroughly investigated. The optimization problems obtained are solved by using appropriate tools from the optimization theory and a number of new spectrum sensing structures are proposed to accommodate the tradeoffs. In addition, performance improvements associated with the proposed spectrum sensing methods are visualized by extensive simulation results.

Keywords: Dynamic spectrum access (DSA), cognitive radio (CR), spectrum sensing, cooperative communications, decision/data fusion, efficiency, nonlinear optimization.

Author

Younes Abdi Mahmoudaliloo
Faculty of Information Technology
University of Jyväskylä
Finland

Supervisor

Professor Tapani Ristaniemi
Faculty of Information Technology
University of Jyväskylä
Finland

Reviewers

Professor Risto Wichman
Department of Signal Processing and Acoustics
School of Electrical Engineering
Aalto University
Finland

Professor Ekram Hossain
Department of Electrical and Computer Engineering
University of Manitoba
Canada

Opponent

Professor Markku Juntti
Center for Wireless Communications
Faculty of Information Technology and Electrical Engineering
University of Oulu
Finland

ACKNOWLEDGEMENTS

First, I would like to thank my supervisor, Prof. Tapani Ristaniemi, for his continuous support and trust, for the regular long meetings and discussions, and for his valuable encouragements which have motivated me through this journey. Especially, I would like to thank him for being available and open to discuss new ideas or challenges and for the freedom I have had in steering my Ph.D. studies.

I would also like to thank my friends and colleagues at the Department of Mathematical Information Technology, University of Jyväskylä, where is the workplace to many young brilliant minds as well as several distinguished experts in the field. Working with them is a great honor and a priceless source of motivation and courage. I am also grateful to the caring and dedicated staff of our department who always work hard to provide a supporting atmosphere for all fellow students, teachers, and researchers.

I owe many thanks to Mr. Mohammad Tabatabaei from the Department of Mathematical Information Technology for his useful discussions and comments regarding the optimization tools we have used in this dissertation.

I would like to acknowledge that the Graduate school in Electronics, Telecommunications, and Automation (GETA) coordinated by Aalto University and the graduate school in Computing and Mathematical Sciences (COMAS) at the University of Jyväskylä have financially supported this research in a generous manner and have created several wonderful networking possibilities for me during the past four years. I am truly grateful to their valuable trust and support.

I am also thankful to my friends Jeff Pilgram, Joshua Bamford, Veera Joro, and Peadar Faherty, all from the University of Jyväskylä, for proofreading the text in this dissertation. In addition, I would like to acknowledge Timo Männikkö's help in preparing the final draft according to our university guidelines.

My special thanks go to my dear Iranian friends at the University of Jyväskylä who have been my family during these four years in Finland. Houra and Ali, Payam and Mahsa, Maryam and Ali, Diyako and Shawnem, and Azadeh, Hojat, Mehdi. A group of kind, valuable, and trustworthy friends who I have plenty of precious memories with and who have (hopefully) made me a better person by showing me new dimensions of life which I had never experienced before. In addition, I am very thankful to my Spanish friend, Iballa Burunat, from the Music Department, University of Jyväskylä, who is an absolute pleasure to discuss with about any topic, especially, the art of signal processing.

And finally, I need to thank my parents, Kamran and Marzieh Abdi, who have dedicated their lives and given up many dreams of their own to make a thriving future for their children. I am not able to articulate properly how much love and care I have received from them during my entire life and for sure I will never be able to thank them the way they deserve.

Dedicated to my parents

LIST OF ACRONYMS

AMI	Advanced metering infrastructure
AWGN	Additive white Gaussian noise
BAN	Body area network
BEP	Bit error probability
BnB	Branch and bound
BS	Base station
BSC	Binary symmetric channel
CAF	Cyclic autocorrelation function
CBRS	Citizens broadband radio service
CEPT	European Conference of Postal and Telecommunications Administrations
CR	Cognitive radio
CRN	Cognitive radio network
CROC	Complementary receiver operating characteristics
DRM	Demand response management
DSA	Dynamic spectrum access
ECG	Equal-gain combining
ETSI	European Telecommunications Standards Institute
FAN	Field area network
FC	Fusion center
FCC	Federal Communications Commission
GAA	General authorized access
FICORA	Finnish Communications Regulatory Authority
HAN	Home area network
IA	Incumbent access
KKT	Karush-Kuhn-Tucker
LAA	Licensed-assisted access
LRT	Likelihood-ratio test
LSA	Licensed shared access
LTE	Long-term evolution
LTE-A	LTE-advanced
MBAN	Medical body area network
MINLP	Mixed-integer nonlinear program
NP	Neyman-Pearson
NPC	Neyman-Pearson criterion
Ofcom	UK Office of Communications
PA	Prioritized access
PDF	Probability distribution function
PU	Primary user
QCQP	Quadratically-constrained quadratic program

QoS	Quality of service
RF	Radio frequency
ROC	Receiver operating characteristic
SDP	Semidefinite programming
SDR	Software-defined radio
SNR	Signal-to-noise ratio
SU	Secondary user
UHF	Ultra-high frequency
VHF	Very high frequency
WAN	Wide area network
WBAN	Wireless body area network

LIST OF FIGURES

CONTENTS

LIST OF INCLUDED ARTICLES

PI Younes Abdi and Tapani Ristaniemi. Joint Local Quantization and Linear Cooperation in Spectrum Sensing for Cognitive Radio Networks. *IEEE Transactions on Signal Processing, vol. 62, no. 17, pp. 4349-4362, Sept. 1, 2014.*

PII Younes Abdi and Tapani Ristaniemi. Extension of Deflection Coefficient for Linear Fusion of Quantized Reports in Cooperative Sensing. *Proc. IEEE 25th Annual International Symposium on Personal, Indoor, and Mobile Radio Communication (PIMRC), pp. 928-932, Washington DC, USA, Sept. 2-5, 2014.*

PIII Younes Abdi and Tapani Ristaniemi. Joint Reporting and Linear Fusion Optimization in Collaborative Spectrum Sensing for Cognitive Radio Networks . *Proc. 9th International Conference on Information, Communications and Signal Processing (ICICS), pp.1-5, Tanian, Taiwan, Dec. 10-13, 2013.*

PIV Younes Abdi and Tapani Ristaniemi. Random Interruptions in Cooperation for Spectrum Sensing in Cognitive Radio Networks. *IEEE Transactions on Communications (submitted for publication)*, 2016.

PV Younes Abdi and Tapani Ristaniemi. Linear Fusion of Interrupted Reports in Cooperative Spectrum Sensing for Cognitive Radio Networks. *Proc. IEEE 26th Annual International Symposium on Personal, Indoor, and Mobile Radio Communication (PIMRC), pp. 365-369, Hong Kong, China, Aug. 30 - Sept. 2, 2015.*

PVI Hossein Shokri-Ghadikolaei, Younes Abdi, and Masoumeh Nasiri-Kenari. Analytical and Learning-Based Spectrum Sensing Time Optimisation in Cognitive Radio Systems. *IET Communications, vol. 7, no. 5, pp. 480 - 489, 2013 (**IET Premium Paper Award 2014**).*

1 INTRODUCTION

1.1 Scope of the Research

Efficient utilization of available resources is a vital requirement in designing modern communication systems. Limited battery lifetime of today's so-called smart wireless devices and the global warming effect [1] are among the challenges which force engineers to reduce the energy consumption of wireless networks. On the other hand, the current dramatic growth rate in the number of bandwidth-hungry mobile systems and applications along with adherent scarcity in the available spectrum resources necessitates developing advanced spectrum-efficient communication techniques. Consequently, cognitive radio technology has been of great interest as an important implementation platform for green and spectrum-efficient wireless communication scenarios, see e.g., [2, 3, 4], and references therein.

In this dissertation, we first overview the notions of dynamic spectrum access and cognitive radio, in particular, in order to highlight the role, impact, and importance of this new communication paradigm in emerging wireless technologies. Specifically, we discuss the current state of spectrum utilization, new rules and regulations facilitating better spectrum use and how cognitive radios are developed as powerful assets to cope with the ever-increasing demand for higher levels of capacity, reliability, flexibility, and interoperability in wireless communication networks. As the core of this dissertation, we investigate spectrum sensing as a major capability in cognitive radios and discuss a number of significant design challenges in spectrum sensing for cognitive radio networks. These challenges cover a diverse collection of functionalities which, as a whole, enable cognitive radio networks to discover transmission opportunities in the underutilized parts of the radio spectrum and increase the efficiency of spectrum use without compromising the integrity of the legacy wireless networks.

In addition, we discuss how cooperative communication techniques are used to enhance the reliability of the spectrum sensing through better utilization of the spatial/user diversities in cognitive radio networks. We study various phases in the commonly-used cooperative sensing architectures in order to

build a solid understating of the role of different building blocks in this cooperation process. The analytical investigations in this dissertation along with their supporting simulation results demonstrate that design of spectrum sensing in cognitive radio networks, in general, involves dealing with various processes which often are different in nature and impose contradicting requirements. In fact, joint design of these processes often leads to a diverse collection of signal processing challenges ranging from signal estimation/detection to signal transmission/reception to decision/data fusion and decision-making processes. All these elements directly affect the overall sensing performance and we show that joint consideration of different processes involved in cooperative sensing can lead to significant performance gains.

Clearly, joint design of different processes involved in cooperative sensing requires joint effect of various variables to be taken into account by complex models and optimization problems. This is an interesting challenge which opens up a set of exciting and valuable research opportunities. The present dissertation addresses a number of important research questions related to this challenge by proposing novel spectrum sensing structures. These new structures are thoroughly analyzed and their associated design issues and tradeoffs are identified and formulated in the form of standard optimization problems. Consequently, proper techniques from the optimization theory are used to solve these problems in an effective and computationally-affordable fashion, while the effectiveness of the proposed spectrum sensing methods is supported by extensive simulations.

It is worth noting that, the set of theories, algorithms, and techniques used for performance optimization of the proposed spectrum sensing schemes consists of a broad range of materials including, standard convex optimization techniques [5], semidefinite relaxation methods for solving nonconvex quadratically-constrained quadratic programs (QCQPs) [6, 7, 8], mixed-integer nonlinear programs (MINLPs) [9, 10], convex-over-convex fractional programs [11], the branc- h-and-bound (BnB) algorithm [9, 10, 11], stochastic programming [12], and neural networks [13, 14, 15].

1.2 Structure of the Dissertation

We start with the radio spectrum in Chapter 2 and discuss why this valuable resource is currently underutilized and how more efficient spectrum utilization techniques are being developed to construct what is referred to as the dynamic spectrum access technology. This discussion leads us to the fundamental concept of cognitive radio for which a formal definition is provided in Section 2.2. In addition, we discuss different components of the cognitive radio, disclose its network architecture, and briefly overview its various emerging applications.

Chapter 3 is about different aspects of spectrum sensing in cognitive radio networks. In particular, we discuss a number of commonly-used signal detection techniques in spectrum sensing, introduce performance metrics for evaluating

the sensing quality, and illustrate how these performance metrics are typically calculated based on the statistical behavior of the received signal. In addition, we introduce the concept of cooperative spectrum sensing and discuss its significance in developing reliable spectrum sensing methods, while providing a brief overview of different components involved in this cooperation process and their respective roles.

Chapter 4 represents the research questions along with the design challenges addressed in this dissertation. Specifically, we introduce several tradeoffs by focusing on different processes in spectrum sensing. In each case, we discuss how the system design leads to conflicting requirements which are properly taken into account in the form of mathematical optimizations. In addition, we explain the solution procedure we have developed in each case for the system performance optimization.

Finally, we provide our concluding remarks in Chapter 5.

1.3 Summary of the Publications Included

In the following, we briefly explain major contributions in each publication included in this dissertation. Further details and discussions regarding the research questions addressed by these publications are provided in Chapter 4.

In [PI], cooperative spectrum sensing in cognitive radio networks is studied as a three-phase process composed of local sensing, reporting, and decision/data fusion. Then, a significant tradeoff in designing the reporting phase, i.e., the effect of the number of bits used in local sensing quantization on the overall sensing performance, is identified and formulated. In addition, a novel approach is proposed to jointly optimize the linear soft-combining scheme at the fusion phase with the number of quantization bits used by each sensing node at the reporting phase. The proposed optimization is represented using the conventional false alarm and missed detection probabilities, in the form of a MINLP. The solution is developed as a BnB procedure based on convex hull relaxation, and a low-complexity suboptimal approach is also provided. Finally, the performance improvement associated with the proposed joint optimization scheme, which is due to better exploitation of spatial/user diversities in cognitive radio networks, is demonstrated by a set of illustrative simulation results.

In [PII], maximizing the so-called deflection coefficient is discussed as an effective approach to design cooperative sensing schemes with low computational complexity. Specifically, an extension to the deflection coefficient is proposed which captures the effects of the quantization processes at the sensing nodes, jointly with the impact of linear combining at the fusion center. The proposed parameter is then used to formulate a new MINLP as a fast suboptimal method to design a distributed detection scenario where the nodes report their sensing outcomes to a fusion center through nonideal digital links. Numerical evaluations show that the performance of the proposed method is very close to the optimal

case.

In [PIII], the linear soft combining scheme at the fusion phase of the centralized cooperative sensing is jointly optimized with two elements of the reporting phase: i) the number of bits used by each node to quantize the local sensing outcomes, and ii) the power level by which each node reports its sensing outcome to the fusion center. The proposed optimization problem is represented by using the conventional false alarm and missed detection probabilities and two straightforward solutions are also provided. In addition, the performance improvement associated with the proposed joint optimization scheme is demonstrated by simulation results.

In [PIV], a new cooperation structure for spectrum sensing in cognitive radio networks is proposed which outperforms the existing commonly-used ones in terms of energy efficiency. The efficiency is achieved in the proposed design by introducing random interruptions in the cooperation process between the sensing nodes and the fusion center, along with a compensation process at the fusion center. Regarding the hypothesis testing problem concerned, first, the proposed system behavior is thoroughly analyzed and its associated likelihood-ratio test is provided. Next, based on a general linear fusion rule, statistics of the global test summary are derived and the sensing quality is characterized in terms of the probability of false alarm and probability of detection. Then, optimization of the overall detection performance is formulated according to the Neyman-Pearson criterion and it is discussed that the optimization required is indeed a decision-making process with uncertainty which incurs prohibitive computational complexity. The Neyman-Pearson criterion is then modified to achieve a good affordable solution by using semidefinite programming (SDP) techniques and it is shown that this new solution is nearly optimal according to the deflection criterion. Finally, the effectiveness of the proposed architecture and its associated SDP are demonstrated by simulation results.

In [PV], joint optimization of the reporting and fusion phases in a cooperative sensing with random interruptions is investigated. This optimization aims at finding the best weights used at the fusion center to construct a linear fusion of the received interrupted reports, jointly with Bernoulli distributions governing the statistical behavior of the interruptions. The problem is formulated by using the deflection criterion and as a nonconvex quadratic program which is then solved for a suboptimal solution, in a computationally-affordable fashion, by a semidefinite relaxation technique. The system performance is then demonstrated by a set of simulation results which compare the performance of the system for the cases with and without the optimal linear fusion.

In [PVI], the average throughput maximization of a secondary user by optimizing its spectrum sensing time is formulated, assuming that a priori knowledge of the presence and absence probabilities of the primary users is available. The energy consumed to find a transmission opportunity is evaluated, and a discussion on the impacts of the number of primary users on the secondary user throughput and consumed energy are presented. To avoid the challenges associated with the analytical method, as a second solution, a systematic adaptive

neural-network-based sensing time optimization approach is also proposed. The proposed scheme is able to find the optimum value of the channel sensing time without any prior knowledge or assumption about the wireless environment. The structure, performance and cooperation of the artificial neural networks used in the proposed method are explained in detail, and a set of illustrative simulation results is presented to validate the analytical results as well as the performance of the proposed learning-based optimization scheme.

1.4 Author's Contributions

The author of this dissertation is the main contributor regarding the analysis and simulations published in [PI, PII, PIII, PIV, PV]. He has also written the text of these publications.

The author of this dissertation was involved in developing the analysis and writing the text in [PVI]. He also proposed the use of neural networks in the system performance optimization. The idea of spectrum sensing time optimization considering the spectrum mobility and handover was proposed by the first author in [PVI] who has also conducted the simulations.

2 DYNAMIC SPECTRUM ACCESS TECHNOLOGY

2.1 Introduction

Availability of radio spectrum is essential to have reliable and high-performance wireless communications. However, rigid spectrum regulatory policies based on traditional *command-and-control* mechanisms make this precious natural resource scars, yet, underutilized. It is well known, as the result of extensive field measurements, that a large portion of the assigned spectrum is used sporadically with high geographical variations and high variance in time [2, 16, 17]. Fig. 1 illustrates the signal strength distribution over a large portion of the radio spectrum [16]. The underutilization is due to the fact that the use of spectrum is strictly licensed by governments. In traditional regulatory procedures, a license, associated with a particular frequency band over a certain geographical area, is granted to an operator which is referred to as licensee or license holder. The license gives, usually on a long-term basis, the licensee an exclusive right of utilizing that spectrum, meaning that no one else is allowed to use it. This is relatively an old process, referred to as *spectrum assignment* and is currently known to be highly inefficient making the assigned spectrum underutilized.

Underutilization of the radio spectrum indicates that there exist bands of frequencies assigned to license holders, which at some particular times and specific geographic locations are not being utilized. These temporarily- and/or spatially-available transmission opportunities are referred to as *spectrum holes* or *white spaces* [17, 18, 19]. The underutilization of spectrum has sparked a great deal of interest in engineering, economics, and regulatory communities in searching for better spectrum management policies and techniques [20, 21].

In order to promote more efficient use of the radio spectrum, altering the old regulations was initiated in December 2003 by the USA Federal Communications Commission (FCC). The FCC issued the first report and order in October 2006 exploring the possibility of allowing fixed wireless access to the TV broadcast bands for license-exempt devices on a non-interfering basis. The FCC further issued the second report and order in November 2008 to allow secondary usage

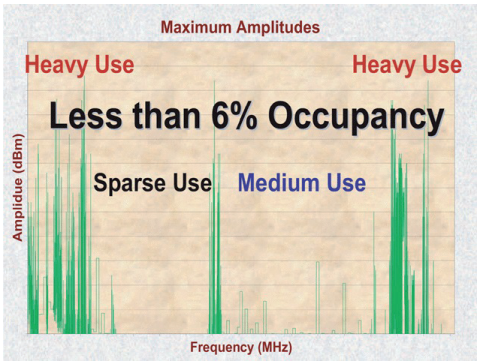

FIGURE 1 Spectrum utilization © 2011 IEEE.

of TV broadcast bands for fixed and mobile devices. European Conference of Postal and Telecommunications Administrations (CEPT), UK Office of Communications (Ofcom) and other countries like Canada, The Netherlands, Finland, and Scotland have followed the FCC and started investigating secondary usage of the radio spectrum, see [21, 22] and references therein. As explained in [23], Europe is proceeding with the finalization of rules and testing of the available technology on a large scale. The European progress is particularly driven by the Ofcom's work and instantiation of a large pilot of license-exempt devices and the underlying enabling technology. All trials within this pilot must operate under Ofcom's prospective rules for license-exempt spectrum access in the TV bands, reflected in ETSI standard [24]. In Finland, the WISE (white space test environment for broadcast frequencies) project [25] aims to construct an open testbed for studying the use of white spaces in the UHF television broadcast bands. The project partners are Finnish Communications Regulatory Authority (FICORA), Aalto University, Digita, Fairspectrum, Nokia, University of Turku, Turku University of Applied Sciences and it is funded by Tekes, the Finnish national technology funding organization.

According to the new regulations, license-exempt access to unused TV bands, known as TV band white spaces, is granted, provided that no harmful interference is made to the incumbent users (i.e., licensed users) present on those bands. In this scenario, the incumbents, which are TV broadcasters and wireless microphones, are considered as *primary users* (PU) with exclusive right of utilizing the spectrum while the license-exempt users are seen as *secondary users* (SU). SUs may only use a particular licensed spectrum when the corresponding PU is not using it and once the PU returns, the SUs have to vacate that band in order to avoid making any harmful interference. This particular access mechanism is referred to as *hierarchical spectrum access* which is further discussed in Section 2.4. Even though the FCC has set strict limits to protect the incumbents against interference in this scenario, valuable data communication opportunities can be realized by the secondary unlicensed access [26]. This is due to the fact that, significantly-large portions of the radio spectrum—especially in the VHF and UHF bands which have excellent propagation characteristics—are not utilized most of the time over large

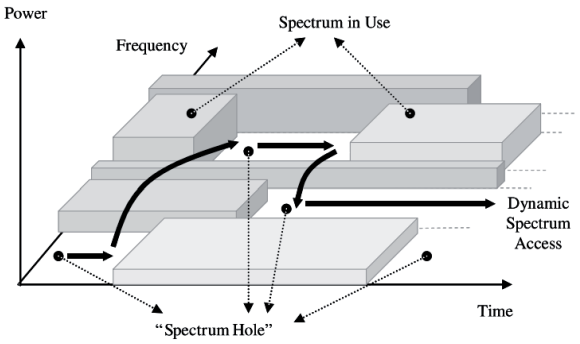

FIGURE 2 The concepts of white space and dynamic spectrum access © 2008 IEEE.

geographical areas. The unlicensed access was first considered for the TV bands as an initial step for extending the rules to other spectrum bands in future.

New opportunities provided by the secondary usage of the spectrum come with new challenges in radio communications. These challenges stem from the fluctuating nature of the white spaces, as well as the diverse quality-of-service (QoS) requirements of various applications [2]. For an SU, the availability of spectrum for access and communication is a random process whose behavior is dictated by the behavior of the PUs. In fact, SUs are supposed to identify the white spaces in a pool of licensed spectrum bands, and reconfigure their internal parameters such as operating frequency, transmission power, and bandwidth, in real time and according to the statistical characteristics of the discovered white spaces as well as their own QoS requirements.

Therefore, the radios used by the SUs need to have some sort of awareness regarding the user needs, the surrounding RF environment, and their current internal parameters and to be able to reconfigure their own parameters in step with changing circumstances in order to access and utilize dynamic spectral opportunities. This behavior is commonly referred to as *dynamic spectrum access* (DSA) [2, 16, 17] which is illustrated in Fig. 2 along with the concept of spectrum hole [17].

Awareness regarding the radio environment and user needs can be seen as *context awareness* whereas awareness with respect to the internal parameters can be considered as radio's *self-awareness* [27]. The changing circumstances may include the change in the propagation characteristics of the wireless environment due to, for example, the mobility of the SU or other entities, change in the behavior of the PUs as well as of other present SUs, and change in the QoS requirements. Significant levels of reconfigurability, required for accessing the dynamically-changing white spaces, are realized by implementing radios major air interface functionalities in software. This type of implementation, termed as *software-defined radio* (SDR), is a radio which could easily be reconfigured to operate on different frequencies with different protocols by software reprogramming [28]. This means that, the protocols based on which an SDR works can be altered without making changes to radio's hardware components.

Hence, we see that the secondary utilization of the spectrum needs to be realized by radios with special capabilities or attributes. These radios are termed as *cognitive radios* (CR) and were first introduced by J. Mitola in [27]. CR is commonly considered as the key enabling technology for realizing the DSA in wireless communication networks. In this chapter, we take a closer look at the concept of CR and provide a definition for it. In addition, we investigate fundamental building blocks commonly considered as major components of a CR and briefly describe their respective roles. Finally, we explain the CR network (CRN) architecture and provide an overview of different applications of the DSA technology.

It is worth noting that, there exist several spectrum sharing mechanisms, falling within the scope of the DSA technology, which are not entirely based on the licensed-exempt spectrum use. In these sharing schemes, the spectrum is dynamically accessed by several parties among which some may in fact be license holders. Moreover, these shared access mechanisms make the DSA technology be considered in other frequency bands rather than only in the TV spectrum. The concepts of licensed share access (LSA) [29, 30], licensed-assisted access (LAA) [31, 32, 33], and citizen broadband radio service (CBRS) [34] can be considered as some examples. We briefly explain these methods in order to present a complete overview of the state of the art. Nevertheless, implementation details of these spectrum sharing schemes are beyond the scope of this dissertation.

LSA is a complementary approach, to exclusive licensing and license-exempt approaches, allowing a spectrum band to be shared between an incumbent spectrum user and a mobile communication network (here, the LSA licensee) with predetermined conditions that resemble exclusive licensing and offer benefits to both parties. The LSA concept has been successfully trialled with a live LTE network in the 2.3 GHz shared band in Finland [29, 30]. A key benefit of the LSA concept is to ensure controlled predictable QoS levels for both incumbent spectrum users and the LSA licensees by considering a limited number of entities involved in the sharing arrangement [29].

LAA is a spectrum sharing approach which enables the use of unlicensed spectrum bands for the licensed services. Specifically, LAA is concerned with sharing the unlicensed spectrum by the licensed and unlicensed users and its main deployment scenario considers the coexistence of LTE-A with WiFi in the 5 GHz band [32]. This allows operators to leverage unlicensed 5 GHz spectrum for improved peak rates and capacity.

CBRS is another hierarchical spectrum access which is recommended by the FCC for the 3.5 GHz. The CBRS consists of a DSA architecture with three tiers [34]: the incumbent users, Priority Access (PA) users and General Authorized Access (GAA) users. In this architecture, existing primary operations in the 3.5 GHz would make up the incumbent access (IA) tier. The CBRS would be divided into PA and GAA tiers of service, each of which would be required to operate on a non-interference basis with the IA tier. As the name suggests, PA users receive protection from the GAA operation while GAA users will receive no interference protection from other CBRS users. The 3.5 GHz band has physical characteristics that make it particularly well-suited for mobile broadband employing small cell

technology. As such, the CBRS is envisioned to represent a major contribution toward making more spectral resources available for broadband use.

2.2 Cognitive Radio

CR is regarded as a promising technology to alleviate the problem of spectrum scarcity via utilizing large amounts of the unused spectrum while not interfering with incumbent devices in frequency bands already licensed [35]. This new communication paradigm is based on radios that can acquire information about their operating environment and adapt their operating characteristics in real-time in order to better utilize the available opportunities. Today, CR techniques are being applied to many different communications systems [28] (see Section 2.5), and hold promise for increasing utilization of radio frequencies and allowing for improved commercial, emergency, and military communication services [36]. Moreover, since the concept of CR is built on top of the SDR, its prominent reconfiguration capabilities make it known as a facilitator of communications for devices which may operate in different bands and/or have incompatible wireless interfaces. All these facts have made CR as the core of many technical discussions and interactions among various academic, industrial, and regulatory groups specialized in wireless communications all over the world.

Considering CR in the context of the radio spectrum and as an enabling technology for more efficient spectrum utilization serves the purposes of the present dissertation appropriately. However, it should be noted that CR can be seen with a broader perspective as a means in general for serving dynamically-changing user needs based on the dynamic availability of resources influenced by changing circumstances in radio's environment. Consequently, we see generic terms about the radio environment and the associated resources in commonly-used definitions of cognitive radio.

There exist several definitions for CR in the literature provided by various regulatory, standardization, and research institutes worldwide as well as some distinguished researchers in the field. In [37] a number of most prominent definitions of CR are reviewed in order to obtain a fundamental understanding of its capabilities. The result obtained by this investigation suggests the following capabilities for a CR [37]:

- Whether directly or indirectly, the radio is capable of acquiring information about its operating environment
- The radio is capable of changing its waveform (protocols)
- The radio is capable of applying information towards a purposeful goal

Accordingly, the following definition is proposed in [37]:

> *A cognitive radio is a radio whose control processes permit the radio to leverage situational knowledge and intelligent processing to autonomously adapt towards some goal.*

Intelligence in this definition is adopted from [38] which defines it as

> *Intelligence is the capacity to acquire and apply knowledge, especially toward a purposeful goal.*

In the CR scenarios considered in this dissertation, the goal pursued is to detect white spaces and to use those white spaces in order to establish wireless communication without having spectrum bands allocated to that communication. Situational knowledge may include information acquired by the CR about its spectral environment. In general, there are several ways in practice to acquire information about radios spectral environment, among which *spectrum sensing* and *geolocation/database* are the most common ones. Spectrum sensing in this context refers to applying signal processing algorithms on the received radio signals in order to detect the presence or absence of the PUs in the frequency bands of interest. Geolocation/database is used when the SUs know their location. In this method, the SUs have access to a (typically) remote database which provides them with a list of available channels at their geolocation when requested. Situational knowledge may also include the user needs characterized by the QoS requirements of the communication. Hence, we see that having situational knowledge covers the context awareness of the cognitive radio. Moreover, situational knowledge may also include information a CR has about its own internal parameters and their implications regarding the radio performance. In other words, the information which gives the CR its self-awareness is covered by situational knowledge in this definition as well.

In the following, we discuss the components of the CR to better illustrate how the situational knowledge is acquired and how it is processed in order to conduct the autonomous adaptation.

2.3 Components of a Cognitive Radio

Fig. 3, which is adapted from [28], provides a high-level view of the components that can be found in a CR. This system is composed of a reconfigurable radio, a reasoning engine, a decision (or configuration) database, and a policy database. The reconfigurable radio is typically used to facilitate autonomous adaptation of radio's operating parameters including, but not limited to, transmission power, frequency, and bandwidth. The sensing module is responsible for inspecting radio's environment to provide information about the available communication resources. The system may contain a policy database which defines a set of rules to determine the acceptable behavior in different circumstances. The appropriate configuration of the system internal parameters is determined by a reasoning module which receives information from the sensing engine and the policy database and may be equipped with learning capabilities. Learning is a function of observations and decisions [27]. For example, performance levels achieved based on prior and current internal states may be compared with expectations

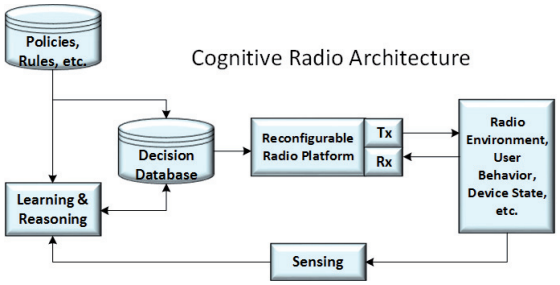

FIGURE 3 Components of a cognitive radio system © 2008 IEEE.

to learn about the effectiveness of the decisions made by the reasoning engine. The current configuration of the radio components, which is determined by the decisions made by the reasoning engine, is stored in a configuration database. A simple CR system might have a single reconfigurable radio component accepting sensing information from a single local node and no external data sources.

It should be noted that the concept of CR roots back to the artificial intelligence theory in which *cognition* is often involved with machine learning. In some references, CR refers to a sophisticated radio device that mimics the human brain in a DSA environment to perceive and learn the radio environment to control and adapt the transmission actions [4]. However, based on several available definitions of CR and the related terms, and as a result of inspecting several commonly-used CR-based communication scenarios, the author concludes that cognition, in the context of the radio technology, is mostly concerned with knowledge and the ability to acquire and use that knowledge. Hence, the processes of building, changing, or even contributing to that knowledge—in the form that can be referred to as learning—may not be a necessary part of a cognitive system, or, at least, a CR. As explained in [28], today, the term CR generally refers to a radio system that has the ability to sense its radio frequency (RF) environment and modify its spectrum usage based on what it detects. Nevertheless, since CR is a relatively new and evolving concept, the machine learning capability will most likely be considered as one of the necessary components of a CR in future.

2.4 Network Architecture

The concept of CRN is built upon the notion of hierarchical spectrum access which is described by the notions of primary and secondary users and primary and secondary networks [17, 18]. In this structure, the legacy license holders, such as cellular network operators and TV broadcasters, are the PUs and their networks are primary networks. Based their license, PUs can utilize the spectrum exclusively, which means that, while they are operating on a certain frequency band, no one else is allowed to use it. A primary network is typically composed of a set of PUs and one or more primary base stations (BS). CR users are the SUs, i.e., they can only access the spectrum and utilize it for communication when PUs

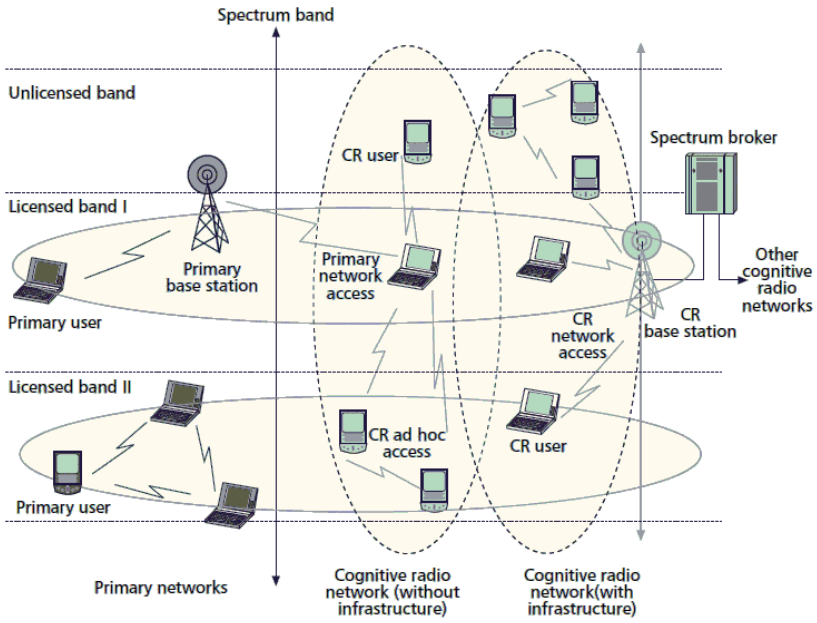

FIGURE 4 The cognitive radio network architecture © 2008 IEEE.

are not using it. Accordingly, the CRNs are referred to as the secondary networks. As clarified in Section 2.1, SUs need to be equipped with cognitive capabilities to be aware of their spectral environment and also to be able to adapt their operating parameters in order to avoid making harmful interference to PUs. Note that besides secondary access to the licensed spectrum, CRNs can use the unlicensed spectrum bands. Availability of different licensed or unlicensed spectrum bands for the secondary use is usually referred to as spectrum heterogeneity in CRNs.

The secondary network may contain a BS, equipped with cognitive functionalities, which coordinates the spectrum access of SUs. This type of secondary network is shown in Fig. 8 as a CRN with infrastructure [17]. However, this may not always be the case and a CRN may be realized as an ad-hoc network. It should be noted that the hierarchical spectrum access does not require the secondary nor the primary networks to be infrastructure-based. Accordingly, we see both types of infrastructure-based and ad-hoc structures for either of the primary or secondary networks in Fig. 8.

SUs typically get aware of their radio environment by spectrum sensing and/or geolocation/database. If several secondary networks share a common set of frequency bands, their spectrum usage may be coordinated by a central network entity, called spectrum broker [18]. The spectrum broker collects operation information from each secondary network and allocates the network resources to achieve efficient and fair spectrum sharing.

The IEEE 802.22 standard [26] is a commonly-used CRN example. This standard concerns the secondary use of the TV bands on a non-interfering basis which is realized by the so-called TV band devices (TVBD). TVBDs have been developed

for the secondary use of the available chunks of TV spectrum (TV white spaces). Since the TV bands have good propagation characteristics, they can increase coverage and the ability to penetrate buildings at low power levels, leading to better broadband access across remote rural areas.

The IEEE 802.22 standard specifies a cellular CRN. In each cell, a BS manages the medium access for all the SUs. In order to properly protect the PUs against harmful interference, both spectrum sensing and geolocation/database techniques have been considered in this standard. In particular, each BS is equipped with a GPS device and has access to a remote database of available channels. Moreover, the BSs as well as the SUs are equipped with spectrum sensing capabilities. The BSs coordinate the local spectrum sensing activities of SUs in their cell and decide which TV bands are unoccupied based on information received from the database, their own sensing outcome, and the sensing results provided by the SUs. This particular type of spectrum sensing in which a network entity coordinates the local spectrum sensing of the SUs and makes the global decision about the presence or absence of the PU based on the data received from the sensing SUs is referred to as *centralized cooperative spectrum sensing*. Cooperative spectrum sensing is discussed in detail in Section 3.3.

2.5 Applications of Cognitive Radio

CRNs can be used in different applications. In what follows, we briefly discuss some of the applications that can benefit from the research conducted in this dissertation. For a more comprehensive overview of CR applications see [36] and the references therein.

2.5.1 Cellular Networks

Cellular networks provide data and voice services for billions of us every day. These networks, as our major communication infrastructures, need to be constantly improved in coverage, efficiency, service quality, and reliability in order to meet the ever-growing demand for wireless communications. At the same time, the spectrum is limited. The DSA technology along with the unlicensed access schemes to the radio spectrum provides more spectral resources for the next generation cellular networks. As such, the cognitive cellular network is considered as one of the key concepts in designing the fifth-generation (5G) mobile communication systems [39]. Employing the CR functionalities, such as spectrum sensing and spectrum sharing, in different components of cellular networks enhances their performance and enable network operators to utilize the available resources more efficiently and more effectively, see, e.g., [40, 41] and references therein.

The tradeoff between energy efficiency and spectral efficiency has always been of major importance in designing cellular communication networks. In fact,

CR and the DSA technology are at the heart of discussions concerning green cellular communications. Since Shannon's communication capacity [42] increases linearly with the available bandwidth while it grows only logarithmically with power, by providing more bandwidth, we can reduce the transmission power in communication systems. Hence, better spectrum management mechanisms realized by the DSA technology can significantly reduce the power consumption in cellular networks [43]. It is shown in [44] that the use of DSA techniques can lead to substantial savings in the power consumption of cellular networks. As another point, it is worth mentioning that, according to the definition provided in Section 2.2, CR is a radio which can autonomously adapt its own parameters to meet a certain objective. Therefore, the cognitive functionalities can be designed in general with the primary goal of power saving. This design strategy reduces the power consumption of wireless cellular networks while maintaining the required QoS levels, under various channel conditions [43].

2.5.2 Public Safety Networks

Public safety networks often suffer from two major drawbacks. First, the radio frequencies allocated for public safety use are congested and cannot meet the growing demand for high-quality wireless communications required by first responders. Second, since first responders from different agencies often use different radio technologies, they are often not able to communicate with each other properly and in accordance with their needs, especially, in disaster situations. Interoperability is hampered by the use of multiple frequency bands, incompatible radio equipment, and a lack of standardization [36].

CR benefits for public safety can be summarized in two main factors as first, DSA which leads to higher communication capacities and second, reconfigurability which facilitates interoperability between communication systems. With cognitive radio, public safety users can use additional spectrum such as license-exempt TV white spaces. Moreover, through appropriate spectrum sharing partnerships with commercial operators, public safety workers can also access licensed spectrum and/or commercial networks [36]. When a natural disaster or terrorist attack destroys existing communication infrastructure, CRNs, deployed rapidly as a set of BSs mounted on emergency responders' vehicles can aid the search and rescue teams. Cognitive capabilities in recognizing spectrum availability and autonomous adaptation for more efficient communication can provide public safety personnel with reliable broadband communication which reduces delay in information transfer when dealing with critical situations [16].

2.5.3 Smart Grid Communications

Smart grid is widely considered as the next generation of power grid. This promising technology is currently being promoted by many governments as an effective means of developing power transmission networks with higher levels of agility, reliability, efficiency, security, economy, and environmental friendliness [16, 45].

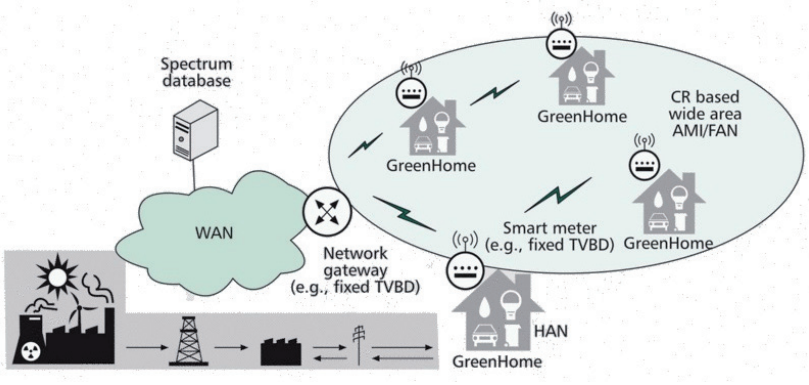

FIGURE 5 An IEEE 802.22-based smart grid architecture © 2011 IEEE.

A reliable and efficient communication infrastructure is the foundation of any smart grid. In fact, optimality and accuracy of demand response management (DRM), which is the core control unit of smart grid, directly depends on the performance of communication facilities incorporated. The communication infrastructure concerned is typically a heterogeneous network providing access to grid components in diverse environments. These network components typically need to spread over large geographical areas including generation, transmission, and distribution to the consumer premises [45].

Fig. 5 shows a basic illustration of the electrical power grid and the smart grid multitier communications network [36]. This network is composed of a so-called home area network (HAN), the advanced metering infrastructure (AMI) or field area networks (FAN) and a wide area network (WAN). HAN is the network of smart meters connected to on-premise appliances, plug-in electrical vehicles, and distributed renewable sources (e.g., solar panels) while FANs carry information between premises and an aggregation unit, which will often be a power substation, a utility pole-mounted device, or a communications tower. The WAN which serves as the backbone for communication, provides links between the grid and core utility systems [36, 45].

Due to different nature of various applications running on these networks, the smart grid communication infrastructure has to accommodate different types of data traffic (e.g., real-time vs. non-real-time, emergency report vs. demand response) with different priorities, and with various QoS requirements in terms of the required bandwidth, latency, etc [16, 46]. Moreover, since an SG is typically a large and costly power network built to serve over large geographical areas for a considerably long time, it is clear that future growth in the number of applications and connected devices must be taken into account in the initial design. However, leaving significant room for future expansions is not an appropriate solution due to high costs [46]. In particular, acquiring additional bandwidth through licensing the spectrum, to facilitate future growth, can be very expensive, if possible.

CR is recognized as a promising technology to enhance capacity, coverage, and scalability in smart grid networks and to reduce the cost associated with

licensing the spectrum. In particular, CR-based AMI/FANs may offer many advantages in terms of bandwidth, distance, and cost, as compared with other wireline/wireless technologies currently available [16]. For instance, TVBDs operating with the IEEE 802.22 standard [26] provide a good solution for connecting the gateways and smart meters which are fixed nodes in a smart grid. Fig. 5 illustrates a DSA-based wide area AMI/FAN. TVBDs provide relatively high transmission power and superior TV band propagation characteristics. Specifically, the BSs coverage area for the IEEE 802.22 can be 33 km if the power level of the customer-premises equipment (CPE) is 4 W, and it can be extended to 100 km if higher power levels are allowed [47]. Therefore, an IEEE 802.22-based network gateway may reach all the smart meters with one or two hops (e.g., covering an entire town). In rural areas available TV white space channels could be abundant, providing low-cost reliable broadband communication facilities for smart grid applications.

2.5.4 Wireless Medical Networks

Wireless communications has been considered as an important factor in improving patient's quality of life in healthcare centers due to reducing the need for having the patient connected to fixed medical equipment. Since patient's mobility plays an important role in fast recovery, especially, after surgical procedures and interventions, developing reliable, scalable, and effective wireless medical devices for monitoring vital signals, is of special interest in today's biomedical engineering. Current use of on-body sensors which are connected by wires to a monitoring device is gradually replaced by the use of wireless body area networks (WBAN). A WBAN typically consists of a collection of low-power, miniaturized, lightweight devices with wireless communication capabilities that operate in the proximity of a human body [48]. Medical BAN (MBAN), which is WBAN for medical applications, refer to a low cost wireless sensor network designed to collect multiple health-care-related parameters simultaneously and relay information wirelessly such that clinicians can monitor their patients and respond quickly to their medical needs without compromising their mobility [36, 48]. Besides improving patient's mobility, the use of MBAN reduces the infection risks associated with using and managing wires in healthcare units.

Many standard solutions for WBAN, such as IEEE 802.15.4 and IEEE 802.15.6, operate in the license-free Industrial Scientific and Medical (ISM) band centered at 2.45 GHz and this leads to coexistence issues with other networks operating in the same band, e.g., IEEE 802.11, a.k.a., WiFi. Cognitive wireless communication paradigms can be used to mitigate the coexistence issues and improve the reliability of WBANs which is a serious issue due to their low transmission power, see [48, 49]. CR-based MBAN architectures with frequency agility and frequency-domain spectrum shaping capabilities are used to facilitate interference avoidance in scenarios where many devices are operating in common spectrum segments and in close proximity to each other, as may occur in locations such as a busy medical center. Besides facilitating coexistence, CR technology can con-

tribute to the effectiveness and reliability of WBANs by providing them with two important characteristics: higher bandwidth and reconfigurability.

3 SPECTRUM SENSING IN COGNITIVE RADIO NETWORKS

3.1 Introduction

In order to protect the PUs against harmful interference, CRs monitor their radio environment by applying signal processing techniques on the received radio signals. This process is referred to as spectrum sensing and is certainly a key capability enabling CRs to find transmission opportunities without making harmful interference on the PUs. Consequently, reliable spectrum sensing is of major importance in designing CRNs. The average throughput of the SUs, their consumed energy, and the amount of interference experienced by the PUs are directly related to the effectiveness of the sensing methods incorporated in CRs.

When sensing the radio spectrum, CRs conduct a binary hypothesis test based on statistical characteristics of the received signals. Conventionally, in this test the null hypothesis, denoted $\mathcal{H}_0$, corresponds to the absence of the PU signal while the alternative hypothesis, denoted $\mathcal{H}_1$, indicates its presence. Techniques used by CRs to transform the radio signals received at their RF front end into a set of statistics representing the state of the PU activities can range from a simple radiometry, a.k.a., *energy detection* to *cyclostationary detection* to *coherent detection* [50]. Energy detection is the most common way of spectrum sensing because of its low computational and implementation complexities. In addition, it does not need any knowledge about the primary users' signal. The signal is detected in this method by comparing the output of the energy detector with a threshold which depends on the noise floor [51]. Cyclostationary detection is a method for detecting PU transmissions by exploiting the cyclostationarity of the received signals. Cyclostationary features are caused by the periodicity in the signal or in its statistics such as mean and autocorrelation. These two techniques are further explained in Section 3.2. In the presence of a known pattern, sensing can be performed by correlating the received signal with a known copy of itself. This method is only applicable when the PU signal patterns are known, and it is termed as coherent detection.

Depending on the DSA scenario considered, CRs may be designed either to monitor a narrow chunk of the radio spectrum based on narrowband spectrum sensing methods or to inspect a wide range of frequencies by wideband sensing schemes. How to choose the best parameter values when designing an appropriate spectrum sensing algorithm is an important consideration in developing reliable CRNs and depends on several factors in general. These factors may include hardware complexity of the CR nodes, amount of available *a priory* knowledge about the behavior and signal statistics of the PUs, propagation characteristics of the radio environment, the detection quality required, and number of signal samples available. In particular, the detection quality is determined based on interference limits to be maintained for protecting the PUs as well as the QoS levels to be provided for the SUs. As a matter of fact, design of reliable, yet low-complexity spectrum sensing schemes is a challenging task, often involving contradictory requirements, with significant impacts on the performance of the CRNs. In the following paragraph, the tradeoff between the sensing time and accuracy [52] is explained as an example.

Typically, spectrum sensing and signal transmission cannot be performed at the same time in a CR [1] [51]. Hence, the time slots used by a CR are usually divided into two parts; one for sensing and the other for data transmission. Sensing time refers to the portion of time slots used for sensing the radio spectrum. For interference avoidance, the sensing time needs to be long enough to achieve sufficient detection accuracy, i.e., longer sensing time provides more signal samples which, in turn, lead to higher sensing accuracy, and hence, to less interference. However, as the sensing time becomes longer, the transmission time of CR users are decreased. Conversely, while a longer transmission time increases the CR throughput, it causes higher interference due to the lack of sensing information. Accordingly, sensing time and transmission time are the sensing parameters that influence the CR performance in two opposite directions and therefore, proper selection of these sensing parameters is critical.

Performance of the spectrum sensing is commonly measured by two probabilities, namely, the *probability of false alarm* and the *probability of detection* (or its complement, the *probability of missed detection*). False alarm occurs when the sensing CR node mistakenly decides the presence of the PU signal while it is absent. In this case, a communication opportunity is lost by treating a spectrum hole as occupied. Therefore, the higher the false alarm probability, the more transmission opportunities missed by the CR. In general, due to inevitable sources of uncertainty, such as thermal and environmental noise, shadowing, and multipath fading, it is difficult in practice to have zero false alarm probability without failing

[1] Simultaneous sensing and transmission is currently possible by the use of full-duplex CRs. However, design of these radios is challenging in the sense that proper techniques must be implemented to mitigate the effect of the resulting self-interference. In fact, a high level of isolation between the transmitter and receiver is necessary in full-duplex CRs. A typical technique to reduce the self-interference in these radios is to use two antennas; one for sensing and the other for data transmission. Mitigating the effect of self-interference in full-duplex CRs is an ongoing research challenge which has recently gained a great deal of interest, see [53] and the references therein.

to detect the PU signals frequently. However, through certain design strategies (which are discussed later) the false alarm probability can be minimized or constrained by a limit in order to achieve an acceptable performance. Probability of detection can be regarded as the dual of the false alarm probability. Detection occurs when the sensing algorithm declares the presence of the PU while it is actually present and active. In this case, the CR node can avoid interfering with the PU by either interrupting its own transmission or directing it to another vacant band. Clearly, the higher the detection probability, the lower the interference level experienced by the PUs. By a similar reasoning as we did for the false alarm probability, we can see that the probability of detection cannot be easily forced to be one without having a high false alarm rate in the signal detection, especially, in low SNR regimes. Nevertheless, performance of the spectrum sensing can be optimized with the aim of maximizing the detection probability or bounding it from below.

Detector design based on the *Neyman-Pearson* (NP) criterion [54] is a commonly-used method for optimizing the spectrum sensing performance in CRs. In an NP detector, the probability of detection is maximized subject to a constant false alarm probability. This design method aims at achieving the maximum protection of the PUs while maintaining the rate of lost transmission opportunities at a certain limit. Alternatively, the false alarm probability can be minimized subject to a constant detection probability. In this way, the CR throughput is maximized while keeping the level of interference experienced by the PUs at a certain level. Since the spectrum sensing performance can depend on various uncertainties, the mathematical representation of the false alarm and detection probabilities may involve complicated nonlinear formulations which, in an NP setting, may lead to complicated nonconvex optimizations. As an alternative method with good performance and often low computational complexity, the deflector design based on the *deflection* criterion is a popular technique in the literature, see e.g., [55, 56, 57] and [PI, PII]. In this method, the so-called deflection coefficient, as a parameter representing the sensitivity of the sensing scheme, is maximized without directly considering the detection and false alarm probabilities.

As mentioned before, the sensing performance is susceptible to impairments caused by the wireless environment. In fact, noise, interference, shadowing, and multipath fading often degrade the CR sensing performance. Moreover, the sensing CR might not be able to detect the PU signal due to its inappropriate location. This particular issue is known as the *hidden node problem* and has to be taken into account when designing the spectrum sensing in CRNs. In order to mitigate these issues, the reliability of the sensing process is enhanced significantly by the so-called *cooperative spectrum sensing*. In this method, spatially-divers sensing CR nodes cooperate with each other in finding the spectrum holes.

Design and analysis of cooperative sensing schemes concern in general with how the observations in different nodes are combined and tested and how the decisions are made. In the *centralized cooperative sensing* [2] the binary hypothesis test is conducted in a special node, referred to as the *fusion center* (FC), which receives and processes local sensing outcomes from the cooperating nodes. This coopera-

tion, which is synchronized and coordinated by the FC, follows a three-step process: *local sensing*, *reporting*, and *decision/data fusion*. In the first step, the sensing nodes perform their individual sensing by using their own built-in sensor. They listen to their wireless environment to detect the PU signals. Hence, the channel between the PU transmitter and the sensing CR nodes are referred to as *listening channels*. Then, they report their sensing results to the FC through a *reporting or control channel* indicated by the FC. Finally, the FC combines the received reports and decides about the presence or absence of the PU. Note that centralized cooperative sensing can occur in either centralized or distributed CR networks. In centralized CR networks, a cognitive BS is naturally the FC. A commonly-used practical example for this case is the IEEE 802.22 standard [58] where the BS is also the FC coordinating the cooperative spectrum sensing process in the CRs. Alternatively, in CR ad hoc networks where a CR BS is not present, any CR user can act as an FC to coordinate the cooperative sensing and combine the sensing information from the cooperating neighbors.

Besides centralized cooperation, there exist other methods, such as *distributed cooperative sensing* and *relay-based cooperative sensing*, in which the information exchange between the CR nodes as well as the decision making process take place differently. Specifically, in the former there is no such node as the FC and the sensing CRs exchange their information directly with each other and converge to a decision iteratively. In the latter, the nodes which experience better reporting channels relay the results from the nodes with weak reporting channel. The relays may be chosen from the ones which do not have a good listening channel. More details can be found in [2] and the references therein. For the purposes of this dissertation, we will focus on the centralized cooperative sensing which is also known as distributed detection with an FC. We will see that design of each different phase in centralized cooperative sensing is in general concerned with a different set of challenges. In local sensing, the problem is how to quickly and effectively detect a radio signal distorted by noise, shadowing, and multipath fading, whereas the design of the reporting phase is mostly concerned with quantization of the sensing outcomes as well as transmit power and/or bandwidth to make efficient use of the available transmission and computation resources. At the fusion phase, we are dealing with the hypothesis testing and decision-making processes which need to properly take into account the PU behavior as well as listening- and reporting- channel characteristics. Therefore, we see that the set of problems to be addressed in each different phase of cooperative sensing is different in nature. However, we show that joint design and optimization of these different phases can lead to significant performance gains in CRNs.

3.2 Signal Detection Methods

Spectrum sensing in CR is, in general, a decision-making problem. By using signal processing tools, the CR converts some statistical features of the PU signal re-

ceived into a decision variable, referred to as *test statistic* or *test summary*, whose value indicates the presence or absence of the PU. The test statistic, which is a random variable, is usually compared against a predefined detection threshold to decide the presence or absence of the PU. The random behavior of the decision variable and the sensing result obtained stem from the uncertainties in the PU behavior as well as the impact of the wireless environment on the received signal. Due to this randomness, the sensing performance is commonly measured by probabilities, i.e., the probability of false alarm and the probability of detection. To measure the sensing performance by these metrics, we first need to evaluate the random behavior of the decision variable and find its probability distribution. In order to illustrate the analysis concerned, in the following, we provide mathematical modeling of the energy detection and cyclostationary detection which are two widely-used sensing schemes in CR systems.

The signal received by the ith sensing node in a CRN can be modeled as

$$\begin{cases} x_i(m) = \nu_i(m), & \mathcal{H}_0 \\ x_i(m) = h_i s(m) + \nu_i(m), & \mathcal{H}_1 \end{cases} \tag{1}$$

where $s(m)$ denotes the signal transmitted by the PU and $x_i(m)$ is the received signal by the ith SU. h_i is the listening channel block fading coefficient. $\nu_i(m)$ denotes the circularly-symmetric zero-mean additive white Gaussian noise (AWGN) at the CR sensor receiver, i.e., $\nu_i(m) \sim \mathcal{CN}(0, \sigma_i^2)$. $s(m)$ and $\{\nu_i(m)\}$ are assumed to be independent of each other.

3.2.1 Energy Detection

Energy detection [50, 51, 52, 55, 56, 59] is the simplest spectrum sensing technique. A CR employing energy detection decides the presence or absence of the PU simply by comparing the energy of the received signal with a predefined threshold. Energy detection is widely used in the literature due to its low computational (and hence implementation) complexity and its fast detection ability. In addition, energy detection assumes no *a priori* knowledge about the PU signal which makes it feasible when there is no such information available.

The sensing outcome generated in the ith CR node applying energy detection on N samples of the received signal can be modeled as

$$u_i = \sum_{m=0}^{N-1} |x_i(m)|^2 \tag{2}$$

This sensing outcome is then compared against a detection threshold γ_i to decide the presence or absence of the PU signal, i.e.,

$$u_i \underset{\mathcal{H}_0}{\overset{\mathcal{H}_1}{\gtrless}} \gamma_i \tag{3}$$

Since u_i is the sum of squares of Gaussian random variables, it can be shown that u_i/σ_i^2 follows a central chi-square χ^2 distribution with N degrees of freedom if

$\mathcal{H}_0$ is true; otherwise, it would follow a noncentral χ^2 distribution with N degrees of freedom and parameter η_i. That is,

$$\frac{u_i}{\sigma_i^2} \sim \begin{cases} \chi_N^2, & \mathcal{H}_0 \\ \chi_N^2(\eta_i), & \mathcal{H}_1 \end{cases} \tag{4}$$

where

$$\eta_i = \frac{E_s |h_i|^2}{\sigma_i^2} \tag{5}$$

and $E_s = \sum_{m=1}^{N} |s(m)|^2$ denotes the PU signal energy. According to central limit theorem [60], if the number of samples N is large enough, the test statistic u_i is asymptotically normally distributed, i.e,

$$u_i \sim \begin{cases} \mathcal{N}\left(E[u_i|\mathcal{H}_0], \mathrm{Var}[u_i|\mathcal{H}_0]\right), & \mathcal{H}_0 \\ \mathcal{N}\left(E[u_i|\mathcal{H}_1], \mathrm{Var}[u_i|\mathcal{H}_1]\right), & \mathcal{H}_1 \end{cases} \tag{6}$$

where

$$E[u_i|\mathcal{H}_0] = N\sigma_i^2 \tag{7}$$

$$E[u_i|\mathcal{H}_1] = (N + \eta_i)\sigma_i^2 \tag{8}$$

$$\mathrm{Var}[u_i|\mathcal{H}_0] = N\sigma_i^4 \tag{9}$$

$$\mathrm{Var}[u_i|\mathcal{H}_1] = (N + 2\eta_i)\sigma_i^4 \tag{10}$$

Therefore, the false alarm and detection probabilities of the ith CR node, denoted respectively as $P_{\mathrm{f}}^{(i)}$ and $P_{\mathrm{d}}^{(i)}$, can be formulated as

$$P_{\mathrm{f}}^{(i)} = \Pr\{u_i > \gamma_i|\mathcal{H}_0\} = \int_{\gamma_i}^{\infty} f_{u_i}(x|\mathcal{H}_0)dx = Q\left(\frac{\gamma_i - E[u_i|\mathcal{H}_0]}{\sqrt{\mathrm{Var}[u_i|\mathcal{H}_0]}}\right) \tag{11}$$

$$P_{\mathrm{d}}^{(i)} = \Pr\{u_i > \gamma_i|\mathcal{H}_1\} = \int_{\gamma_i}^{\infty} f_{u_i}(x|\mathcal{H}_1)dx = Q\left(\frac{\gamma_i - E[u_i|\mathcal{H}_1]}{\sqrt{\mathrm{Var}[u_i|\mathcal{H}_1]}}\right) \tag{12}$$

where $Q(x) \triangleq \frac{1}{\sqrt{2\pi}} \int_x^{\infty} e^{-x^2/2} dx$.

It is worth noting that, energy detection is not able to distinguish between the PU signal and noise and suffers from a poor performance in low signal-to-noise ratio (SNR) regimes. Reliability of spectrum sensing in low SNR can be improved significantly by establishing cooperation among the sensing nodes in a CR network. We discuss cooperative sensing in Section 3.3.

3.2.2 Cyclostationary Detection

Cyclostationary detection [50, 51, 57, 61] is capable of distinguishing the PU signal from the interference and noise. In this method, the signal detection is based on estimating the discrete-time cyclic autocorrelation function (CAF) of the received signal $R_i^{(f_0)}(l)$ defined for $0 \leq l \leq L$ as [50]

$$\hat{R}_i^{(f_0)}(l) \triangleq \frac{1}{N-l} \sum_{m=0}^{N-l-1} x_i(m+l) x_i^*(m) e^{-j2\pi f_0 m} \tag{13}$$

where $f_0 = 1/T_0$ and T_0 denotes the symbol period in the digitally-modulated PU signal. CAF estimations corresponding to different lags are collected in a vector as

$$\hat{\mathbf{r}} \triangleq \left[\mathcal{R}e\{\hat{R}_i^{(f_0)}(0)\}, ..., \mathcal{R}e\{\hat{R}_i^{(f_0)}(L)\}, \mathcal{I}m\{\hat{R}_i^{(f_0)}(0)\}, ..., \mathcal{I}m\{\hat{R}_i^{(f_0)}(L)\}\right] \quad (14)$$

where $\mathcal{R}e$ and $\mathcal{I}m$ denote the real and imaginary parts, respectively.

Then, the signal detection is conducted based on the statistical behavior of $\hat{\mathbf{r}}$ [62]. Note that cyclostationary detection assumes that T_0 is known *a priori*. This information about the PU signal behavior enables cyclostationary detection to distinguish the PU signal from noise and interference.

For simplicity, we focus here on the so-called single-cycle detector which refers to a detector with $L = 0$. In this case, the CAF estimation is derived as

$$\hat{R}_i^{(f_0)}(0) = \frac{1}{N}\sum_{m=0}^{N-1} |x_i(m)|^2 e^{-j2\pi f_0 m} \quad (15)$$

and the test statistic is [57]

$$u_i \triangleq |\hat{R}_i^{(f_0)}(0)|^2 \quad (16)$$

Assuming that N is large enough, $\hat{R}_i^{(f_0)}(0)$ follows a normal distribution. Replacing $x_i(m)$ with its model in (1), we obtain the mean and variance of $\hat{R}_i^{(f_0)}(0)$ under $\mathcal{H}_0$ and $\mathcal{H}_1$, i.e.,

$$E[\hat{R}_i^{(f_0)}(0)|\mathcal{H}_0] = 0 \quad (17)$$

$$\mathrm{Var}[\hat{R}_i^{(f_0)}(0)|\mathcal{H}_0] = \frac{\sigma^4}{N} \quad (18)$$

$$E[\hat{R}_i^{(f_0)}(0)|\mathcal{H}_1] = |h_i|^2 P_s^{(f_0)} \quad (19)$$

$$\mathrm{Var}[\hat{R}_i^{(f_0)}(0)|\mathcal{H}_1] = \frac{\sigma^2}{N}(2|h_i|^2 P_s + \sigma^2) \quad (20)$$

where $P_s^{(f_0)} \triangleq \frac{1}{N}\sum_{m=0}^{N-1} |s(m)|^2 e^{-j2\pi f_0 m}$ and $P_s \triangleq \frac{1}{N}\sum_{m=0}^{N-1} |s(m)|^2$.

Hence, when $\mathcal{H}_0$ is true, $\hat{R}_i^{(f_0)}(0)$ is a zero-mean complex-valued Gaussian random variable. Therefore, under $\mathcal{H}_0$, our test summary u_i follows a central χ^2 distribution with two degrees of freedom. When $\mathcal{H}_1$ is true however, $\hat{R}_i^{(f_0)}(0)$ is a complex-valued Gaussian random variable with nonzero mean which makes u_i follow a non-central χ^2 distribution. Therefore, when $\mathcal{H}_0$ is true we have,

$$\frac{u_i}{\sigma^2_{\mathcal{H}_0}} \sim \chi^2_2 \quad (21)$$

whereas under $\mathcal{H}_1$ we obtain

$$\frac{u_i}{\sigma^2_{\mathcal{H}_1}} \sim \chi^2_2(\eta_i) \quad (22)$$

where $\sigma^2_{\mathcal{H}_0} \triangleq \mathrm{Var}[\hat{R}_i^{(f_0)}(0)|\mathcal{H}_0]$ and $\sigma^2_{\mathcal{H}_1} \triangleq \mathrm{Var}[\hat{R}_i^{(f_0)}(0)|\mathcal{H}_1]$, while $\eta_i \triangleq \frac{|E[\hat{R}_i^{(f_0)}(0)|\mathcal{H}_1]|^2}{\sigma^2_{\mathcal{H}_1}}$. Consequently, the false alarm and detection probabilities of this detector are obtained as

$$P_{\mathrm{f}}^{(i)} = \Pr\{u_i > \gamma_i|\mathcal{H}_0\} = \int_{\gamma_i}^{\infty} f_{u_i}(x|\mathcal{H}_0)dx = e^{-\gamma_i/2\sigma^2_{\mathcal{H}_0}} \tag{23}$$

$$P_{\mathrm{d}}^{(i)} = \Pr\{u_i > \gamma_i|\mathcal{H}_1\} = \int_{\gamma_i}^{\infty} f_{u_i}(x|\mathcal{H}_1)dx = Q_1\left(\sqrt{\eta_i}, \frac{\sqrt{\gamma_i}}{\sigma_{\mathcal{H}_1}}\right) \tag{24}$$

where Q_1 is the first-degree Marcum Q-function.

3.2.3 Other Sensing Methods

There exist several other spectrum sensing methods which constitute a rich collection of signal processing tools to trade computational (and therefore, hardware complexity) for the detection performance. Applicability of these methods depends in general on how well the PU signal behavior is known *a priori*. Here we provide a brief explanation of two important sensing methods, i.e., *covariance-based detection* and *coherent detection*. A survey of existing spectrum sensing techniques can be found in [50, 51].

Covariance-based detection is a spectrum sensing method which exploits the correlation between the received PU signal samples. In this method, based on estimating the covariance matrix of the received signal samples, a decision variable is constructed and compared to a predefined threshold to decide the presence or absence of the PU signal. In general, when the PU is active the covariance matrix exhibits different features compared to the case in which the only received signal is the white noise. The decision variable can be considered as the ratio of the minimum and maximum eigenvalues of the covariance matrix, the ratio of its diagonal and off-diagonal elements, or its maximum eigenvalue. Clearly, performance of the covariance-based detection depends on how correlated the PU signal samples behave.

Coherent detection, a.k.a. wave-form-based sensing, is a spectrum sensing method based on detection of known patterns in the PU signal of interest. This method, which is capable of distinguishing the PU signal from the interference and noise, requires the availability of known patterns in the PU signal and is realized by matched filtering which is known to be the optimal detection method in such cases. Known patterns are usually utilized in wireless systems to assist synchronization or for other purposes. Such patterns include preambles, midambles, regularly transmitted pilot patterns, spreading sequences etc [51]. A preamble is a known sequence transmitted before each burst and a midamble is transmitted in the middle of a burst or slot.

Other alternative spectrum sensing methods include multitaper spectral estimation, wavelet transform based estimation, Hough transform, and time-frequency analysis [50, 51].

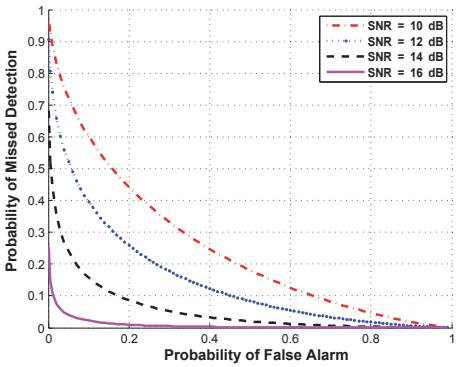

FIGURE 6 CROC curves representing performance of energy detection scheme in different SNRs.

3.2.4 Receiver Operating Characteristics

The receiver operating characteristics (ROC) curve is a graphical representation of the performance of signal detection schemes. This curve is derived by plotting the system detection probability against its false alarm probability for different values of the detection threshold. Equivalently, the same information regarding the system performance can be represented by a so-called complementary ROC (CROC) curve which depicts the system missed detection probability versus its false alarm probability. In this dissertation, we use the CROC curves to demonstrate the performance of spectrum sensing methods. It is clear that a spectrum sensing method with a better performance exhibits, in general, a CROC curve closer to the origin, i.e., closer to point $(0,0)$. As an example, note that we can remove γ_i from (11) and (12) and express the detection probability for a given false alarm probability of $P_{\mathrm{f}}^{(i)} = \alpha$ as

$$P_{\mathrm{d}}^{(i)}(\alpha) = Q\left(\frac{Q^{-1}(\alpha)\sqrt{\mathrm{Var}[u_i|\mathcal{H}_0]} - E[u_i|\mathcal{H}_1] + E[u_i|\mathcal{H}_0]}{\sqrt{\mathrm{Var}[u_i|\mathcal{H}_1]}}\right) \tag{25}$$

Now plotting $1 - P_{\mathrm{d}}^{(i)}$ for different values of α gives the CROC curve of the detector. Fig. 6 depicts the CROC curves of this detector for different SNR levels. We see that by increasing the SNR, the CROC curves get closer to the origin, indicating lower missed detection and false alarm probabilities.

3.3 Cooperative Spectrum Sensing

3.3.1 The Need for Cooperation

The performance of spectrum sensing can be severely degraded due to impairments such as shadowing and multipath fading associated with typical wireless

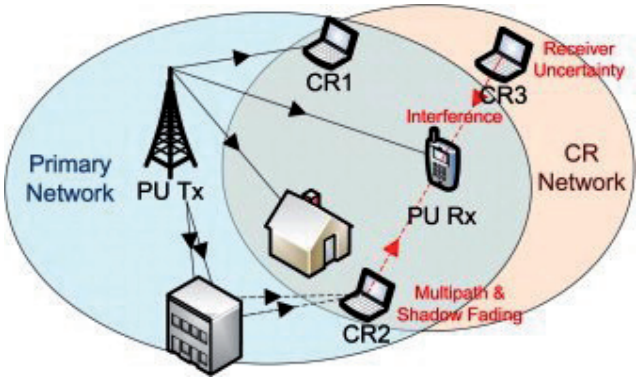

FIGURE 7 The hidden node problem in a CRN © 2011 IEEE.

environments. In fact, a CR may fail to detect the PU signal, even though it is present and active, since the PU may be hidden form the sensing CR node. Consequently, if not properly taken into account, the hidden node problem can cause severe interference on PUs. Fig. 7 illustrates this issue. In this figure, the PU transmitter is active and is transmitting PU signals to the PU receivers. CR1 is able to detect the PU signal and avoid interfering with it. However, since the signal level received by CR2, which is located within the range of the PU transmitter, is severely attenuated by shadowing and multipath fading, CR2 is not able to detect the PU signal and may perceive the situation as a transmission opportunity. CR3 may also misclassify the occupied spectrum as vacant, since it is located outside the range of the PU transmitter. Therefore, both CR2 and CR3 may cause interference on the PU receiver if they solely rely on their own spectrum sensing processes.

The hidden node problem can be mitigated by establishing cooperation among spatially-diverse sensing nodes in the CRN. In fact, cooperative spectrum sensing is known as an effective technique to maintain acceptable QoS levels for the SUs while protecting the PUs against harmful interference. In this way, that is when CRs share their sensing information with each other, the PU can be protected more reliably even when some of the sensing CR nodes are not able to properly detect the PU signal individually.

3.3.2 Network Configuration

Fig. 8 depicts general configuration of a centralized cooperative spectrum sensing [2]. There are K sensing CR nodes which use their own spectrum sensing module to sense the PU signal. These CR nodes send their sensing outcomes, u_i, $i = 1, \ldots, K$, through a nonideal but dedicated reporting channel to the FC where the received reports are combined and transformed into a decision variable based on a *fusion rule*. The decision variable, which is commonly referred to as *global test summary*, is then compared with a threshold to decide the presence or absence of the PU.

We collect the local sensing outcomes in vector $\mathbf{u} \triangleq [u_1, ..., u_K]^T$ and the

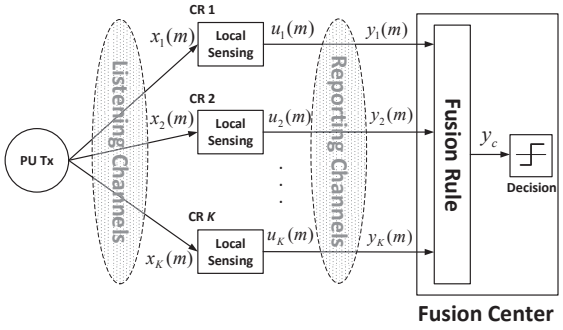

FIGURE 8 Basic configuration of centralized cooperative spectrum sensing.

received reports at the FC in $\mathbf{y} \triangleq [y_1, ..., y_K]^T$. It is clear that, due to reporting channel contaminations, the received reports are not necessarily equal to the local sensing outcomes transmitted to the FC. The fusion method incorporated at the FC can either be *soft-* or *hard-decision fusion*. Soft-decision fusion is when the sensing CR nodes directly report the data generated by their built-in sensor to the FC without making any local decision themselves. In this case, the FC processes a set of statistics received from the cooperating nodes to make the global decision. In hard-decision fusion, the global decision is still made by the FC, however, instead of local sensing outcomes, the sensing nodes report their local decisions about the presence or absence of the PU. These local decisions can be sent to the FC as one-bit binary signals consuming considerably lower communication resources allocated to the reporting phase. We know that the soft decision fusion scheme outperforms the hard decision fusion method at the expense of higher communication cost at the reporting phase. Note also that when sending the sensing outcomes to the FC through the reporting channels with a limited bandwidth, the CR nodes need to quantize this data. So the FC combines the quantized data received from the cooperating nodes in this case. This process is referred to as *quantized soft fusion*. In the following, we briefly explain the soft and hard fusion schemes. The quantized soft decision fusion method is thoroughly investigated in [PI].

3.3.3 Soft Fusion in Cooperative Sensing

The statistical behavior of the decision variable constructed at the FC depends in general on the joint probability distribution of the received reports $f(\mathbf{y})$ which, in turn, depends on the behavior of the reporting channel, characterized by $f(\mathbf{y}|\mathbf{u})$, as well as the statistical behavior of the local sensing outcomes specified by $f(\mathbf{u})$. The optimal fusion rule is found based on the NP test. In an NP test, the objective is to maximize the overall detection probability given the target false alarm probability of α, where α is referred to as the *significance level of the detector*. It is shown in [54] that the NP test is equivalent to the *likelihood-ratio test* (LRT) where

the decision variable, denoted Λ, is constructed and compared to a threshold as

$$\Lambda(\mathbf{y}) \triangleq \frac{f(\mathbf{y}|\mathcal{H}_1)}{f(\mathbf{y}|\mathcal{H}_0)} \underset{\mathcal{H}_0}{\overset{\mathcal{H}_1}{\gtrless}} \gamma_\Lambda \tag{26}$$

This test is computationally-expensive in the sense that, to find the optimal threshold γ_Λ we need to find the probability distribution function (PDF) of the decision variable Λ which, in turn, involves complicated multidimensional integrations. As an alternative to the LRT, *optimal linear combining* is commonly used as a low-complexity soft fusion rule with a very good performance [55, 56, 59, 63]. In this method, the received reports are combined linearly at the FC to form a global test summary y_c which is compared with a threshold to make the global decision, i.e.,

$$y_c \triangleq \mathbf{w}^T\mathbf{y} \underset{\mathcal{H}_0}{\overset{\mathcal{H}_1}{\gtrless}} \gamma_c \tag{27}$$

The main idea of linear combining is that the combining weight for the signal from a particular user represents its contribution to the global decision. For example, if a CR generates a reliable (i.e., high-SNR) signal that may lead to correct detection on its own, it should be assigned a larger weighting coefficient. For those SUs experiencing deep fading or shadowing, their weights are decreased in order to reduce their negative contribution to the decision fusion.

Assuming that the sensing CR nodes conduct energy detection with a large number of samples, u_i can be considered as a normal random variable. Hence, modeling the reporting media as AWGN channels between the FC and the CR, we can conclude that y_i is also a normal random variable. Consequently, the global test summary y_c follows a normal distribution with the mean and variance represented (for $h = 0, 1$) by

$$E[y_c|\mathcal{H}_h] = \mathbf{w}^T\boldsymbol{\mu}_{\mathbf{y}|\mathcal{H}_h} \tag{28}$$

$$\mathrm{Var}[y_c|\mathcal{H}_h] = \mathbf{w}^T\mathbf{C}_{\mathbf{y}|\mathcal{H}_h}\mathbf{w} \tag{29}$$

where $\boldsymbol{\mu}_{\mathbf{y}|\mathcal{H}_h} \triangleq E[\mathbf{y}|\mathcal{H}_h]$ and $\mathbf{C}_{\mathbf{y}|\mathcal{H}_h} \triangleq E[(\mathbf{y} - \boldsymbol{\mu}_{\mathbf{y}|\mathcal{H}_h})(\mathbf{y} - \boldsymbol{\mu}_{\mathbf{y}|\mathcal{H}_h})^T|\mathcal{H}_h]$. Consequently, the overall detection and false alarm probabilities are derived as

$$P_\mathrm{f} = \Pr\{y_c > \gamma_c|\mathcal{H}_0\} = Q\left(\frac{\gamma_c - \mathbf{w}^T\boldsymbol{\mu}_{\mathbf{y}|\mathcal{H}_0}}{\sqrt{\mathbf{w}^T\mathbf{C}_{\mathbf{y}|\mathcal{H}_0}\mathbf{w}}}\right) \tag{30}$$

$$P_\mathrm{d} = \Pr\{y_c > \gamma_c|\mathcal{H}_1\} = Q\left(\frac{\gamma_c - \mathbf{w}^T\boldsymbol{\mu}_{\mathbf{y}|\mathcal{H}_1}}{\sqrt{\mathbf{w}^T\mathbf{C}_{\mathbf{y}|\mathcal{H}_1}\mathbf{w}}}\right) \tag{31}$$

Removing γ_c from (30) and (31) for a target false alarm probability $P_\mathrm{f} = \alpha$, we have

$$P_\mathrm{d}^{(\alpha)}(\mathbf{w}) = Q\left(\frac{Q^{-1}(\alpha)\sqrt{\mathbf{w}^T\mathbf{C}_{\mathbf{y}|\mathcal{H}_0}\mathbf{w}} - \mathbf{a}^T\mathbf{w}}{\sqrt{\mathbf{w}^T\mathbf{C}_{\mathbf{y}|\mathcal{H}_1}\mathbf{w}}}\right) \tag{32}$$

where $P_{\mathrm{d}}^{(\alpha)}$ denotes the detection probability given the false alarm probability of α and $\mathbf{a} \triangleq \boldsymbol{\mu}_{\mathbf{u}|\mathcal{H}_1} - \boldsymbol{\mu}_{\mathbf{u}|\mathcal{H}_0}$. The system performance is then optimized by finding a $\mathbf{w}$ which maximizes $P_{\mathrm{d}}^{(\alpha)}$. This optimization can be solved either by applying the Karush-Kuhn-Tucker (KKT) conditions [59] or by the quadratic programming techniques [63].

3.3.4 Hard Fusion in Cooperative Sensing

Regarding the hard-decision-based cooperative sensing, it is shown in [64] that when the reporting facility comprises nonideal analogue communication channels between the distributed nodes and FC, the globally-optimal structure is to perform the LRT both at individual nodes and at the FC. However, how to efficiently find the optimal LRT thresholds for individual nodes and for the FC is still unknown, see [56, 64].

Several suboptimal decision fusion methods have been introduced and investigated in the literature. In these methods, the global test summary is built at the FC as a binary variable whose value is obtained by a logic operation on the received local binary decisions. This logic operation can be an OR function, an AND operation, a majority fusion rule or, more generally, a so-called k-out-of-N fusion rule[2] [50, 65]. With the OR fusion rule, the global sensing outcome is 1, indicating (let's say) the presence of the PU, if at least one of the received local decisions is 1. The AND fusion rule indicates that the global decision is 1 only when all the received reports are 1. As clarified by the name, in a cooperative sensing with the majority fusion rule, the global decision is the case supported by the majority of the sensing nodes. Note that the OR, AND, and majority fusion rules are all special cases of the k-out-of-N fusion method in which the global sensing outcome is 1 when at least k out of N received reports indicate 1 as the local decision. The performance of different hard-decision fusion rules in the presence of reporting channel errors is investigated in [65] where it is shown that the majority rule outperforms other commonly-used hard fusion methods in cooperative sensing with erroneous reporting channels.

It is worth noting that, the binary symmetric channel (BSC) is a common choice for modeling the reporting facility in analyzing the hard-decision-based as well as quantized soft-decision-based cooperation. By using the BSC the effect of reporting channel impairments on the overall sensing performance is captured into the system model by the notion of reporting bit error probability (BEP), as it is a convenient and widely applicable method to model the end-to-end performance of the system including the transmitter, the channel, and the receiver [65].

---

[2] N refers here to the number of cooperating nodes.

4 TRADEOFFS IN SPECTRUM SENSING

4.1 Introduction

As we have seen so far, the performance of CRNs significantly depends on the effectiveness of their spectrum sensing while the spectrum sensing performance itself depends in general on several factors including the SU needs, affordable hardware complexity, the radio environment, and the PU behavior. Generally speaking, the design of reliable spectrum sensing often involves conflicting requirements which need to be taken into account in the form of tradeoffs formulated as optimization problems. In this chapter, we investigate several design issues in spectrum sensing for CRs and introduce a number of important challenges which need to be addressed properly in order to realize effective and efficient spectrum sensing.

We first focus on the local spectrum sensing process and investigate the problem of the sensing time optimization. This investigation involves addressing the throughput-energy tradeoff in CRNs while taking into account two fundamental processes, namely, *spectrum mobility* and *spectrum handover*. We have discussed these concepts in [PVI] where their effects on the throughput and energy consumption of CRs are analyzed and formulated. Specifically, we construct an optimization problem which aims at finding the best sensing time in a CRN with spectrum mobility. In this analysis, we find the overall average throughput of a CR system which incorporates the energy detection and *sequential spectrum sensing* method to find spectrum holes among N_p channels allocated to the PUs. We also find the average number of spectrum handovers required to find a transmission opportunity and take into account, in the proposed optimization, the energy consumed for spectrum sensing and for spectrum handover. Consequently, the proposed optimization enables the SU to have control over its consumed energy and the achieved average throughput. Further details are provided in Section 4.2.

Next, we work on the centralized cooperative spectrum sensing. In particular, we analyze the overall detection performance considering the effect of three fundamental processes as *i)* quantization of the sensing outcomes at the CR

nodes, *ii)* reporting the quantized sensing outcomes to the FC, and *iii)* the fusion rule at the FC. The quantization process prepares the sensing outcomes at CR nodes to be sent to the FC through a reporting channel with limited capacity. Our analytical and simulation-based investigations reveal that increasing the quality of local quantization does not necessarily lead to a better overall detection performance since there is a tradeoff between the local quantization quality and the degradation caused by the reporting channel. Formulation of this tradeoff in an NP setting allows us to propose a better cooperative sensing scheme which comes as a benefit for better exploitation of the spatial/user diversities in CRNs. In addition, we extend the notion of deflection coefficient to take into account the impact of the number of quantization levels used at the sensing nodes jointly with optimal linear combining at the FC. The extended deflection coefficient provides a practically-appealing fast suboptimal solution for the proposed joint optimization. Further details are provided in Section 4.3.

In studying cooperative sensing schemes, we develop our formulations based on the optimal linear combining method. Linear fusion is a widely-used method and this popularity mainly stems from two important factors, the ease of implementation and the close-to-LRT performance. We redesign the optimal linear combining scheme from a different perspective aiming at more efficient use of the available signal processing and communication resources in CRNs. In particular, we show that the idea of discriminating between the different sensing nodes by assigning different weights to their received reports is not an efficient approach. We then develop a new idea to realize the discrimination in a more efficient way and propose a new cooperative sensing structure which outperforms the existing ones by better utilization of the available resources. This new design is based on two mechanisms added to the commonly-used cooperation structure. Specifically, the first mechanism is realized as a set of random energy-saving interruptions in the cooperation between the sensing CR nodes and the FC, while the second mechanism is a compensation process at the FC. This compensation, which is realized as a linear estimator, aims at recovering the local test summaries out of degradations caused jointly by the interruptions and reporting channel contaminations. The estimation of the local test summaries is realized in the proposed system by using the spatio-temporal cross-correlations of the sensor outcomes as well as auto-covariance functions characterizing the behavior of the reporting channels. Through comprehensive analytical investigations, novel optimization procedures, and extensive simulations, we show that this new structure can significantly improve the efficiency in utilizing the available resources in CRNs which employ centralized cooperative spectrum sensing. Although the idea of random interruptions is developed by investigating the linear cooperation structure, the results obtained are not constrained to this particular cooperation scheme. The use of linear fusion and linear estimation processes at the FC does not limit the applicability scope of the proposed idea and is only for maintaining tractability in the proposed analysis and optimization. Further details are provided in Section 4.4.

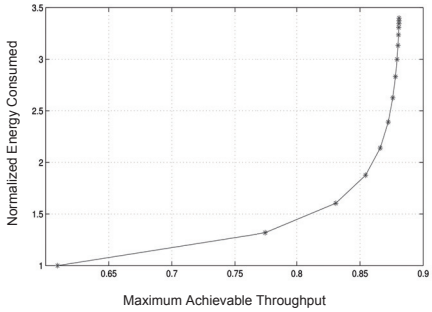

FIGURE 9 Energy consumed by a sensing CR vs. the maximum throughput achieved.

4.2 The Sensing-Throughput Tradeoff

In this section, we discuss the effect of spectrum mobility and spectrum handover on the energy-throughput tradeoff in CRNs. Spectrum mobility refers to the dynamic availability of transmission opportunities in a CRN due to the dynamic behavior of the PUs, while spectrum handover, or simply handover (HO), is used to describe the process of vacating a spectrum band and switching to another white space when a PU arrives. Taking these two important factors into account, we propose a new formulation of the problem of spectrum sensing time optimization in CRNs. In the proposed modeling and optimization we assume that the SU performs *sequential channel sensing* in order to find the next available white space. The sequential channel sensing means that the SU starts sensing the channels from the top of a list, referred to as the *sensing sequence*, and if the channel considered is sensed as occupied, then the SU senses the next one and this process is continued until an idle spectrum is found. We formulate the average throughput maximization of an SU by optimizing its spectrum sensing time, assuming that *a priori* knowledge of the presence and absence probabilities of the PUs is available. More specifically:

> *We formulate the throughput of an SU in terms of its sensing time duration when the spectrum mobility and consequent HOs affect the SU performance. In addition, the energy cost of HOs is considered in the proposed modeling in order to address the energy-throughput tradeoff encountered in designing portable and/or green CR systems.*

Consequently, we evaluate the energy consumed to find a transmission opportunity, and discuss the impact of the number of PU channels on the SU achievable throughput and its consumed energy. In particular, we show that, see Fig. 9, there is a saturation behavior in the relationship between the spectrum sensing time and the throughput achieved by an SU. Hence, we show that:

> *At the cost of a small reduction in the maximum throughput, the consumed energy of a CR can be substantially decreased. We use this saturation effect to increase the energy efficiency of the spectrum sensing in CRNs.*

We propose a learning-based approach for solving the proposed optimization. We first decompose the spectrum sensing time optimization into two distinct parts as *i)* obtaining the mapping between the sensing time and the SU throughput and *ii)* finding the optimum value for the sensing time based on the derived mapping. For the first part, we use a *multilayer feedforward neural network* [15] which learns the mapping between the parameters of interest and for the second part we use a *Kennedy-Chua neural network* [14] which finds the optimal sensing time based on the learned mapping. The neural-network-based method proposed has several advantages over an analytical solution. These advantages can be summarized as:

> *First, no prior knowledge about the link behavior, such as the presence or absence probabilities of the PUs is required. Second, the limited consistency of the mathematical models with the real wireless environment does not affect the optimality of the derived spectrum sensing time. And third, by using this learning-based optimization scheme, an adaptive system is proposed which is capable of effectively following the variations in the link and keeping the average throughput at the maximum level in non-stationary conditions.*

4.3 Joint Local Quantization and Linear Cooperation

As mentioned before, cooperative sensing in CRNs is often concerned with three different phases; local sensing, reporting, and decision/data fusion. Since the overall detection performance is affected in general by the joint effect of all the elements involved, enhancing the performance quality of a certain phase does not necessarily lead to a better overall detection performance. Consequently, a joint design of the different phases, taking into account their joint impact on the overall detection performance, can lead to a better cooperation structure. We show the effectiveness of this design strategy in [PI] by joint consideration of all the three phases. In particular, we identify, analyze, and take into account the following tradeoff:

> *For a given set of radio resources dedicated to the reporting phase in terms of transmission power and bandwidth, increasing the number of quantization bits influences the overall sensing performance in two opposite directions. Specifically, on one side, increasing the number of quantization levels leads to a better quantization process and consequently, lowers the quantization errors affecting the reported local sensing outcomes, improving the cooperation performance. On the other side however, increasing the quantization bits raises the BEP induced by the reporting channels and reduces the received sensing outcomes quality at the FC, degrading the overall sensing performance.*

Fig. 10 shows the basic configuration and major elements of the cooperative sensing in detail. K CR nodes cooperate for spectrum sensing by reporting their sensing outcomes to an FC through an erroneous digital channel. As shown in Fig. 10,

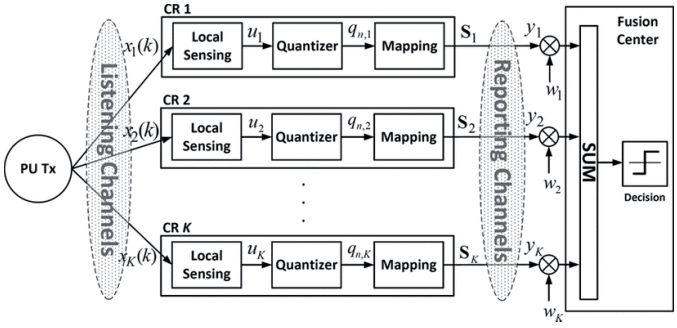

FIGURE 10 Linear fusion of quantized reports in cooperative sensing.

our analysis considers the joint impact of the following processes in detail: local sensing, quantization, mapping the quantizer outputs onto bit strings, transmission of the bit strings to the FC, and the linear fusion process along with the decision-making at the FC. Through considering all these elements, we develop solid understanding of the role of different components in a cooperative spectrum sensing and address this particular problem:

> *How precisely the local sensing outcomes should be quantized at each node, and how to linearly combine the received statistics at the FC, when the reporting facility is a digital communication link with a given bandwidth and transmission power?*

In order to properly address this question, we develop a new model for analyzing the reporting channel contaminations and, based on this model, we provide a comprehensive set of mathematical relations for evaluating the reporting channel effect on the bit sequences generated by an arbitrary mapping process. In particular:

> *The proposed analysis leads to exact as well as practical approximate relationships describing the joint impact of the quantization, reporting, and linear fusion processes.*

Based on these results, we formulate the system performance optimization in an NP setting and develop a computationally-efficient solution for it. The proposed optimization is a MINLP problem. We develop its solution as a fast BnB procedure which is based on the convex hull relaxation of the nonlinear factors in the derived new formulations. It is worth noting that, the BnB procedure is a standard method for solving MINLPs and it has been shown that under very general conditions, a BnB solution procedure always converges [66, 67]. Moreover, although the worst-case complexity of such a procedure is exponential, the actual running time is fast when all partition variables are integers. In addition, we extend the notion of deflection coefficient to accommodate the proposed joint optimization [PI, PII]. In particular, we have developed fast deflection-based suboptimal solutions for the proposed problem. The computational complexity of these solutions increases linearly with the number of sensing nodes involved in cooperation. Therefore:

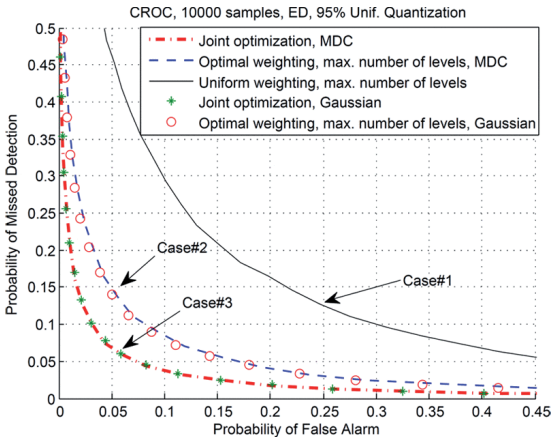

FIGURE 11 Performance of the proposed joint reporting-fusion optimization scheme compared with the optimal linear combining.

We provide a complete set of solutions which are practical, and scientifically-appealing even when dealing with large-scale networks.

We evaluate the proposed system performance by a comprehensive set of simulations. In these simulations, three distinct cases are considered as:

Case#1: Uniform linear combining at the FC and maximum number of quantization bits at the sensing nodes.

Case#2: Optimal linear combining at the FC and maximum number of quantization bits at the sensing nodes.

Case#3: The proposed joint optimization, i.e., optimal linear combining at the FC and optimal number of quantization bits at the sensing nodes.

Case#1 corresponds to a system design with no optimization involved. Equal weights are used at the FC and the quantization is performed based on the maximum number of bits available. This case plays the role of a baseline in our performance comparisons. In *Case#2* optimization only concerns the fusion process. This case represents the existing works in [55, 56, 59]. We aim at showing that this optimization is not comprehensive enough since it ignores the effect of local quantization at the sensing CR nodes. *Case#3* represents the proposed design which takes into account the local quantization jointly with its effect of reporting degradations and the fusion rule at the FC.

As depicted in Fig. 11, the system performance in each case is illustrated by their corresponding CROC curves. We see in this figure that the proposed method leads to significant performance gains compared to the existing methods. This better performance is due to that fact that, in the proposed design the spatial/user diversities regarding the listening and reporting channels are considered in a more comprehensive optimization approach.

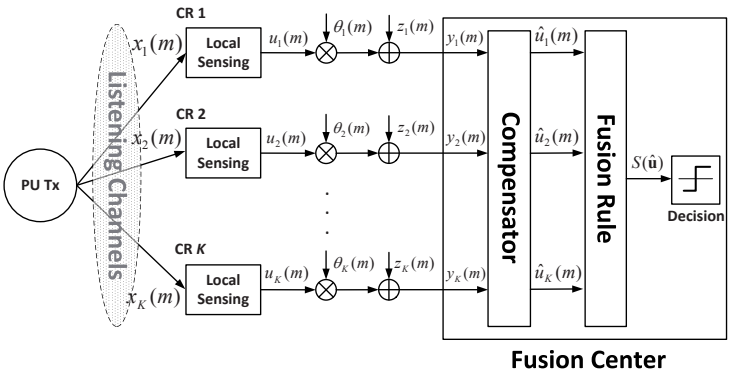

FIGURE 12 Random interruptions in cooperation for spectrum sensing.

4.4 Random Interruptions in Cooperation

In this section, we discuss how to increase efficiency in utilizing the available resources when designing centralized cooperative sensing schemes for CRNs. We know that in order to achieve a better cooperation performance, it is necessary to discriminate between the reliable and unreliable sensing nodes. This discrimination is commonly achieved by a linear fusion method which linearly combines the received reports while assigning different weights to the reports from different sensing nodes. In this fusion method, by assigning higher weights to the more reliable sensing nodes, their impact on the global decision is emphasized, whereas the degrading effect of the unreliable reports is suppressed by assigning relatively smaller weights to the nodes operating under deep fading or shadowing. Although linear combining is known to be an effective and computationally-affordable technique in designing cooperative sensing schemes, it is not energy-efficient. In particular, we point out the following issue with the linear fusion scheme in cooperative sensing:

> *Regardless of the channel conditions experienced by different sensing nodes, they all provide their sensing outcomes at the same cost which manifests itself as the energy consumed during the local sensing and reporting phases. When the contribution of a particular node to the global decision is suppressed by assigning a small weight to it, the energy and signal processing resources consumed by that node for the local sensing and reporting processes are relatively wasted.*

We propose in [PIV] a more efficient method to realize the required discrimination between the sensing nodes which experience different channel conditions. Fig. 12 shows the proposed cooperation structure (for comparison, see Fig. 8). In this method, instead of suppressing the contribution of nodes working under deep fading or shadowing, they are occasionally ordered not to cooperate. This interruption is modeled by a set of binary random variables—depicted in Fig. 12 as θ_i, $i = 1, 2, ..., K$—multiplied by the sensing outcomes. These random numbers

control the behavior of the sensing nodes, i.e., a CR node performs the local sensing and reporting processes in a time slot only when the corresponding random number is 1 in that time slot. Otherwise, the CR saves its energy and signal processing resources during that time slot by going to a sleep mode. By switching the sensing nodes on and off we can save considerable energy in general, however, we are deliberately imposing degradations on the reported sensing outcomes as well. We compensate for these degradations by adding an estimation process to the FC. This estimation process, depicted as *compensator* in Fig. 12, aims at recovering the reported sensing outcomes out of degradations caused jointly by the random interruptions and reporting channel contaminations. In this structure, the more reliable a sensor, the more likely it is to contribute to the overall sensing process.

We model and thoroughly analyze the proposed system to derive the global test summary statistics in terms of probability distributions of the random interruptions. By using the statistics obtained, we formulate the proposed system performance optimization according to the NP and deflection criteria. Specifically, first, we analyze the global test summary statistics and characterize the system performance by providing closed-form relations for the probability of false alarm and the probability of detection. We then derive the detection threshold for a fixed false alarm probability and formulate the system performance optimization, in the NP setting, subject to a constraint on the energy consumed at the local sensing and reporting phases. Consequently, we formulate a significant tradeoff concerning the overall detection quality along with the joint energy consumption of the local sensing and reporting phases. We discuss that the obtained optimization is a stochastic program with prohibitive computational complexity and then, we consider the optimization as a decision-making process with uncertainty. By using this decision-making structure, we show the link between the NP and deflection criteria for the proposed cooperative sensing structure.

Regarding the deflection criterion, we formulate the performance optimization as a convex-over-convex fractional programming problem. This fractional program, which is solved by a BnB algorithm, gives the optimal distributions of the random interruptions for maximizing the overall detection performance, subject to a constraint on the energy consumed at the local-sensing and reporting phases. Through delicate algebraic manipulations, we convert the fractional program into a set of nonconvex QCQPs whose solution can be obtained in polynomial time by using standard techniques in nonconvex quadratic programming. Therefore, we construct an effective low-complexity method for solving the proposed optimization even when dealing with a large number of sensing nodes. Based on these investigations, we obtain the following results:

> *The required discrimination between the reliable and unreliable sensors is achieved by the proposed interruption-compensation structure while significant savings in the available resources can be achieved. This efficiency is obtained by optimizing the random-interruptions-based cooperation considering a constraint on the energy consumed in the local sensing and reporting phases. More specifically, we*

find optimal distributions associated with the random number generators, assuming a general linear fusion rule at the FC. In addition, we discuss and highlight the differences between the proposed method and the existing energy-efficient cooperation schemes and justify that the proposed method outperforms the commonly-used energy-efficient methods, such as censoring-based methods and sensor selection/scheduling algorithms, by better utilizing the available resources.

In addition, we formulate the joint optimization of the reporting and fusion phases in the proposed interruption-based cooperation [PV]. This optimization aims at finding the best weights used at the FC to construct a linear fusion of the received interrupted reports, jointly with the best Bernoulli distributions governing the statistical behavior of the interruptions. We construct this new problem by using the deflection criterion and as a nonconvex quadratic program which can be solved for a good suboptimal solution, in polynomial time complexity, by a semidefinite relaxation technique. We then demonstrate the proposed system performance by a set of simulation results which compare the performance of the system for the cases with and without the optimal linear fusion. The results obtained by this joint optimization demonstrate that:

When random interruptions are employed, there is no more need for discriminating between the reliable and unreliable nodes by the fusion process.

5 SUMMARY

Significant levels of flexibility and adaptability are realized in wireless networks by employing the CR technology which is developed through adding certain artificial-intelligence-based capabilities, such as self-awareness, context-awareness, and machine learning, to software-defined radios. Due to these prominent capabilities, CR has been of great interest in developing more efficient wireless communications for various applications. In fact, wireless cellular communications, public safety networks, smart grid, and wireless body area networks can be named as some of the major applications of this new promising communication paradigm.

Spectrum sensing is the key capability in the CR systems and enables the SUs to get informed about their radio environment and establish communication without having any particular spectrum band assigned to them. The design of reliable spectrum sensing in CRNs often requires dealing with contradictory requirements which are represented and accounted for in the form of optimization problems. These optimizations are constructed in general based on mathematical modeling of the radio environment, the PU behavior and its signal characteristics, and the target false alarm and detection probabilities. The optimizations involved are often in nonlinear/nonconvex forms which make it a challenge to develop a solution with affordable complexity. Therefore, a major step in developing efficient and effective spectrum sensing schemes is to use proper tools from the optimization theory and construct a scalable solution for the problem.

5.1 Conclusions

In this dissertation, we have identified and thoroughly investigated a number of important tradeoffs in spectrum sensing for CRNs. We have considered all the major phases in cooperative spectrum sensing, i.e., the local sensing, reporting, and fusion processes. We have modeled and evaluated the joint impact of different parameters in cooperative sensing on the overall detection performance and

developed novel design methods to increase the effectiveness and reliability of the spectrum sensing. In particular, the following items constitute a summarizing list of the results obtained:

- We have addressed the sensing-throughput tradeoff in a CR system with the sequential spectrum sensing by formulating the SU throughput in terms of its sensing time duration while taking into account the energy cost of spectrum handovers due to the spectrum mobility effect of the radio environment. Accordingly, we have provided an analytical and a learning-based method for spectrum sensing time optimization in CRNs. We have shown that at the cost of a small reduction in the maximum throughput, the consumed energy of a CR can be substantially decreased.

- After providing a structured study of major phases in a centralized cooperative sensing scheme, we have introduced the effect of the number of bits used in local sensing quantization on the overall sensing performance in a CRN with cooperative sensing. We have then proposed a joint optimization approach to optimize the linear soft-combining scheme at the fusion phase with the number of quantization bits used by each sensing node at the reporting phase. The presented analytical expressions followed by simulation results demonstrate that, through joint consideration of the reporting and fusion phases in a cooperative sensing scheme, considerable performance gains can be obtained. This better performance stems from better exploitation of spatial/user diversities in CRNs. The proposed joint optimization scheme leads to more powerful distributed detection performance, especially when the sensing nodes have to work at low SNR regimes.

- We have proposed an extension to the deflection coefficient which captures the effects of the quantization processes at the sensing nodes, jointly with the impact of the linear combining at the FC. The proposed parameter has been used to formulate a new MINLP problem as a fast suboptimal method to design a distributed detection scenario where the nodes report their sensing outcomes to a FC through nonideal digital links. Numerical results demonstrate the effectiveness of the proposed design approach.

- We have proposed a novel energy-efficient structure for spectrum sensing in CRNs based on making random interruptions in the cooperation process among the CRs. We have thoroughly modeled and analyzed the proposed system behavior, and developed an optimization problem in order to formulate a tradeoff taking into account the energy consumption at the local sensing and reporting processes jointly with the overall detection performance. Analytical solution of the optimization problem and the presented numerical results demonstrate that, significant levels of energy efficiency can be achieved by the proposed architecture. This energy efficiency is due to the fact that, unlike in existing cooperative sensing schemes, in the pro-

posed design the discrimination between reliable and unreliable nodes is obtained while no energy is wasted. Moreover, we have shown that, the sensitivity of the overall detection to degradations in the local sensing and reporting processes is significantly reduced by the proposed architecture, leading to a more reliable cooperative spectrum sensing.

– We have jointly optimized the reporting and fusion phases of cooperative spectrum sensing scheme with linear fusion at the FC and random interruptions in cooperation of the sensing nodes with the FC. The results achieved based on maximizing the modified deflection coefficient in this system demonstrate that, when random interruptions are employed, there is no more need for discriminating between the reliable and unreliable nodes by the fusion process, and the equal-gain combining scheme at the FC is enough to nearly have the optimal overall detection performance.

5.2 Future Research

There exist numerous possibilities for future research based on the findings presented in this dissertation. In the following, we provide some cases which can be investigated in future:

Multiband cooperative sensing with random interruptions: Extension of the proposed random-interruptions-based cooperation to multiband cooperative spectrum sensing is an interesting research question to be investigated. More specifically, formulation of the performance of the centralized cooperative sensing in a multiband joint detection scenario with random interruptions can be considered as a direct extension of the analysis provided in [PIV]. This investigation aims at finding the aggregate opportunistic throughput [55] of the CRN on a (typically) wide range of frequency bands along with the aggregate interference experienced by the PUs operating on those bands. Then, the system performance is optimized by maximizing the aggregate opportunistic throughput subject to a constraint on the aggregate interference, while restricting the energy and signal processing resources consumed to stay below a certain threshold.

Hard-decision fusion with random interruptions in cooperative sensing: Since the hard-decision fusion is a commonly-used method in cooperative sensing schemes for CRNs, developing analytical foundations for implementing the proposed random interruptions in a hard-fusion-based cooperation could be an interesting future work providing important tools for realizing the proposed energy efficient cooperation in a variety of commonly-used detection scenarios. In this research, the notion of random interruptions will be extended to cooperative sensing schemes where the sensing nodes report to the FC their local decisions of the presence and absence of the primary user signal. In particular, analyzing the system behavior, finding closed-form relations for the system detection and false alarm probabilities, and establishing the system performance optimization in an

NP setting are the expected research results.

Network lifetime optimization in cooperative spectrum sensing with random interruptions: Fair and effective distribution of the load of spectrum sensing among the cooperating nodes is of critical importance in designing CRNs. In this research, first, the effect of random interruptions in extending the network lifetime is taken into account by formulating an optimization problem to minimize the energy consumption of the sensing nodes while maintaining a predefined cooperative sensing quality. Then, based on this optimization problem, the tradeoff between the network lifetime and fairness in distributing the sensing load among the cooperating nodes is investigated by considering well accepted, axiomatically-justified notions of fairness such as the proportional fairness and max-min fairness [68]. The results obtained from this research are expected to provide valuable guidelines for researchers and system designers in incorporating the random interruptions more effectively.

Security in DSA infrastructures: Considering the fact that the main source of security threats in a distributed CRN setting is manipulation of the spectrum sensing process by the adversaries [69], the knowledge developed in this dissertation provides an excellent foundation for more investigations towards mitigating the security threats in DSA networks. Currently, there exist several open research topics concerning the security of DSA networks. For instance, the security and reliability tradeoff in wireless communications in the presence of eavesdropping attacks is still an open issue [70]. In addition, there are several security attacks identified in several layers and cross-layer designs taking into account these threats are currently of great importance. Energy efficient and low-complexity security algorithms are desirable to make the CR technology a viable solution for the future generation wireless communications and achieving these features with highly robust cross-layer security mechanisms is still a very demanding topic of research [70]. Since the models and analyses presented in this dissertation provide a deep insight into the role and impact of the key components in spectrum sensing, they can be used in future to better investigate these open issues.

YHTEENVETO (FINNISH SUMMARY)

Tulevaisuuden kognitiiviradioverkoissa on tärkeää kerätä tietoa ympäröivästä radioympäristöstä, kuten siitä mitkä taajuudet ovat kulloinkin varattuina ja mitkä vapaina käytettäviksi tiedonsiirtoon. Tätä tilannetiedon keräämistä kognitiiviradioverkoissa kutsutaan yleisesti spektrin aistinnaksi, jonka luotettavuus on välttämätön ehto luotettavalle ja tehokkaalle tiedonsiirrolle. Tässä väitöskirjassa tutkitaan tapoja parantaa spektrin aistinnan onnistumista ja siihen käytettävää energiaa. Erityisesti tutkitaan nk. keskitettyä yhteistyöhön perustuvaa aistintaa, jossa monet spektriä aistivat radiot lähettävät aistintainformaationsa keskitettyyn päätelaitteeseen tai verkkoelementtiin fuusioitavaksi ja näin ollen osallistuvat yhteistyöhön vapaan taajuuden etsinnässä. Tutkimuksessa otetaan huomioon kaikki olennaiset vaiheet koko prosessissa kuten itse aistinta, tulosten raportointi eteenpäin radioteitse ja lopuksi päätöksenteko datafuusion jälkeen. Näin ollen tutkimuksessa spektrin aistinta analysoidaan ja optimoidaan kokonaisena prosessina, poiketen näin siitä muusta alan laajasta tutkimuksesta, jossa yleensä optimoidaan jokin yksittäinen prosessin vaihe. Tutkimuksen tuloksina saavutettiin useita rakenteita, joilla spektrin aistintaa voidaan parantaa kokonaisuutena joko suorituskyvyn tai aistintaan käytettävän energiankulutuksen suhteen. Kyseiset suorituskyvyt ja niiden parannukset esitetään niin analyyttisesti kuin monin numeerisin esimerkeinkin.

REFERENCES

[1] *Climate Change 2013: The Physical Science Basis. Contribution of Working Group I to the Fifth Assessment Report of the Intergovernmental Panel on Climate Change*. Cambridge, United Kingdom and New York, NY, USA: Cambridge University Press, 2013.

[2] I. F. Akyildiz, B. F. Lo, and R. Balakrishnan, "Cooperative spectrum sensing in cognitive radio networks: A survey," *Elsevier Physical Communications*, vol. 4, no. 1, pp. 40–62, March 2011.

[3] Z. Hasan, H. Boostanimehr, and V. Bhargava, "Green cellular networks: A survey, some research issues and challenges," *Communications Surveys Tutorials, IEEE*, vol. 13, no. 4, pp. 524–540, Nov. 2011.

[4] E. Hossain, D. Niyato, and D. I. Kim, "Evolution and future trends of research in cognitive radio: a contemporary survey," *Wireless Communications and Mobile Computing*, no. 11, pp. 1530–1564, 2015.

[5] S. Boyd and L. Vandenberghe, *Convex optimization*. New York, NY, USA: Cambridge University Press, 2004.

[6] Z.-Q. Luo, W.-K. Ma, A.-C. So, Y. Ye, and S. Zhang, "Semidefinite relaxation of quadratic optimization problems," *IEEE Signal Processing Magazine*, vol. 27, no. 3, pp. 20–34, May 2010.

[7] K. M. Anstreicher, "Semidefinite programming versus the reformulation-linearization technique for nonconvex quadratically constrained quadratic programming," *Journal of Global Optimization*, vol. 43, no. 2-3, pp. 471–484, 2009.

[8] X. Bao, N. V. Sahinidis, and M. Tawarmalani, "Semidefinite relaxations for quadratically constrained quadratic programming: A review and comparisons," *Mathematical Programming*, vol. 129, no. 1, pp. 129–157, 2011.

[9] P. Belotti, J. Lee, L. Liberti, F. Margot, and A. Wachter, "Branching and bound tightening techniques for non-convex MINLP," *IBM Research Report*, Aug. 2008.

[10] S. Burer and A. N. Letchford, "Non-convex mixed-integer nonlinear programming: a survey," *Surveys in Operations Research and Management Science*, vol. 17, no. 2, pp. 97–106, 2012.

[11] H. P. Benson, "Maximizing the ratio of two convex functions over a convex set," *Naval Research Logistics*, vol. 53, no. 4, pp. 309–317, June 2006.

[12] A. Shapiro, D. Dentcheva *et al.*, *Lectures on stochastic programming: modeling and theory*. SIAM, 2014, vol. 16.

[13] J. E. Dayhoff, *Neural network architectures: an introduction*. Van Nostrand Reinhold Co., 1990.

[14] M. P. Kennedy and L. O. Chua, "Neural networks for nonlinear programming," *IEEE Transactions on Circuits and Systems*, vol. 35, no. 5, pp. 554–562, 1988.

[15] T. L. Fine, *Feedforward Neural Network Methodology*, 1st ed. New York: Springer, 1999.

[16] B. Wang and K. Liu, "Advances in cognitive radio networks: A survey," *IEEE Journal of Selected Topics in Signal Processing*, vol. 5, no. 1, pp. 5–23, 2011.

[17] I. F. Akyildiz, W.-Y. Lee, M. C. Vuran, and S. Mohanty, "A survey on spectrum management in cognitive radio networks," *IEEE Communications Magazine*, vol. 46, no. 4, pp. 40–48, 2008.

[18] ——, "Next generation/dynamic spectrum access/cognitive radio wireless networks: a survey," *Computer Networks*, vol. 50, no. 13, pp. 2127–2159, 2006.

[19] S. Haykin, "Cognitive radio: brain-empowered wireless communications," *IEEE Journal on Selected Areas in Communications*, vol. 23, no. 2, pp. 201–220, 2005.

[20] Q. Zhao and B. M. Sadler, "A survey of dynamic spectrum access," *IEEE Signal Processing Magazine*, vol. 24, no. 3, pp. 79–89, 2007.

[21] Y. Zeng, Y. Liang, S. W. O. Z. Lei, F. Chin, and S. Sun, "Worldwide regulatory and standardization activities on cognitive radio," in *Proc. IEEE DySPAN 2010*, Washington DC, April 6-9 2010, pp. 1–9.

[22] E. Pietrosemoli and M. Zennaro, *TV White Spaces, a Pragmatic Approach*. ICTP-The Abdus Salam International Centre for Theoretical Physics. Trieste, 2013.

[23] O. Holland, S. Ping, A. Aijaz, J. M. Chareau, P. Chawdhry, Y. Gao, Z. Qin, and H. Kokkinen, "To white space or not to white space: That is the trial within the Ofcom TV white spaces pilot," in *Proc. IEEE DySPAN 2015*, Sept 2015, pp. 11–22.

[24] ETSI EN 301598, "White space devices (WSD); wireless access systems operating in the 470 MHz to 790 MHz frequency band; harmonized EN covering the essential requirements of article 3.2 of the R&TTE directive," vol. 1.1.1, 2014.

[25] CEPT/ECC SE 43(11)81, "Wise-project measurement report: WSD maximum power indoor measurements in Turku test network," in *12th SE43 meeting*, Cambridge, UK, December 2011.

[26] C. Cordeiro, K. Challapali, D. Birru, and S. Shankar N, "IEEE 802.22: An introduction to the first wireless standard based on cognitive radios," *Journal of Communications*, vol. 1, no. 1, pp. 38–47, 2006.

[27] J. Mitola, *Cognitive Radio—An Integrated Agent Architecture for Software Defined Radio*. Royal Institute of Technology (KTH), 2000.

[28] M. Sherman, A. N. Mody, R. Martinez, C. Rodriguez, and R. Reddy, "IEEE standards supporting cognitive radio and networks, dynamic spectrum access, and coexistence," *IEEE Communications Magazine*, vol. 46, no. 7, pp. 72–79, 2008.

[29] M. Marja, H. Okkonen, M. Palola, S. Yrjola, P. Ahokangas, and M. Mustonen, "Spectrum sharing using licensed shared access: the concept and its workflow for LTE-advanced networks," *IEEE Wireless Communications*, vol. 21, no. 2, pp. 72–79, 2014.

[30] M. Palola, M. Matinmikko, J. Prokkola, M. Mustonen, M. Heikkila, T. Kippola, S. Yrjola, V. Hartikainen, L. Tudose, A. Kivinen *et al.*, "Description of Finnish licensed shared access (LSA) field trial using TD-LTE in 2.3 GHz band," in *Proc. IEEE DySPAN 2014*, McLean, VA USA, April 1-4, 2014, pp. 374–375.

[31] N. Rupasinghe and I. Guvenc, "Licensed-assisted access for WiFi-LTE coexistence in the unlicensed spectrum," in *IEEE Globecom Workshops (GC Wkshps)*, Austin, TX USA, December 8-12, 2014, pp. 894–899.

[32] R. Ratasuk, N. Mangalvedhe, and A. Ghosh, "LTE in unlicensed spectrum using licensed-assisted access," in *IEEE Globecom Workshops (GC Wkshps)*, Austin, TX USA, December 8-12, 2014, pp. 746–751.

[33] Q. Chen, G. Yu, R. Yin, A. Maaref, G. Y. Li, and A. Huang, "Energy efficiency optimization in licensed-assisted access," *IEEE Journal on Selected Areas in Communications*, Early Access 2016.

[34] M. M. Sohul, M. Yao, T. Yang, and J. H. Reed, "Spectrum access system for the citizen broadband radio service," *IEEE Communications Magazine*, vol. 53, no. 7, pp. 18–25, July 2015.

[35] M. Guizani, C. Hsiao-Hwa, and W. Chonggang, *The Future of Wireless Networks: Architectures, Protocols, and Services*. Taylor & Francis, 2015.

[36] J. Wang, M. Ghosh, and K. Challapali, "Emerging cognitive radio applications: A survey," *IEEE Communications Magazine*, vol. 49, no. 3, pp. 74–81, 2011.

[37] J. O. Neel, "Analysis and design of cognitive radio networks and distributed radio resource management algorithms," Ph.D. dissertation, Virginia Polytechnic Institute and State University, 2006.

[38] *The American Heritage dictionary of the English language*, 4th ed. Houghton Mifflin Company, 2000.

[39] X. Hong, J. Wang, C.-X. Wang, and J. Shi, "Cognitive radio in 5g: a perspective on energy-spectral efficiency trade-off," *IEEE Communications Magazine*, vol. 52, no. 7, pp. 46–53, 2014.

[40] C.-I. Badoi, N. Prasad, V. Croitoru, and R. Prasad, "5g based on cognitive radio," *Wireless Personal Communications*, vol. 57, no. 3, pp. 441–464, 2011.

[41] A. Gupta and R. K. Jha, "A survey of 5g network: Architecture and emerging technologies," *IEEE Access*, vol. 3, pp. 1206–1232, 2015.

[42] J. G. Proakis, *Digital Communications*, 3rd ed. New York: McGraw-Hill, 1995.

[43] Z. Hasan, H. Boostanimehr, and V. K. Bhargava, "Green cellular networks: A survey, some research issues and challenges," *IEEE Communications Surveys & Tutorials*, vol. 13, no. 4, pp. 524–540, 2011.

[44] O. Holland, V. Friderikos *et al.*, "Green spectrum management for mobile operators," in *IEEE Globecom Workshops*, 2010, pp. 1458–1463.

[45] R. Deng, J. Chen, X. Cao, Y. Zhang, S. Maharjan, and S. Gjessing, "Sensing-performance tradeoff in cognitive radio enabled smart grid," *IEEE Transactions on Smart Grid*, vol. 4, no. 1, pp. 302–310, 2013.

[46] A. Ghassemi, S. Bavarian, and L. Lampe, "Cognitive radio for smart grid communications," in *Proc. First IEEE International Conference on Smart Grid Communications (SmartGridComm)*, Gaithersburg, MD, USA, 2010, pp. 297–302.

[47] V. C. Gungor and D. Şahin, "Cognitive radio networks for smart grid applications: A promising technology to overcome spectrum inefficiency," *IEEE Vehicular Technology Magazine*, vol. 7, no. 2, pp. 41–46, 2012.

[48] R. Cavallari, F. Martelli, R. Rosini, C. Buratti, and R. Verdone, "A survey on wireless body area networks: technologies and design challenges," *IEEE Communications Surveys & Tutorials*, vol. 16, no. 3, pp. 1635–1657, 2014.

[49] R. Chávez-Santiago, K. E. Nolan, O. Holland, L. De Nardis, J. M. Ferro, N. Barroca, L. M. Borges, F. J. Velez, V. Gonçalves, and I. Balasingham, "Cognitive radio for medical body area networks using ultra wideband," *IEEE Wireless Communications*, vol. 19, no. 4, pp. 74–81, 2012.

[50] J. Ma and G. Y. L. B. H. Juang, "Signal processing in cognitive radio," *Proceedings of the IEEE*, vol. 97, no. 5, pp. 805–823, 2009.

[51] T. Yücek and H. Arslan, "A survey of spectrum sensing algorithms for cognitive radio applications," *IEEE Communications Surveys & Tutorials*, vol. 11, no. 1, pp. 116–130, 2009.

[52] P. Paysarvi-Hoseini and N. Beaulieu, "Optimal wideband spectrum sensing framework for cognitive radio systems," *IEEE Transactions on Signal Processing*, vol. 59, no. 3, pp. 1170–1182, March 2011.

[53] T. Riihonen and R. Wichman, "Energy detection in full-duplex cognitive radios under residual self-interference," in *Proc. 9th IEEE International Conference on Cognitive Radio Oriented Wireless Networks and Communications (CROWNCOM)*, Oulu, Finland, June 2–4, 2014, pp. 57–60.

[54] S. M. Kay, *Fundamentals of Statistical Signal Processing: Estimation Theory*. Upper Saddle River, NJ, USA: Prentice-Hall, Inc., 1998.

[55] Z. Quan, S. Cui, A. H. Sayed, and H. V. Poor, "Optimal multiband joint detection for spectrum sensing in cognitive radio networks," *IEEE Transactions on Signal Processing*, vol. 57, no. 3, pp. 1128–1140, March 2009.

[56] Z. Quan, S. Cui, and A. H. Sayed, "Optimal linear cooperation for spectrum sensing in cognitive radio networks," *IEEE Journal on Selected Topics in Signal Processing*, vol. 2, no. 1, pp. 28–40, Feb. 2008.

[57] M. Derakhshani, T. Le-Ngoc, and M. Nasiri-Kenari, "Efficient cooperative cyclostationary spectrum sensing in cognitive radios at low SNR regimes," *IEEE Transactions on Wireless Communications*, vol. 10, no. 11, pp. 3754–3764, Nov. 2011.

[58] C. Cordeiro, K. Challapali, D. Birru, and N. Sai Shankar, "IEEE 802.22: the first worldwide wireless standard based on cognitive radios," in *Proc. IEEE DySPAN 2005*, Baltimore, MD, USA, Nov 2005, pp. 328–337.

[59] G. Taricco, "Optimization of linear cooperative spectrum sensing for cognitive radio networks," *IEEE Journal on Selected Topics in Signal Process.*, vol. 5, no. 1, pp. 77–86, Feb. 2011.

[60] A. Papoulis and S. U. Pillai, *Probability, random variables and stochastic processes*. New York: McGraw-Hill, 2002.

[61] J. Lundén, V. Koivunen, A. Huttunen, and H. V. Poor, "Collaborative cyclostationary spectrum sensing for cognitive radio systems," *IEEE Transactions on Signal Processing*, vol. 57, no. 11, pp. 4182–4195, Nov. 2009.

[62] A. V. Dandawate and G. B. Giannakis, "Statistical tests for presence of cyclostationarity," *IEEE Transactions on Signal Processing*, vol. 42, no. 9, pp. 2355–2369, 1994.

[63] Z. Quan, W. Ma, S. Cui, and A. H. Sayed, "Optimal linear fusion for distributed detection via semidefinite programming," *IEEE Transactions on Signal Processing*, vol. 58, no. 4, pp. 2431–2436, 2010.

[64] B. Chen and P. K.Willett, "On the optimality of the likelihood-ratio test for local sensor decision rules in the presence of nonideal channels," *IEEE Transactions on Information Theory*, vol. 51, pp. 693–699, Feb. 2005.

[65] S. Chaudhari, J. Lunden, V. Koivunen, and H. V. Poor, "Cooperative sensing with imperfect reporting channels: Hard decisions or soft decisions?" *IEEE Transactions on Signal Processing*, vol. 60, no. 1, pp. 18–28, Jan. 2012.

[66] Y. Shi, Y. T. Hou, and H. Zhou, "Per-node based optimal power control for multi-hop cognitive radio networks," *IEEE Transactions on Wireless Communications*, vol. 8, no. 10, pp. 5290–5299, Oct. 2009.

[67] H. D. Sherali and W. P. Adams, *A Reformulation-Linearization Technique for Solving Discrete and Continuous Nonconvex Problems*. Kluwer Academic Publishers, 1999.

[68] D. Bertsimas, V. F. Farias, and N. Trichakis, "The price of fairness," *Operations research*, vol. 59, no. 1, pp. 17–31, 2011.

[69] A. Attar, H. Tang, A. V. Vasilakos, F. R. Yu, and V. Leung, "A survey of security challenges in cognitive radio networks: Solutions and future research directions," *Proceedings of the IEEE*, vol. 100, no. 12, pp. 3172–3186, 2012.

[70] R. K. Sharma and D. B. Rawat, "Advances on security threats and countermeasures for cognitive radio networks: A survey," *IEEE Communications Surveys & Tutorials*, vol. 17, no. 2, pp. 1023–1043, 2015.

ORIGINAL PAPERS

PI

JOINT LOCAL QUANTIZATION AND LINEAR COOPERATION IN SPECTRUM SENSING FOR COGNITIVE RADIO NETWORKS

by

Younes Abdi and Tapani Ristaniemi

IEEE Transactions on Signal Processing, vol. 62, no. 17, pp. 4349-4362, Sept. 1, 2014

Joint Local Quantization and Linear Cooperation in Spectrum Sensing for Cognitive Radio Networks

Younes Abdi, *Student Member, IEEE*, and Tapani Ristaniemi, *Senior Member, IEEE*

***Abstract*—In designing cognitive radio networks (CRNs), protecting the license holders from harmful interference while maintaining acceptable quality-of-service (QoS) levels for the secondary users is a challenge effectively mitigated by cooperative spectrum sensing schemes. In this paper, cooperative spectrum sensing in CRNs is studied as a three-phase process composed of local sensing, reporting, and decision/data fusion. Then, a significant tradeoff in designing the reporting phase, i.e., the effect of the number of bits used in local sensing quantization on the overall sensing performance, is identified and formulated. In addition, a novel approach is proposed to jointly optimize the linear soft-combining scheme at the fusion phase with the number of quantization bits used by each sensing node at the reporting phase. The proposed optimization is represented using the conventional false alarm and missed detection probabilities, in the form of a mixed-integer nonlinear programming (MINLP) problem. The solution is developed as a branch-and-bound procedure based on convex hull relaxation, and a low-complexity suboptimal approach is also provided. Finally, the performance improvement associated with the proposed joint optimization scheme, which is due to better exploitation of spatial/user diversities in CRNs, is demonstrated by a set of illustrative simulation results.**

***Index Terms*—Cognitive radio (CR), cooperative spectrum sensing, decision fusion, non-ideal reporting channel, quantization.**

I. Introduction

PROMOTING more efficient use of the radio spectrum as a valuable resource has been of the first priority in many scientific debates and research activities worldwide, see e.g., [1], [2]. Consequently, Cognitive Radio (CR) as the best implementation candidate for the emerging Dynamic Spectrum Management procedures has been the core of most related technical discussions and interactions among various academic, industrial, and regulatory groups specialized in wireless communications all over the world, see [3], [4], and the references therein.

Conceptually, CR is an adaptive communication system which offers the promise of intelligent radios that can learn from and adapt to their environment [5]. As a matter of fact, spectrum sensing is the key element in each CR system and enables its user, commonly referred to as Secondary User (SU), to find transmission opportunities in spectrum resources allocated exclusively to license holders. In this context, the license holders are called Primary Users (PUs) and have the exclusive right of using the spectrum. So the aim of a CR Network (CRN) generally is to achieve radio resources for communication within the spectrum band of the PUs without causing any harmful interference and the spectrum sensing capability enables CRs to detect active PUs and avoid causing interference for them. However, due to impairments like shadowing and multipath fading associated with typical wireless environments, there might be some cases in which not all the CRs are able to detect the PU signal, even though it is present and active. This significant issue is known as the Hidden Node Problem and is a major concern in designing CRNs.

Conventionally, the hidden node problem is mitigated by cooperation among spatially diverse sensing nodes, leading to the concept of Cooperative Spectrum Sensing. As a common design strategy, the cooperative sensing is coordinated by and the overall sensing outcome is generated in a special node called the Fusion Center (FC) which might be considered as a more powerful node, like a base station or an access point. This cooperation of the CR nodes with the FC is generally performed as a three-phase process. In the first phase which we call Local Sensing, each node performs spectrum sensing individually, by using its own built-in sensing scheme. In other words, the nodes listen to their environment to detect the PU signal. Accordingly, the wireless channels between the PU and the sensing nodes are referred to as Listening Channels. In the second phase, called Reporting, the sensing nodes send their local sensing outcomes to the FC through dedicated [6]–[8] or non-dedicated [9], [10] Reporting Channels. Finally, in the third phase, i.e., Fusion, the FC combines the received local sensing outcomes by using a soft-decision (SD) [8], [11]–[16] or hard-decision (HD) [17]–[19] method to decide the presence or absence of the PU.

A. Assumed Architecture: Linear Fusion of Quantized Reports

The architecture assumed in this paper has two main parts, namely, the fusion rule at the FC and the reporting links. We have assumed that the FC performs linear combining on the local test summaries which are reported through non-ideal (i.e., erroneous) digital channels. The main considerations motivating us to adopt this structure are as follows.

It has been shown in [20] that for a distributed detection problem with nonideal analogue communication channels between the distributed nodes and FC, the globally optimal structure is to perform the Likelihood Ratio Test (LRT) both at individual nodes and at the FC. However, how to efficiently find

Manuscript received January 27, 2014; revised June 02, 2014; accepted June 03, 2014. Date of publication June 12, 2014; date of current version August 05, 2014. The associate editor coordinating the review of this manuscript and approving it for publication was Prof. Paolo Banelli. This work has been financially supported by the Graduate school in Electronics, Telecommunications, and Automation (GETA) coordinated by Aalto University, Espoo, Finland.

The authors are with the Faculty of Information Technology, University of Jyväskylä, FIN-40014, Jyväskylä, Finland (e-mail: younes.abdi@jyu.fi; tapani.ristaniemi@jyu.fi).

Color versions of one or more of the figures in this paper are available online at http://ieeexplore.ieee.org.

Digital Object Identifier 10.1109/TSP.2014.2330803

the optimal LRT thresholds for individual nodes and for the FC is still unknown, see [8], [20]. For the quantized SD case, i.e., when the reporting is performed through nonideal digital links, a solution for optimizing the local quantization levels jointly with the LRT threshold at the FC may or may not exist [21]. Even if an optimal solution exists, the threshold calculations are not trivial, and complex optimization schemes are needed to solve them. The complexity cost further rises as these optimizations have to be done each time the listening or reporting channels change. Moreover, the optimal rules are derived under strict assumptions that may not hold in a practical scenario, resulting in lack of robustness [22]. These difficulties are commonly avoided by assuming a linear fusion scheme [8], [12]–[14] which is the base for our considered architecture. In particular, linear combining is shown in [8] to perform very closely to the optimal LRT method but with much less computational complexity.

Two approaches are commonly used in the literature to model the reporting phase. In the first approach, the reporting links are modeled as analogue, i.e., additive white Gaussian noise (AWGN) channels [8], [12]–[14], which is the simplest assumption leading to analytically-tractable formulations. The alternative approach is based on assuming nonideal digital communication links, i.e., Binary Symmetric Channels (BSC) through which the quantized test summaries are sent to the FC [15], [19], [22]. Digital reporting is more practically appealing since, first, the reporting channel bandwidth is limited in practice, and, second, in many cases, the FC is the access point, base station (BS), or network coordinator which performs a set of resource allocation activities besides decision/data fusion, see e.g., the BS in the IEEE 802.22 standard. These tasks basically require establishment of a set of digital communication links between the FC and CR nodes, which can also be used for the reporting purposes. When modeling the reporting facility as a digital link, the effect of reporting channel impairments on the overall sensing performance is captured into the system model by reporting Bit Error Probability (BEP), as it is a convenient and widely applicable method to model the end-to-end performance of the system including the transmitter, the channel, and the receiver.

B. Related Work

Optimal linear combining is a non-convex problem studied in [8] and [23], where it is broken into several subproblems and the optimal solution is derived through a tedious iterative process which fails to cover all possible cases. As an alternative approach, the authors in [8] have proposed a suboptimal solution based on the so-called Modified Deflection Coefficient (MDC) and showed that this method provides very close results to the ones obtained by the optimal LRT method, but with lower complexity. The MDC approach is also used in other works like [11] and [24] to optimize the detection performance where direct formulation of the false alarm and missed detection probabilities leads to a non-convex problem. In [12], a semidefinite programming approach with a divide-and-conquer process is proposed for the linear combining problem, but the most straightforward and complete solution is developed in [13], which covers all the possible cases. The method in [13] is simple to implement in the sense that it only requires solving a polynomial equation in a single scalar variable over a given interval depending on the system parameters. The effect of reporting channel impairments on the overall sensing performance has been investigated in [19], [22], and [25], where the reporting channels are modeled as BSCs that cause errors with a certain BEP. Existence of a BEP wall has been demonstrated in these works for both soft- and hard-decision combining schemes, and it is shown that if the BEP of the reporting channel is above the BEP wall value, the constraints on the cooperative detection performance cannot be met at the FC, regardless of the signal quality at the listening channels. Moreover, the authors in [22] compare the performance of the HD- and SD-based fusion methods and illustrate that, in general, the SD significantly outperforms the HD scheme when nonideal reporting channels are considered. In [26], a seesaw analogy for distributed detection based on Rayleigh-faded quantized reports is introduced and evaluated. The fusion rule in [26] is based on assigning weights to the quantization levels rather than to reporting nodes.

C. Contribution

In this paper, we jointly optimize the reporting and fusion phases of the cooperative spectrum sensing in CRNs. In particular and different from the previous works, we optimize the linear soft-combining at the FC considering the effect of reporting channel impairments in designing the quantization scheme used at the sensing nodes. In our novel design, we identify, formulate, and take into account a tradeoff which is described in the following paragraph.

For a given set of radio resources dedicated to the reporting phase in terms of transmission power and bandwidth, increasing the number of quantization bits influences the overall sensing performance in two opposite directions. Specifically, on one side, increasing the number of quantization levels leads to a better quantization process and consequently, lowers the quantization errors affecting the reported local sensing outcomes, improving the cooperation performance. On the other side however, increasing the quantization bits raises the BEP induced by the reporting channels and reduces the received sensing outcomes quality at the FC, degrading the overall sensing performance.

We derive exact as well as practical approximate relationships describing the joint impact of the quantization, reporting, and linear fusion processes. Therefore, the spatial/user diversities regarding the listening and reporting channels are considered in a more comprehensive optimization approach, promising a better overall sensing performance.

The rest of the paper is organized as follows. In Section II, general modeling assumptions and details of the CRN considered are introduced. In Section III, the overall structure of the proposed joint optimization problem is presented, and its detailed mathematical formulations are derived. In Section IV, the MINLP problem is formally constructed, and its solution procedures are developed. The effectiveness of the proposed joint optimization is demonstrated through simulation results in Section V, followed by concluding remarks provided in Section VI.

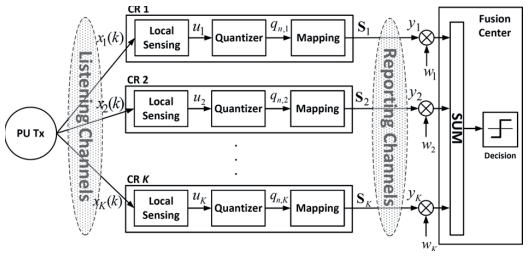

Fig. 1. Basic configuration of cooperative spectrum sensing including the listening and reporting channels, PU, SUs, and FC.

II. System Model

A CRN with K sensing nodes is considered. These nodes cooperatively sense the radio spectrum to find temporal and/or spatial vacant bands for their data communication. Fig. 1 shows the basic configuration and major elements in a CRN exploiting cooperative spectrum sensing.

A. Local Sensing and Quantization

In our adopted model, the kth sample of the received PU signal at the ith CR node is represented as

$$\begin{cases} x_i(k) = \nu_i(k), & \mathcal{H}_0 \\ x_i(k) = h_i s(k) + \nu_i(k), & \mathcal{H}_1 \end{cases} \tag{1}$$

where $\mathcal{H}_1$ and $\mathcal{H}_0$ denote the hypotheses representing the presence or absence of the PU, respectively. $s(k)$ denotes the signal transmitted by the PU and $x_i(k)$ is the received signal by the ith SU. h_i is the listening channel block fading gain. Listening channel gains are assumed to be independent circularly-symmetric Gaussian random variables. $\nu_i(k)$ denotes the circularly-symmetric zero-mean AWGN at the CR sensor receiver, i.e., $\nu_i(k) \sim \mathcal{CN}(0, \sigma^2_{\nu_i})$. Without loss of generality, $s(k)$ and $\{\nu_i(k)\}$ are assumed to be independent of each other.

CR node $i, i = 1, \ldots, K$ performs spectrum sensing by using its built-in sensor (which can be of any common types like Energy Detection (ED), Cyclostationary Detection (CSD), etc.) to derive a local test statistic u_i, and then uses the following quantization rule to map it on a bit sequence of length d_i

$$\psi_i(u_i) = q_{n,i} \text{ if } t_{n,i} \leqslant u_i < t_{n+1,i} \tag{2}$$

where $\psi_i(\cdot)$ denotes the quantization process at the ith SU, $q_{n,i}$, $n = 1, \ldots, 2^{d_i}$ is its nth quantization level, while $t_{n,i}$ and $t_{n+1,i}$ denote the corresponding boundaries.

Let $\mathbf{d} \triangleq [\, d_1, \ldots, d_K \,]^T$ denote the number of quantization bits used in all sensing nodes. As described in [22] several quantization methods for signal detectors can be considered here such as Maximum Output Entropy (MOE) quantization and Minimum Average Error (MAE) quantization. Without loss of generality, we have considered uniform and MOE quantization schemes in this paper. We describe the uniform quantization method in the following. For details of the MOE quantization, see [22].

In the uniform quantization incorporated in the ith sensing node, the range covered by the quantization levels is $(\mu_i - m\sigma_i, \mu_i + m\sigma_i)$, where m is determined by the Chebyshev inequality such that $\mathbf{Pr}\{|u_i - \mu_i| \geq m\sigma_i\} \leq \frac{1}{m^2}$. This coverage range is then divided into 2^{d_i} equally-spaced levels, whose boundaries are denoted by

$$t_{n,i} = \mu_i + m\sigma_i \left(\frac{2(n-1)}{2^{d_i} - 1} - 1 \right). \tag{3}$$

The quantization level $q_{n,i}$ lies in the middle of $t_{n-1,i}$ and $t_{n,i}$, i.e.,

$$q_{n,i} = \mu_i + m\sigma_i \left(\frac{2n-1}{2^{d_i} - 1} - 1 \right). \tag{4}$$

And the conditional probability of having level $q_{n,i}$ at the ith quantizer output is

$$\mathbf{Pr}\{\psi_i(u_i) = q_{n,i} | \mathcal{H}_j\} = \int_{t_{n-1,i}}^{t_{n,i}} f_{u_i}(x|\mathcal{H}_j) dx \tag{5}$$

where $f_{u_i}(\cdot|\mathcal{H}_j)$ denotes the probability density function (pdf) of u_i conditioned on $\mathcal{H}_j, j = 0, 1$.

The generated reporting bit sequences are then transmitted to the FC through the reporting channel in an orthogonal manner. The effect of reporting channel impairments on the transmitted bit sequences of the ith CR node is modeled as a BEP denoted by $P_{\mathrm{b},i}$. The reporting channel is assumed to affect each node's transmitted reporting bit sequence independently. Moreover, errors introduced on different bits in a transmitted reporting sequence by the reporting channel are assumed to be independent and identically distributed (i.i.d). Therefore, the received quantized test statistics at the FC, y_i, $i = 1, \ldots, K$ are independent discrete random variables whose probability mass functions (pmf) can be represented (for $j = 0, 1$) as [22]

$$\mathbf{Pr}\{y_i = q_{n,i} | \mathcal{H}_j\} = \sum_{k=1}^{2^{d_i}} P_{\mathrm{b},i}^{D_{n,k}} \left(1 - P_{\mathrm{b},i}\right)^{d_i - D_{n,k}} \mathbf{Pr}\{\psi_i(u_i) = q_{k,i} | \mathcal{H}_j\} \tag{6}$$

where $D_{n,k}$ is the Hamming distance between bit sequences corresponding to levels $q_{n,i}$ and $q_{k,i}$.

B. Mapping and Bit Sequences

In analyzing the system behavior, it is worth considering the BSC effect on the reported bit sequences and relate it to the received test summary statistics. Therefore, focusing on transmitted and received bit strings in the reporting phase, we model the effect of the BSC using the eXclusive OR (XOR) operator as

$$r_i = s_i \oplus e_i \tag{7}$$

where d_i-bit (scalar) random variables s_i, r_i, and e_i denote the sent and received bit sequences and error caused by the BSC, respectively. If we denote the value of s_i associated with the

nth quantization level (i.e., $q_{n,i}$) by $s_{n,i}$, the following invertible mapping describes the correspondence between the quantization levels and the bit sequences

$$\begin{cases} \Gamma : \{1, 2, \ldots, 2^{d_i}\} \rightarrow \{0, 1, \ldots, 2^{d_i} - 1\} \\ s_{n,i} = \Gamma(n). \end{cases} \tag{8}$$

In other words, $s_i = \Gamma(n)$ if and only if $\psi_i = q_{n,i}$, or equivalently, $s_i = n$ if and only if $\psi_i = q_{\Gamma^{-1}(n),i}$. Therefore, the pmf of s_i can be expressed as (for $n = 0, 1, \ldots, 2^{d_i} - 1$, and $j = 0, 1$)

$$P_{s_i|\mathcal{H}_j}(n) \triangleq \mathbf{Pr}\{s_i = n|\mathcal{H}_j\} = \mathbf{Pr}\{\psi_i = q_{\Gamma^{-1}(n),i}|\mathcal{H}_j\}. \tag{9}$$

Without loss of generality, we have assumed the same mapping process for all CR nodes.

Given the BEP $P_{b,i}$, each bit in the random variable e_i follows the Bernoulli distribution. Consequently, the pmf of e_i is derived as (for $n = 0, 1, \ldots, 2^{d_i} - 1$)

$$P_{e_i}(n) = P_{b,i}^{w_H(n)} (1 - P_{b,i})^{d_i - w_H(n)} \tag{10}$$

where $w_H(n)$ denotes the Hamming weight of the binary representation of n.

In order to derive the pmf of r_i, we use the fact that the assumed reporting channel contamination does not depend on the reported bit sequence s_i, nor the behavior of the PU. Therefore,

$$\begin{aligned} P_{r_i|\mathcal{H}_j}(n) &= \sum_{k=0}^{2^{d_i}-1} \mathbf{Pr}\{r_i = n|e_i = k|\mathcal{H}_j\} \mathbf{Pr}\{e_i = k\} \\ &= \sum_{k=0}^{2^{d_i}-1} \mathbf{Pr}\{s_i = n \oplus k|e_i = k|\mathcal{H}_j\} \mathbf{Pr}\{e_i = k\} \\ &= \sum_{k=0}^{2^{d_i}-1} P_{s_i|\mathcal{H}_j}(n \oplus k) P_{b,i}^{w_H(k)} (1 - P_{b,i})^{d_i - w_H(k)}. \end{aligned} \tag{11}$$

C. Reporting Channel Error

Assuming a general M-ary modulation for the reporting channel, the reporting BEP can be expressed as

$$P_{\mathrm{b},i} = c_M Q\left(\sqrt{c'_M \gamma_{\mathrm{r},i}}\right) \tag{12}$$

where $Q(x) \triangleq \int_x^\infty \exp(-t^2/2)dt/\sqrt{2\pi}$ is the Q-function, c_M and c'_M are two constants determined by the modulation type and $\gamma_{\mathrm{r},i}$ is the reporting link signal-to-noise ratio (SNR). The reporting SNR depends on the number of bits used in the reporting bit sequence d_i as

$$\gamma_{\mathrm{r},i} = \frac{|h_{\mathrm{r},i}|^2 E_{\mathrm{r}}}{N_0 d_i \log_2 M} \tag{13}$$

where $h_{\mathrm{r},i}$, E_{r}, and N_0 denote the reporting channel gain, reporting signal energy, and noise power spectral density, respectively. Therefore, the reporting BEP is a continuous function of d_i

$$P_{\mathrm{b},i} = c_M Q\left(\sqrt{\frac{c''_M}{d_i}}\right) \tag{14}$$

where $c''_M = \frac{c'_M |h_{\mathrm{r},i}|^2 E_r}{N_0 log_2 M}$.

D. Linear Combining

Linear combining is performed at the FC, meaning that the global test statistic y_c is constructed as a weighted sum of the received quantized levels, i.e.,

$$y_{\mathrm{c}} = \sum_{i=1}^{K} w_i y_i = \mathbf{w}^T \mathbf{y} \tag{15}$$

where $\mathbf{w} \triangleq [w_1, \ldots, w_K]^T$ and $\mathbf{y} \triangleq [y_1, \ldots, y_K]^T$.

Finally, y_c is compared against a predefined threshold ξ to decide the presence or absence of the PU, i.e.,

$$\begin{cases} \mathcal{H}_1, & y_{\mathrm{c}} \geq \xi \\ \mathcal{H}_0, & y_{\mathrm{c}} < \xi. \end{cases} \tag{16}$$

The detector performance is commonly measured using two probabilities, namely the probability of false alarm $P_{\mathrm{fa}} = \mathbf{Pr}\{y_{\mathrm{c}} \geq \xi|\mathcal{H}_0\}$ and the probability of missed detection $P_{\mathrm{md}} = \mathbf{Pr}\{y_{\mathrm{c}} < \xi|\mathcal{H}_1\}$. Both false alarm and missed detection probabilities depend on the probability distribution of the global test statistic y_c, which can be derived as a convolution of the pmfs of K independent random variables $\{y_i\}_{i=1}^K$, i.e.,

$$p(y_{\mathrm{c}}) = p(y_1/w_1) * \ldots * p(y_K/w_K) \tag{17}$$

where $p(\cdot)$ and $*$ stand for pmf and convolution, respectively.

III. Problem Formulation

Our problem is to jointly optimize the reporting and fusion phases. Specifically, the goal is to jointly optimize $\mathbf{w}$ and $\mathbf{d}$ to achieve the best cooperative sensing performance. We determine the weighting vector $\mathbf{w}$ at the FC and $\mathbf{d}$ used by the sensing nodes through jointly considering the effects of both the listening and reporting channels while taking into account the significant tradeoff explained earlier in specifying the optimal number of quantization bits.

A. Problem Structure

We formulate our proposed optimization based on minimizing the missed detection probability subject to an upper bound on the false alarm probability

$$\begin{aligned} &\min_{\mathbf{w},\mathbf{d}} P_{\mathrm{md}} \\ &\text{s.t.} \quad P_{\mathrm{fa}} \leq \alpha \end{aligned} \tag{P1}$$

where α is the given upper limit on the false alarm probability.

According to the Central Limit Theorem (CLT), if K is large enough, we can assume a Gaussian distribution for y_c. In Appendix I, we have shown that Lyapunov's CLT condition [27] holds for y_is. Consequently, the false alarm and missed detection probabilities can be expressed in closed form as

$$P_{\mathrm{fa}} = Q\left(\frac{\xi - \boldsymbol{\mu}_{\mathcal{H}_0}^T \mathbf{w}}{\sqrt{\mathbf{w}^T \boldsymbol{\Sigma}_{\mathcal{H}_0} \mathbf{w}}}\right) \tag{18}$$

$$P_{\mathrm{md}} = 1 - Q\left(\frac{\xi - \boldsymbol{\mu}_{\mathcal{H}_1}^T \mathbf{w}}{\sqrt{\mathbf{w}^T \boldsymbol{\Sigma}_{\mathcal{H}_1} \mathbf{w}}}\right) \tag{19}$$

where (for $j = 1, 2$) $\boldsymbol{\mu}_{\mathcal{H}_j} \triangleq \mathrm{E}[\mathbf{y}|\mathcal{H}_j]$ and $\boldsymbol{\Sigma}_{\mathcal{H}_j} \triangleq \mathrm{E}\left[\mathbf{y}\mathbf{y}^T|\mathcal{H}_j\right] = \mathrm{diag}(\sigma^2_{y_1|\mathcal{H}_j}, \ldots, \sigma^2_{y_K|\mathcal{H}_j})$. We have found through numerical evaluations that Gaussian distribution fits well for $K \geq 5$.

Now, if we eliminate ξ in (18) and (19) by considering a target false alarm probability $P_{\mathrm{fa}} = \alpha$, (P1) is converted to

$$\max_{\mathbf{w},\mathbf{d}} Q\left(\frac{Q^{-1}(\alpha)\sqrt{\mathbf{w}^T\boldsymbol{\Sigma}_{\mathcal{H}_0}\mathbf{w}} - \mathbf{a}^T\mathbf{w}}{\sqrt{\mathbf{w}^T\boldsymbol{\Sigma}_{\mathcal{H}_1}\mathbf{w}}}\right) \tag{P2}$$

where $Q^{-1}(\cdot)$ is the functional inverse of the Q-function, $\mathbf{a} \triangleq [a_1, \ldots, a_K]^T \triangleq \boldsymbol{\mu}_{\mathcal{H}_1} - \boldsymbol{\mu}_{\mathcal{H}_0}$ and, for $i = 1, \ldots, K$, we have $a_i \triangleq \mathrm{E}[y_i|\mathcal{H}_1] - \mathrm{E}[y_i|\mathcal{H}_0]$. a_i and $\sigma^2_{y_i|\mathcal{H}_j}$ are related to the number of quantization bits d_i through the total probability theorem as

$$a_i = \sum_{n=1}^{2^{d_i}} q_{n,i} \sum_{k=1}^{2^{d_i}} P_{\mathrm{b},i}^{D_{n,k}} (1 - P_{\mathrm{b},i})^{d_i - D_{n,k}} \times \left[\Pr(\psi_i = q_{k,i}|\mathcal{H}_1) - \Pr(\psi_i = q_{k,i}|\mathcal{H}_0)\right] \tag{20}$$

$$\sigma^2_{y_i|\mathcal{H}_j} = \sum_{n=1}^{2^{d_i}} q^2_{n,i} \sum_{k=1}^{2^{d_i}} P_{\mathrm{b},i}^{D_{n,k}} (1 - P_{\mathrm{b},i})^{d_i - D_{n,k}} \Pr(\psi_i = q_{k,i}|\mathcal{H}_j) - \left[\sum_{n=1}^{2^{d_i}} q_{n,i} \sum_{k=1}^{2^{d_i}} P_{\mathrm{b},i}^{D_{n,k}} (1 - P_{\mathrm{b},i})^{d_i - D_{n,k}} \Pr(\psi_i = q_{k,i}|\mathcal{H}_j)\right]^2. \tag{21}$$

It is worth noting that the Hamming distance $D_{n,k}$ in (20) and (21) is a complicated term which depends on the number of quantization bits d_i, as well as on the mapping process Γ between the quantization levels and the reported bit sequences. We use two approaches to derive explicit formulas describing the effect of d_i on the desired test statistics at the FC. In the first approach, two simplifying but practical assumptions considering the mapping process and reporting BSC are used to derive approximate relationships. In the second approach, the quantization and mapping processes are considered separately, and exact formulas for the desired statistics are derived in general case. These approaches follow as the next two subsections.

B. Gray Coding and Reliable Reporting

We first assume that Gray coding is used to map the reporting bit sequences to their corresponding quantization levels. In other words, we assume that the bit sequences representing the adjacent quantization levels, differ only in one bit. Secondly, we assume a reliable reporting channel, i.e., small $P_{b,i}$s. Consequently, we neglect the cases in which more than one bit in a sequence arrive erroneously at the FC. Then, we use the following lemma which relates the bit sequences with one-bit distance in a Gray-encoded mapping mechanism.

Lemma 1: Let $s_{n,i}$, $n = 1, \ldots, 2^{d_i}$ denote the d_i-bit Gray-coded bit string corresponding to $q_{n,i}$. By flipping the l_eth bit in $s_{n,i}$, it turns into $s_{k,i}$ where k can be derived as a function of n and l_e as

$$k(n, l_e) = n + 2^{l_e} - 2\mathrm{mod}(n - 1, 2^{l_e}) - 1. \tag{22}$$

Proof: Please refer to Appendix II. ■

Hence, we know that if $q_{n,i}$ (whose bit string is $s_{n,i}$) is sent by the ith CR node and the reporting channel changes only the l_eth element of the reported bit sequence, then $q_{k(n,l_e),i}$ will be received at the FC. In addition, by setting $l_e = 0$, (22) yields $k = n$, i.e., no change in the code index. So we can consider $l_e = 0$ for the error-free bit sequences which arrive at the FC. *Lemma 1* and the aforementioned assumptions lead to the following simplified forms of a_i and $\sigma^2_{y_i|\mathcal{H}_j}$

$$a_i \approx \sum_{n=1}^{2^{d_i}} q_{n,i} \sum_{l_e=0}^{d_i} P_{\mathrm{b},i}^{1-\delta_{l_e,0}} (1 - P_{\mathrm{b},i})^{d_i + \delta_{l_e,0} - 1} \times \left[\mathbf{Pr}(\psi_i = q_{k(n,l_e),i}|\mathcal{H}_1) - \mathbf{Pr}(\psi_i = q_{k(n,l_e),i}|\mathcal{H}_0)\right] \tag{23}$$

where $\delta_{l_e,0}$ equals 1 when $l_e = 0$ and 0 otherwise. $\sigma^2_{y_i|\mathcal{H}_j}$ has been expressed in (24) at the bottom of the page.

C. Bit-by-Bit Considerations

Now we proceed with the second approach to derive exact relations for the desired statistics in general case. We relate the bit-sequence interpretations to our detector optimization by considering a general mapping process. For simplicity, first assume a linear mapping scheme, i.e.,

$$s_{n,i} = n - 1, \quad n = 1, \ldots, 2^{d_i}. \tag{25}$$

Extension to the general case will be considered later. Using uniform quantization (4) at the CR nodes, the quantization levels correspond to the bit sequences according to

$$q_{n,i} = \mu_i + m\sigma_i \left(\frac{2s_{n,i} + 1}{2^{d_i} - 1} - 1\right). \tag{26}$$

$$\sigma^2_{y_i|\mathcal{H}_j} \approx \sum_{n=1}^{2^{d_i}} q^2_{n,i} \sum_{l_e=0}^{d_i} P_{\mathrm{b},i}^{1-\delta_{l_e,0}} (1 - P_{\mathrm{b},i})^{d_i + \delta_{l_e,0} - 1} \mathbf{Pr}(\psi_i = q_{k,i}|\mathcal{H}_j) - \left[\sum_{n=1}^{2^{d_i}} q_{n,i} \sum_{l_e=0}^{d_i} P_{\mathrm{b},i}^{1-\delta_{l_e,0}} (1 - P_{\mathrm{b},i})^{d_i + \delta_{l_e,0} - 1} \mathbf{Pr}(\psi_i = q_{k,i}|\mathcal{H}_j)\right]^2. \tag{24}$$

This correspondence can be expressed in terms of random variables ψ_i and s_i as

$$\psi_i = \mu_i + m\sigma_i \left(\frac{2s_i + 1}{2^{d_i} - 1} - 1 \right). \tag{27}$$

Thus, at the FC, the relation between the received bit sequences and quantization levels is

$$y_i = \mu_i + m\sigma_i \left(\frac{2r_i + 1}{2^{d_i} - 1} - 1 \right) \tag{28}$$

which indicates that we can derive the desired statistics, i.e., a_i and $\sigma^2_{y_i|\mathcal{H}_j}$, in terms of the received code statistics as

$$a_i = \frac{2m\sigma_i}{2^{d_i} - 1} \left(E[r_i|\mathcal{H}_1] - E[r_i|\mathcal{H}_0] \right) \tag{29}$$

$$\sigma^2_{y_i|\mathcal{H}_j} = \left(\frac{2m\sigma_i}{2^{d_i} - 1} \right)^2 \sigma^2_{r_i|\mathcal{H}_j}. \tag{30}$$

These moments are calculated using (11) as (for $j = 0, 1$)

$$E[r_i|\mathcal{H}_j] = \sum_{n=0}^{2^{d_i}-1} n P_{r_i|\mathcal{H}_j}(n) \tag{31}$$

$$\sigma^2_{r_i|\mathcal{H}_j} = \sum_{n=0}^{2^{d_i}-1} n^2 P_{r_i|\mathcal{H}_j}(n) - \left[\sum_{n=0}^{2^{d_i}-1} n P_{r_i|\mathcal{H}_j}(n) \right]^2. \tag{32}$$

To clearly recognize the role of d_i in the derived statistics, we now focus on the pmf of the received bit sequences, i.e., $P_{r_i|\mathcal{H}_j}(n)$. More specifically, we reconsider (11) from a bit-by-bit perspective to deal with the XOR operator and the Hamming weight $w_H(\cdot)$ by using the following lemma.

Lemma 2: For two d_i-bit integers n, and k, if $w_H(k) = n_e$, and $n_e \neq 0$ then

$$n \oplus k = g(n, k_1, k_2, \ldots, k_{n_e}) \tag{33}$$

where

$$\begin{aligned} g(n, k_1, k_2, \ldots, k_{n_e}) \triangleq\, & n + \left[2u(0.5 - b_{k_1}(n)) - 1\right] 2^{k_1 - 1} \\ & + \left[2u(0.5 - b_{k_2}(n)) - 1\right] 2^{k_2 - 1} + \cdots \\ & + \left[2u(0.5 - b_{k_{n_e}}(n)) - 1\right] 2^{k_{n_e} - 1} \end{aligned} \tag{34}$$

where $k_i, i = 1, \ldots, n_e$ denotes the location of ith 1 in k, $b_j(n)$, $j = 1, \ldots, d_i$ denotes the value of jth bit in n and $u(\cdot)$ is the step function, which equals to 1 when its argument is positive and 0 otherwise.

Proof: The proof is given in Appendix III. ∎

Now we can eliminate the XOR operator and Hamming weights in (11) and rewrite it as (35) (see Equation (35) at the bottom of the page), where n_e acts as the number of errors introduced by the BSC in the reported bit sequences and g represents the index of bit sequences with n_e-bit distance from the nth sequence.

In addition, *Lemma 2* enables us to approximate our desired statistics by limiting the maximum number of errors considered. Specifically, by adopting N_e, $1 \leq N_e \leq d_i$ as the upper limit of the first summation in (35), we derive an approximation whose accuracy can be controlled by N_e. For instance, if we have a reliable reporting channel, we can neglect the cases with more than one-bit error by using the following approximation, which is derived by restricting the first summation in (35) to $n_e = 1$

$$\begin{aligned} P_{r_i|\mathcal{H}_j}(n) \approx\, & (1 - P_{b,i})^{d_i} P_{s_i|\mathcal{H}_j}(n) \\ & + P_{b,i} (1 - P_{b,i})^{d_i - 1} \sum_{k_1=1}^{d_i} P_{s_i|\mathcal{H}_j}(g(n, k_1)). \end{aligned} \tag{36}$$

By relaxing the linear mapping and uniform quantization assumptions, the developed analysis structure remains the same. However, there will no longer be linear relationships (29), and (30) between the statistics of the received bit sequences r_i, and their corresponding quantization levels y_i. Nevertheless, the moments of y_i are obtained in terms of the received bit-sequence pmfs as (for $j = 0, 1$)

$$E[y_i^\lambda|\mathcal{H}_j] = \sum_{n=1}^{2^{d_i}} q_{n,i}^\lambda P_{r_i|\mathcal{H}_j}(\Gamma(n)), \quad \lambda = 1, 2, \ldots \tag{37}$$

and the desired statistics are obtained accordingly. Hence, through analyzing the received bit sequences, we can derive the desired test statistics a_i and $\sigma^2_{y_i|\mathcal{H}_j}$ in terms of the number of quantization bits d_i in general case.

IV. Joint Reporting-Fusion Optimization

So far, we have thoroughly investigated the statistics governing our joint reporting-fusion optimization and derived analytical formulations describing the effect of local test summary quantization on the overall cooperative sensing performance. Now, we are ready to consider the joint optimization problem. Recall that we are dealing with (P2), which aims at joint optimization of $\mathbf{w}$ and $\mathbf{d}$.

For a given $\mathbf{d}$, (P2) can be solved for optimal weighting vector $\tilde{\mathbf{w}}$ through considering the Lagrange dual problem and Karush-Kuhn-Tucker (KKT) conditions [13] which yield

$$\tilde{\mathbf{w}} = \mathbf{\Sigma}_{\mathcal{H}_0}^{-1/2} \left[Q^{-1}(\alpha) \mathbf{I}_K + \zeta \mathbf{A} \right]^{-1} \mathbf{c} \tag{38}$$

$$P_{r_i|\mathcal{H}_j}(n) = (1-P_{b,i})^{d_i} P_{s_i|\mathcal{H}_j}(n) + \sum_{n_e=1}^{d_i} P_{b,i}^{n_e} (1-P_{b,i})^{d_i - n_e} \sum_{k_1=1}^{d_i} \sum_{\substack{k_2=1 \\ k_2 \neq k_1}}^{d_i} \cdots \sum_{\substack{k_{n_e}=1 \\ k_{n_e} \neq k_1, \ldots, k_{n_e-1}}}^{d_i} P_{s_i|\mathcal{H}_j}(g(n, k_1, k_2, \ldots, k_{n_e})). \tag{35}$$

where $\mathbf{A} \triangleq \mathbf{\Sigma}_{\mathcal{H}_1}\mathbf{\Sigma}_{\mathcal{H}_0}^{-1}$ and $\mathbf{c} \triangleq \mathbf{\Sigma}_{\mathcal{H}_0}^{-1/2}\mathbf{a}$. ζ is the single root of the polynomial equation

$$\left\|[Q^{-1}(\alpha)\mathbf{I}_K + \zeta\mathbf{A}]^{-1}\mathbf{c}\right\| = 1 \tag{39}$$

and satisfies

$$Q^{-1}(\alpha)\mathbf{I}_K + \zeta\mathbf{A} \succ \mathbf{0} \tag{40}$$

where $\mathbf{0}$ stands for the null matrix and $\succ$ represents the element-wise inequality. Note that (39) and (40) specify a unique ζ as a function of $\mathbf{d}$.

Now, using (38), (39), and (40), we remove $\mathbf{w}$ from (P2) and convert it to an optimization in $\mathbf{d}$ and ζ. In addition, since the number of quantization levels cannot be infinite in practice, we limit $\mathbf{d}$ to lie between a minimum $\mathbf{d}_{\min}$ and a maximum value $\mathbf{d}_{\max}$. Moreover, as the Q-function is strictly decreasing with respect to its argument, we remove it from (P2) and turn the problem into a minimization, i.e.,

$$\min_{\mathbf{d},\zeta} \varphi(\mathbf{d},\zeta) \tag{P3}$$
$$\text{s.t.} \begin{cases} \left\|[Q^{-1}(\alpha)\mathbf{I}_K + \zeta\mathbf{A}]^{-1}\mathbf{c}\right\| = 1 \\ Q^{-1}(\alpha)\mathbf{I}_K + \zeta\mathbf{A} \succ \mathbf{0} \\ \mathbf{d}_{\min} \preceq \mathbf{d} \preceq \mathbf{d}_{\max} \end{cases}$$

where

$$\varphi(\mathbf{d},\zeta) \triangleq \frac{Q^{-1}(\alpha)\sqrt{\tilde{\mathbf{w}}^T\mathbf{\Sigma}_{\mathcal{H}_0}\tilde{\mathbf{w}}} - \mathbf{a}^T\tilde{\mathbf{w}}}{\sqrt{\tilde{\mathbf{w}}^T\mathbf{\Sigma}_{\mathcal{H}_1}\tilde{\mathbf{w}}}}. \tag{41}$$

The cost function in (P3) is a nonlinear function of a_i, $\sigma^2_{y_i|\mathcal{H}_0}$, $\sigma^2_{y_i|\mathcal{H}_1}$ (for $i = 1,\ldots,K$). As we have already studied, and derived these parameters in terms of the number of quantization bits (i.e., d_i), we can clearly see that the cost function in (P3) is highly sophisticated and nonlinear. Since $\mathbf{d}$ represents the number of quantization levels used in the CR nodes, (P3) is a MINLP problem, which is NP hard in general [28]. We develop a Branch-and-Bound (BnB) algorithm to solve this MINLP.

A. The Branch-and-Bound Algorithm

Our optimization problem is a nonlinear program further constrained by integrality restrictions. Clearly, the optimal value of cost function in a continuous linear relaxation of (P3) will always be a lower bound on the optimal value of our cost function. Moreover, in any minimization, any feasible point always specifies an upper bound on the optimal cost function value. The idea of the BnB is to utilize these observations to subdivide MINLP's feasible region into more-manageable subdivisions and then, if required, to further partition the subdivisions. These subdivisions make a so-called *enumeration tree* whose branches can be pruned in a systematic search for the global optimum.

Table I shows the pseudocode of our BnB algorithm. Assuming φ^* as the global minimum of the cost function in (P3), this algorithm provides a $(1-\varepsilon)$ optimal solution φ_ε, which means φ_ε is close enough to φ^* such that $\varphi^* \geq (1-\varepsilon)\varphi_\varepsilon$.

In this algorithm, a lower bound for the cost function is first derived through solving a linear relaxation of (P3) denoted by (LP) (see line 3 in Table I). Construction of the linear relaxation is described later. Then, a local search is performed around

TABLE I
JOINT REPORTING-FUSION OPTIMIZATION AS A BRANCH-AND-BOUND PROCEDURE

1. Define set L of subproblems;
2. $L \leftarrow \{(P3)\}$; $B_U \leftarrow +\infty$; $\varphi_\varepsilon \leftarrow \varnothing$;
3. Solve (LP) for $\tilde{\mathbf{d}}_1$ and denote its minimum cost function by $B_L^{(1)}$;
4. **while** $L \neq \varnothing$
5. Choose $\mathcal{P}_K \in L$ with the minimum $B_L^{(K)}$;
6. $L \leftarrow L \backslash \{\mathcal{P}_K\}$;
7. $B_L \leftarrow B_L^{(K)}$;
8. Find a feasible solution $\tilde{\varphi}$ for (P3) via local search around $\tilde{\mathbf{d}}_K$;
9. $B_U^{(K)} \leftarrow \tilde{\varphi}$;
10. **if** $B_U^{(K)} < B_U$
11. $\varphi_\varepsilon \leftarrow B_U^{(K)}$;
12. $B_U \leftarrow B_U^{(K)}$;
13. **if** $B_L \geq (1-\varepsilon)B_U$
14. output φ_ε;
15. **else**
16. Remove from L all $\mathcal{P}_{K'}$ with $B_L^{(K')} \geq (1-\varepsilon)B_U$;
17. **end if**
18. **end if**
19. Choose a branching variable d_i and a branching point d_{branch};
20. Create subproblems $\mathcal{P}_{K+}$ and $\mathcal{P}_{K-}$;
21. Solve linear relaxations of $\mathcal{P}_{K+}$ and $\mathcal{P}_{K-}$ for $\tilde{\mathbf{d}}_{K+}$ and $\tilde{\mathbf{d}}_{K-}$ and denote their optimal cost functions by $B_L^{(K+)}$ and $B_L^{(K-)}$;
22. **if** $B_L^{(K+)} \leq (1-\varepsilon)B_U$
23. $L \leftarrow L \cup \{\mathcal{P}_{K+}\}$;
24. **end if**
25. **if** $B_L^{(K-)} \leq (1-\varepsilon)B_U$
26. $L \leftarrow L \cup \{\mathcal{P}_{K-}\}$;
27. **end if**
28. **end while**
29. output φ_ε;

the solution of the linear program to obtain a feasible point for (P3) and an upper bound for the global minimum (line 8). Note that any feasible solution of (P3) gives an upper bound on the minimum of φ. This process, i.e., finding the lower and upper bounds for the cost function, is called *bounding*. The algorithm terminates if the derived upper and lower bounds are within the ε-vicinity of each other (lines 13, 14). Otherwise, it continues with the so-called *branching* step, which refers to dividing the feasible region of the problem into two narrower subsets (lines 19, 20).

In this algorithm, maximum relaxation error is considered as metric for choosing the branching variable. That is, the variable d_i with maximum relaxation error is selected for the branching process. The relaxation error for the variable d_i is defined as $\left|d_i^{\text{ls}} - d_i^{\text{lp}}\right|$, where d_i^{ls} and d_i^{lp} denote the value of d_i obtained by the local search and by solving the linear program, respectively. The branching point is $d_{\text{branch}} = \left\lfloor d_i^{\text{lp}} \right\rfloor$, i.e., the problems $\mathcal{P}_{K-}$ and $\mathcal{P}_{K+}$ are constructed through imposing the constraints $d_i \leq \left\lfloor d_i^{\text{lp}} \right\rfloor$ and $d_i \geq \left\lceil d_i^{\text{lp}} \right\rceil$ on $\mathcal{P}_K$, respectively.

Through an iterative branching procedure, subsets are further divided into smaller ones, and the enumeration tree is built. This tree structure allows the algorithm to remove some branches and search for the solution in a very effective way. Moreover, narrowing down the subsets of the optimization variables leads to tighter linear relaxations (i.e., increases B_L) and provides the next local search processes with a closer starting point to the

TABLE II
DECOMPOSITION OF (P3) INTO SMALL BLOCKS AND SIMPLE CONSTRAINTS USED IN CONVEX HULL RELAXATION

Elements of $\mathbf{X}_{\mathcal{H}_k}^{(j)}$, $\mathbf{Z}_{\mathcal{H}_k}$, and $\mathbf{z}$ for $j = 1, ..., 7$, and $k = 0, 1$.
$X_{i,n}^{(1)} = m\sigma_i \left(\frac{2(n-1)}{Z_{i,1}} - 1\right)$, $X_{i,n|\mathcal{H}_k}^{(2)} = Q\left(X_{i,n}^{(1)}/\sigma_{i|\mathcal{H}_k}\right)$, $X_{i,n|\mathcal{H}_k}^{(3)} = X_{i,n|\mathcal{H}_k}^{(2)} - X_{i,n+1|\mathcal{H}_k}^{(2)}$, $X_{i,n|\mathcal{H}_k}^{(4)} = \sum_{k_1=1}^{d_i} X_{i,g(n,k_1)|\mathcal{H}_k}^{(3)}$, $X_{i,n|\mathcal{H}_k}^{(5)} = Z_{i,5} X_{i,n|\mathcal{H}_k}^{(4)}$, $X_{i,n|\mathcal{H}_k}^{(6)} = Z_{i,2|\mathcal{H}_k} X_{i,n|\mathcal{H}_k}^{(3)}$, $X_{i,n|\mathcal{H}_k}^{(7)} = X_{i,n|\mathcal{H}_k}^{(5)} + X_{i,n|\mathcal{H}_k}^{(6)}$.
$Z_{i,1} = 2^{d_i} - 1$, $Z_{i,2} = c_M Q\left(\sqrt{c''_M/d_i}\right)$, $Z_{i,3} = 1 - d_i Z_{i,2}$, $Z_{i,4} = Z_{i,2} + Z_{i,3}$, $Z_{i,5} = Z_{i,2} Z_{i,4}$, $Z_{i,6|\mathcal{H}_k} = \sum_{n=0}^{2^{d_i}-1} n X_{i,n|\mathcal{H}_k}^{(7)}$, $Z_{i,7} = Z_{i,6|\mathcal{H}_1} - Z_{i,6|\mathcal{H}_0}$, $Z_{i,8} = \frac{2m\sigma_i}{Z_{i,1}} Z_{i,7}$, $Z_{i,9|\mathcal{H}_k} = \left(Z_{i,6|\mathcal{H}_k}\right)^2$, $Z_{i,10|\mathcal{H}_k} = \sum_{n=0}^{2^{d_i}-1} n^2 X_{i,n|\mathcal{H}_k}^{(7)}$, $Z_{i,11|\mathcal{H}_k} = Z_{i,10|\mathcal{H}_k} - Z_{i,9|\mathcal{H}_k}$, $Z_{i,12|\mathcal{H}_k} = \zeta Z_{i,11|\mathcal{H}_k}$, $Z_{i,13} = Q^{-1}(\alpha) Z_{i,11|\mathcal{H}_0} + Z_{i,12|\mathcal{H}_1}$, $Z_{i,14} = Z_{i,8}^2$, $Z_{i,15} = \frac{Z_{i,14}}{Z_{i,13}}$, $Z_{i,16|\mathcal{H}_k} = Z_{i,14} Z_{i,11|\mathcal{H}_k}$, $Z_{i,17} = Z_{i,13}^2$, $Z_{i,18|\mathcal{H}_k} = \frac{Z_{i,16|\mathcal{H}_k}}{Z_{i,17}}$, $Z_{i,19|\mathcal{H}_k} = \frac{Z_{i,16|\mathcal{H}_k}}{Z_{i,17}}$.
$z_1 = Q^{-1}(\alpha) - \sum_{i=1}^{K} Z_{i,15}$, $z_2 = \sum_{i=1}^{K} Z_{i,18}$, $z_3 = \sqrt{z_2}$, $z_4 = \sum_{i=1}^{K} Z_{i,19|\mathcal{H}_0} - 1$, $z_5 = z_1/z_3$.

optimal solution (i.e., reduces B_U). Hence, the gap between B_L and B_U is reduced as the process continues. More specifically, at each iteration, the global lower bound B_L is updated to contain the minimum of the lower bounds of all subsets (lines 5, 7). The global upper bound B_U is also updated at each iteration (lines 10, 12), and the branches with a lower bound greater than $(1-\varepsilon)B_U$ are pruned (line 16). This procedure is continued until the difference between the global lower and upper bounds satisfy the accuracy ε (lines 13, 14). Clearly, we may lose the global optimum by pruning the branches. However, if the global optimum is in a pruned branch with the lower bound $B_L^{(K)}$, then $\varphi^* \geq B_L^{(K)}$, and consequently, $\varphi^* \geq (1-\varepsilon)B_U$. Therefore, the current best feasible solution with objective value B_U is already an $(1-\varepsilon)$ optimal solution, and we can still guarantee $(1-\varepsilon)$ optimality. Indeed, this guarantee is the key feature of the BnB algorithm which makes it very effective in solving the MINLPs.

It has been shown that under very general conditions, a BnB solution procedure always converges [29], [30]. Moreover, although the worst-case complexity of such a procedure is exponential, the actual running time could be fast when all partition variables are integers (e.g., the problem considered in this paper).

B. Convex Hull Relaxation

To derive a linear relaxation of our joint optimization problem, we reconfigure (P3) by introducing a number of auxiliary variables along with some additional constraints. In this process, the cost and constraints in (P3) are decomposed into a set of small easy-to-handle functions. We refer to these small functions as *blocks*. These blocks build a set of simple constraints which, as a whole, represent (P3). Finally, the derived constraint functions are replaced by appropriate linear inequalities.

We have decomposed our cost and constraint functions into a set of blocks represented in Table II. Through combination of these blocks, it can be easily verified that the following optimization problem is equivalent to (P3)

$$\text{(P4)} \quad \min_{\mathbf{v}} z_5 \quad \text{s.t.} \begin{cases} \text{Constraints in Table II} \\ z_4 = 0 \\ Z_{i,13} > 0, \text{ for } i = 1, \ldots, K \\ \mathbf{v}_{\min} \preceq \mathbf{v} \preceq \mathbf{v}_{\max} \end{cases}$$

where $\mathbf{v}$ contains the old optimization variables, namely, $\mathbf{d}$ and ζ, as well as the new ones defined in Table II, i.e.,

$$\mathbf{v} \triangleq [\mathfrak{X}_{\mathcal{H}_0}^{(1)}, \ldots, \mathfrak{X}_{\mathcal{H}_0}^{(7)}, \mathfrak{X}_{\mathcal{H}_1}^{(1)}, \ldots, \mathfrak{X}_{\mathcal{H}_1}^{(7)}, \mathfrak{Z}_{\mathcal{H}_0}, \mathfrak{Z}_{\mathcal{H}_1}, \mathbf{z}, \mathbf{d}^T, \zeta]^T \tag{42}$$

in which row vectors $\mathfrak{X}_{\mathcal{H}_k}^{(j)}$ and $\mathfrak{Z}_{\mathcal{H}_k}$, $j = 1, \ldots, 7$, $k = 0, 1$, denote the vectorized forms of $\mathbf{X}_{\mathcal{H}_k}^{(j)}$ and $\mathbf{Z}_{\mathcal{H}_k}$ respectively, i.e., $\mathfrak{X}_{\mathcal{H}_k}^{(j)} \triangleq \text{vec}\left(\mathbf{X}_{\mathcal{H}_k}^{(j)}\right)$ and $\mathfrak{Z}_{\mathcal{H}_k} \triangleq \text{vec}\left(\mathbf{Z}_{\mathcal{H}_k}\right)$. The elements of $\mathbf{X}_{\mathcal{H}_k}^{(j)}$, $\mathbf{Z}_{\mathcal{H}_k}$, and $\mathbf{z}$ represent the blocks defined in Table II. These elements are denoted as[1]

$$\left[\mathbf{X}_{\mathcal{H}_k}^{(j)}\right]_{i,n} \triangleq X_{i,n|\mathcal{H}_k}^{(j)} \tag{43}$$

$$\left[\mathbf{Z}_{\mathcal{H}_k}\right]_{i,j} \triangleq Z_{i,j|\mathcal{H}_k} \tag{44}$$

$$\mathbf{z} \triangleq [z_1, \ldots, z_5]. \tag{45}$$

The vectors $\mathbf{v}_{\min}$ and $\mathbf{v}_{\max}$ denote the lower and upper bounds on the elements of $\mathbf{v}$, respectively. These bounds are directly obtained by applying $\mathbf{d}_{\min} \preceq \mathbf{d} \preceq \mathbf{d}_{\max}$ on the blocks.

It is worth noting that any element v_i in $\mathbf{v}$ can be represented as a function of other elements, i.e., for $v_i \in [v_{i,\min}, v_{i,\max}]$, we have $v_i = \vartheta_i(\mathbf{v})$. ϑ_i is either a convex (or concave) function or it represents a product (or ratio) of two elements in $\mathbf{v}$, i.e., $\vartheta_i(\mathbf{v}) = v_k v_j$.

If ϑ_i is convex, we linearize it by partitioning each interval $[v_{l,\min}, v_{l,\max}]$ into $N_{\text{lin}} - 1$ subintevals, $1 \leq l \leq |\mathbf{v}|$. This partitioning is realized by considering N_{lin} points as $v_{l,\min} = \hat{v}_{l,1} \leq \hat{v}_{l,2} \leq \cdots \leq \hat{v}_{l,N_{\text{lin}}} = v_{l,\max}$. In this way, we make a grid over the space $\mathbf{v}_{\min} \preceq \mathbf{v} \preceq \mathbf{v}_{\max}$. Now for any subspace within this grid $\hat{\mathbf{v}}_k \preceq \mathbf{v} \preceq \hat{\mathbf{v}}_{k+1}$, $k \in \{1, \ldots, N_{\text{lin}}\}$, we have the following linear lower bound for v_i

$$v_i \geq \vartheta_i(\tilde{\mathbf{v}}) + \nabla\vartheta_i(\tilde{\mathbf{v}})^T(\mathbf{v} - \tilde{\mathbf{v}}) \tag{46}$$

where $\tilde{\mathbf{v}}$ can be any point such that $\hat{\mathbf{v}}_k \preceq \tilde{\mathbf{v}} \preceq \hat{\mathbf{v}}_{k+1}$, and $\hat{\mathbf{v}}_k \triangleq \left[\hat{v}_{1,k}, \ldots, \hat{v}_{|\mathbf{v}|,k}\right]$. The number of points N_{lin} can be used to control the precision of the partitioning process.

For $v_i \in [v_{i,\min}, v_{i,\max}]$, the upper bound in our linearization is denoted by the following relation,

$$v_i \leq \vartheta_i(\mathbf{v}_{\min}) + \frac{\vartheta_i(\mathbf{v}_{\max}) - \vartheta_i(\mathbf{v}_{\min})}{v_{k,\max} - v_{k,\min}}(v_k - v_{k,\min}) \tag{47}$$

[1]We have dropped $\mathcal{H}_k$ from the element representations whenever there is no difference between the element values for $\mathcal{H}_0$ and $\mathcal{H}_1$.

where v_k can be any element in $\mathbf{v}$ such that $\partial\vartheta_i/\partial v_k \neq 0$, and $v_{k,\min}$, and $v_{k,\max}$ denote the minimum and maximum values of v_k, respectively. Similar bounds can be obtained for the concave functions.

For the blocks which represent the product of two elements, i.e., $\vartheta_i(\mathbf{v}) = v_k v_j$, the tightest linear constraints are denoted by [31], [32]

$$v_i \geq v_{j,\min} v_k + v_{k,\min} v_j - v_{j,\min} v_{k,\min} \tag{48}$$
$$v_i \geq v_{j,\max} v_k + v_{k,\max} v_j - v_{j,\max} v_{k,\max} \tag{49}$$
$$v_i \leq v_{j,\min} v_k + v_{k,\max} v_j - v_{j,\min} v_{k,\max} \tag{50}$$
$$v_i \leq v_{j,\max} v_k + v_{k,\min} v_j - v_{j,\max} v_{k,\min}. \tag{51}$$

Applying (46)–(51) on the functions defined in Table II, we derive a linear relaxation of (P4) whose solution provides a tight lower bound on the minimum value of our cost function in (P3). This linear program can be expressed as

$$\min_{\mathbf{v}} z_5 \tag{LP}$$
$$\text{s.t.} \begin{cases} \text{Linear constraints } (46)-(51) \\ z_4 = 0 \\ Z_{i,13} > 0, \text{ for } i = 1, \ldots, K \\ \mathbf{v}_{\min} \preceq \mathbf{v} \preceq \mathbf{v}_{\max} \end{cases}$$

which is solved in polynomial time.

C. Low-Complexity Suboptimal Solution

As mentioned earlier, a commonly used suboptimal approach for the design of linear cooperation is based on maximizing the MDC. The MDC provides a good measure of the detection capability, as it characterizes the system performance as the variance-normalized distance between the centers of two conditional pdfs of the global test summary y_c. Therefore, we propose an alternative approach for the discussed joint reporting-fusion optimization based on the MDC, which leads to nearly optimal performance with much less effort. The MDC is defined as

$$\Delta_m^2 \triangleq \frac{(\mathrm{E}[y_c|\mathcal{H}_1] - \mathrm{E}[y_c|\mathcal{H}_0])^2}{\mathrm{Var}\{y_c|\mathcal{H}_1\}}. \tag{52}$$

Replacing y_c with its weighted sum definition, we have

$$\Delta_m^2 = \frac{(\mathbf{a}^T\mathbf{w})^2}{\mathbf{w}^T\boldsymbol{\Sigma}_{\mathcal{H}_1}\mathbf{w}}. \tag{53}$$

Using the MDC approach, we aim at finding $\mathbf{w}$ and $\mathbf{d}$ such that

$$\max_{\mathbf{w},\mathbf{d}} \Delta_m^2 \tag{P5}$$
$$\text{s.t.} \begin{cases} \|\mathbf{w}\| = 1 \\ \mathbf{d}_{\min} \preceq \mathbf{d} \preceq \mathbf{d}_{\max} \end{cases}.$$

The constraint on the weight vector norm is necessary here to derive a unique solution since the MDC does not depend on $\|\mathbf{w}\|$.

In order to derive an analytical solution for (P5), we first eliminate $\mathbf{w}$ as follows. Through the linear transformation [8]

$$\mathbf{w}' = \boldsymbol{\Sigma}_{\mathcal{H}_1}^{1/2}\mathbf{w} \tag{54}$$

the MDC is converted to

$$\Delta_m^2 = \frac{\mathbf{w}'^T\boldsymbol{\Sigma}_{\mathcal{H}_1}^{-T/2}\mathbf{a}\mathbf{a}^T\boldsymbol{\Sigma}_{\mathcal{H}_1}^{-1/2}\mathbf{w}'}{\mathbf{w}'^T\mathbf{w}'} \leq \left\|\boldsymbol{\Sigma}_{\mathcal{H}_1}^{-T/2}\mathbf{a}\right\|^2 \tag{55}$$

and the equality is achieved when $\mathbf{w}' = \boldsymbol{\Sigma}_{\mathcal{H}_1}^{-T/2}\mathbf{a}$. Therefore, the optimal $\mathbf{w}$ which maximizes the MDC is derived as function of $\mathbf{d}$ as

$$\mathbf{w}_{\mathrm{mdc}} = \frac{\boldsymbol{\Sigma}_{\mathcal{H}_1}^{-1/2}\mathbf{w}'}{\left\|\boldsymbol{\Sigma}_{\mathcal{H}_1}^{-1/2}\mathbf{w}'\right\|}. \tag{56}$$

Replacing $\mathbf{w}$ with its MDC-optimal value $\mathbf{w}_{\mathrm{mdc}}$, the MDC can be rewritten as a function of $\mathbf{d}$

$$\Delta_m^2 = \mathbf{a}^T\boldsymbol{\Sigma}_{\mathcal{H}_1}^{-1}\mathbf{a} = \sum_{i=1}^{K} \frac{a_i^2}{\sigma^2_{y_i|\mathcal{H}_1}}. \tag{57}$$

Therefore, (P5) is converted to the following system of optimization problems

$$\text{for } i = 1, \ldots, K, \quad \max_{d_i} \frac{a_i^2}{\sigma^2_{y_i|\mathcal{H}_1}} \tag{P6}$$
$$\text{s.t.} \quad d_{i,\min} \leq d_i \leq d_{i,\max}.$$

We are now dealing with K one-dimensional problems and it is clear that the computational complexity of solving this set of optimizations linearly increases with the number of sensing nodes K.

V. Numerical Results

Two typical distributed detection scenarios have been considered to illustrate the effectiveness of the proposed optimization scheme. In the first scenario, the ED and uniform quantization have been adopted as local sensing and test summary quantization methods at the CR nodes, respectively. As the second scenario, CSD and MOE quantization have been considered. Although not presented here, we also tested other combinations such as CSD with uniform quantization and ED with MOE quantization and obtained similar results, which are expected since our proposed optimization does not depend on any specific local sensing or quantization scheme. In all simulations, there are $K = 5$ cooperating nodes which transmit their sensing outcomes over the reporting channels using the Binary Phase Shift Keying (BPSK) modulation. The PU signal is modeled as a Direct-Sequence (DS) spread-spectrum BPSK signal by using Walsh-Hadamard code with the length of 16, i.e., the processing gain of 16 is considered in all simulation results. The maximum number of quantization bits in each node is 7.

In ED, the energy of the received PU signal is measured using N signal samples, i.e.,

$$u_i = \sum_{k=1}^{N} |x_i(k)|^2 \tag{58}$$

and in CSD the test summary is formed as an estimation of the PU signal autocorrelation function as

$$u_i = \frac{1}{N-\tau} \sum_{k=1}^{N-\tau} x(k+\tau)x^*(k)e^{-j2\pi fk} \tag{59}$$

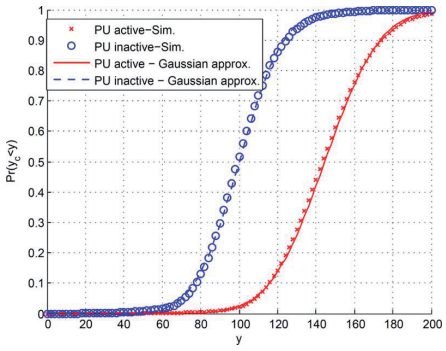

Fig. 2. Cumulative probability distribution of y_c under hypotheses $\mathcal{H}_0$ (the two leftmost curves) and $\mathcal{H}_1$ (the two rightmost curves). Solid curves correspond to the analytic Gaussian approximations. Marked curves are obtained by Monte-Carlo simulation.

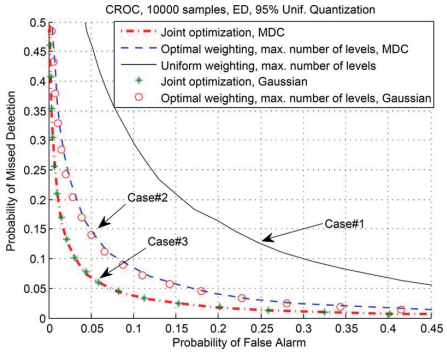

Fig. 3. CROC curves for the energy detection using 20 samples of the PU signal and uniform quantization with Chebyshev probability of 95%. The listening channel SNR levels at sensor inputs are $\{0, -2.7, -3.1, -1.4, -6.9\}$ in dB. The reporting channel SNR levels are $\{10, 13, 12, 14, 11\}$ in dB. The results are obtained using 10,000 realizations.

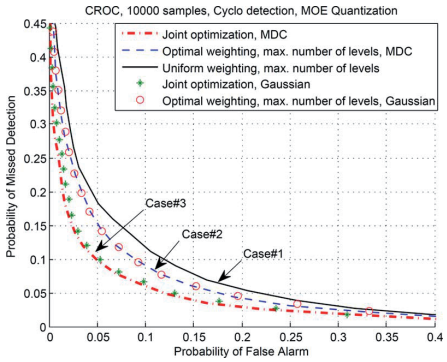

Fig. 4. CROC curves for the cyclostationary detection using 100 samples of the PU signal and MOE quantization. The local SNR levels at sensor inputs are $\{5, 2.3, 1.9, 3.6, -1.9\}$ in dB. The reporting channel SNR levels are $\{11, 14, 13, 12, 11\}$ in dB. The results are obtained using 10,000 realizations.

where f is the cycle frequency, and τ is the lag used in calculating the autocorrelation.

The number of PU signal samples N used in ED is 20 and the Chebyshev probability for the uniform quantization coverage interval has been set to 95%. When CSD is considered, the cyclic autocorrelation function is estimated in each node using $N = 100$ samples of the PU signal and the estimated autocorrelation corresponds to $f = 1/T_c$ and $\tau = 0$. T_c is the chip period of the PU signal. For the ED, the local listening channel SNR levels at sensor inputs are $\{0, -2.7, -3.1, -1.4, -6.9\}$ in dB, and the reporting channel SNRs are $\{10, 13, 12, 14, 11\}$ in dB. For the CSD, $\{5, 2.3, 1.9, 3.6, -1.9\}$ in dB are the listening channel SNR levels and the reporting channel SNRs are $\{11, 14, 13, 12, 11\}$ in dB. Each point on the CROC curves has been derived by averaging over 10,000 realizations. The averaging has been performed on the noise for a fixed set of channel gains and noise variances as in [8], [13].

Fig. 2 shows why Gaussian approximation works well for the global test statistic in (17). It depicts the cumulative distribution function (CDF) of the global test summary y_c when ED is used as the local sensing method at $K = 5$ sensing nodes, assuming both hypotheses $\mathcal{H}_1$ and $\mathcal{H}_0$. It can be seen by comparing the simulation and asymptotic results that y_c behaves very similarly to a normal random variable while the PU is either present or absent.

Fig. 3, and Fig. 4 depict the results derived as Complementary Receiver Operational Characteristics (CROC) curves for both energy and cyclostationary detectors. Specifically, for each detector three cases have been considered as

Case#1: Depicts the performance of uniform linear combining at the FC and maximum number of quantization bits at the sensing nodes,

Case#2: Depicts the performance of optimal linear combining at the FC and maximum number of quantization bits at the sensing nodes,

Case#3: Depicts the performance of the proposed joint optimization, i.e., optimal linear combining at the fusion center and optimal number of quantization bits at the sensing nodes.

It is worth noting that in both figures Case#1, Case#2, and Case#3 represent the detector design without any optimization, only with optimal weighting, and with joint reporting-fusion optimization, respectively. The plots clearly illustrate the effectiveness of our proposed detector in terms of lower false alarm and missed detection probabilities which are shown as CROC curves closer to the origin. Moreover, it can be observed that the achieved optimization results from both the Gaussian approximation and MDC are in close agreement with each other. As another point, we see that performance improvement due to the proposed optimization is higher when ED is used as the local sensing method. This observation is reasonable since ED is known to be more sensitive to the PU signal SNR than the cyclostationary detection. In fact, the linear combining scheme at the FC is a technique to exploit spatial diversity among different sensing nodes to increase the effective SNR level experienced by the detector. For a comparison between ED and CSD performances, see [33]. Note also that we have adopted the parameter values to have almost equal performances in both detectors before applying the proposed optimization. More specifically, by comparing the curves labeled Case#2 in Figs. 2 and 3, we see

almost-equal performances. In fact, we have set the parameters in a way that both detectors meet $P_{\rm fa} = 0.1$, and $P_{\rm md} = 0.1$ (both curves nearly pass the point 0.1, 0.1). In other words, although the SNR levels and sensing times are different, we have evaluated the achieved performance gain by using nearly-equal detectors.

In order to evaluate the performance gain achieved by the proposed joint optimization method, we define the listening channel SNR gain as follows

$$\text{SNR gain (dB)} = \text{SNR}_{\text{maxq}}\,(\text{dB}) - \text{SNR}_{\text{optq}}\,(\text{dB}) \quad (60)$$

where SNR_{maxq} is the minimum SNR required at the SUs to meet $P_{\rm fa} = \alpha$ and $P_{\rm md} = \beta$ when they use the maximum number of quantization levels with optimal weighting and SNR_{optq} is the minimum SNR required at the SUs when they use optimal number of quantization levels and optimal weighting vector derived through the proposed joint optimization scheme.

Fig. 5 depicts the SNR gain at the listening channels vs. the average SNR at the reporting channels. It represents the case in which $K = 5$ sensing nodes experience different SNRs on their listening and reporting channels. The corresponding SNRs for both the reporting and listening channels of $K = 5$ sensing nodes are $[\text{SNR}_0 + 2\Delta\ \text{SNR}_0 + \Delta\ \text{SNR}_0\ \text{SNR}_0 - \Delta\ \text{SNR}_0 - 2\Delta]$, where SNR_0 is the average SNR over the 5 channels and $\Delta = 1\,(\text{dB})$. The target false alarm and missed detection probabilities are both set to 5%. As shown in Fig. 5, the proposed joint optimization leads to a significant performance gain, especially at low SNR regimes experienced at the reporting channels. This superior performance of the proposed design at low SNRs stems from the fact that, the local sensing quantization is also considered when optimizing the linear combining at the FC. Hence, the effect of reporting channel impairments is reduced and, consequently, the proposed detector experiences the reporting channel BEP wall (see [19] and [22]) at lower SNR values, compared to the design which only optimizes the linear fusion. In other words, by decreasing the reporting channel SNR levels, at a certain point, the detector with the maximum number of quantization levels can not meet the target false alarm and missed detection probabilities, no matter how high the SNR levels at the listening channels are. But the proposed detector still reaches the desired performance for a moderate average SNR level at the listening channels. This observation demonstrates the importance of the proposed method, especially when the sensing nodes face stringent energy consumption constraints due to e.g., limited battery life time or green communication considerations, which force the designer to reduce the transmission power used for the reporting phase.

A set of significant observations is obtained by evaluating the derived quantization levels for different listening-channel and reporting-channel SNRs (Table III). In particular, we observe that, when the sensing nodes experience high SNR levels at the listening channel, the proposed optimization scheme reduces the number of quantization levels as much as possible. This clearly means that, when the PU signal is strong, only a small precision in quantizing the sensing outcomes is enough to have the desired detection performance. Therefore, the optimizer takes the advantage of this effect by reducing the number of quantization levels to decrease the reporting channel contaminations on the reported sensing outcomes. Moreover, as long as the listening channel SNR is high, the optimal number of quantization levels remains low for low-, medium-, and high-level reporting SNRs. This means, for the high listening-channel SNR, that the optimal number of levels is not sensitive to the reporting channel SNR levels. In other words, when the local detection processes are reliable, the overall system performance is not affected significantly by the reporting channel degradations. However, we observe a different behavior when the listening-channel SNR is low, i.e., when cooperation in sensing is highly necessary. Specifically, since the local sensing has to be performed on weak PU signals in this case, the uncertainty in determining whether the PU is active or not is quite high. The optimizer tries to compensate for this uncertainty (or not to contribute to this uncertainty) by increasing the precision of the local quantization process at the expense of suffering a higher degradation at the reporting phase. Recall that increasing the number of levels improves the quality of local quantization but increases the BEP of the reporting channel as well. As an important conclusion, the proposed joint optimization approach enables the system to trade the reporting channel quality for the local sensing quality in order to achieve the best overall detection performance. These observations are illustrated in Table III, which shows the optimal number of quantization levels for various listening and reporting SNRs.

Table IV shows typical values of the obtained optimal weighting and quantization vectors for sensing nodes operating in different listening- and reporting-channel conditions.

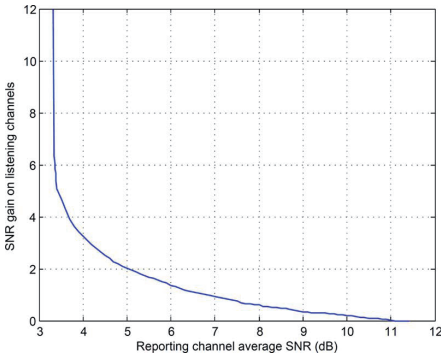

Fig. 5. SNR gains obtained by the proposed joint reporting-fusion optimization scheme vs. the average reporting SNR level experienced by $K = 5$ sensing nodes (SNR_0) and with reporting SNR deviation of $\Delta = 1\,(\text{dB})$.

TABLE III
OPTIMAL NUMBER OF QUANTIZATION LEVELS FOR DIFFERENT LISTENING AND REPORTING SNRS

$\text{SNR}_r \downarrow$, $\text{SNR}_l \rightarrow$	-15 dB	-10 dB	0 dB
0 dB	15	15	4
5 dB	30	15	4
15 dB	31	16	4

VI. CONCLUSION

In this paper, after a structured study of major phases in a centralized cooperative sensing scheme, the effect of the

TABLE IV
OPTIMAL FUSION WEIGHTS, AND OPTIMAL NUMBER OF QUANTIZATION LEVELS FOR NODES OPERATING IN DIFFERENT LISTENING-CHANNEL AND REPORTING-CHANNEL CONDITIONS

SNR_l (dB)	-15	-10	0
SNR_r (dB)	15	5	0
Opt. Weights	0.0037	0.0171	0.9998
Opt. No. of Levels	31	16	4

number of bits used in local sensing quantization on the overall sensing performance in a CRN with cooperative sensing has been introduced and a joint optimization approach has been proposed to optimize the linear soft-combining scheme at the fusion phase with the number of quantization bits used by each sensing node at the reporting phase. The presented analytical expressions followed by simulation results demonstrate that, through joint consideration of the reporting and fusion phases in a cooperative sensing scheme, considerable performance gains can be obtained. This better performance stems from better exploitation of spatial/user diversities in CRNs. The proposed joint optimization scheme leads to more powerful distributed detection performance, especially when the sensing nodes have to work at low SNR regimes.

APPENDIX I
PROOF OF LYAPUNOV'S CLT CONDITION FOR THE RECEIVED QUANTIZED TEST SUMMARIES

Proof: For simplicity, we consider the uniform quantization here. Other quantization schemes can be treated similarly. For any $\delta > 0$, we have (for either $\mathcal{H}_0$ or $\mathcal{H}_1$)

$$E\left[\left|y_i - \overline{y}_i\right|^{2+\delta}\right] \leq (2m\sigma_i)^{2+\delta} \leq (2m\sigma_{\max})^{2+\delta} \tag{61}$$

where $\overline{y}_i$ denotes the mean of y_i, and $\sigma_{\max}$ denotes the maximum standard deviation of the sensing outcomes. We also have

$$s_K^2 \triangleq \sum_{i=1}^{K} \sigma_{y_i}^2 \geq K\sigma_{y_i,\min}^2 \tag{62}$$

where $\sigma_{y_i,\min}^2$ denotes the minimum variance of the received test summaries. Using the above inequalities, we can set an upper bound on the ratio in Lyapunov's condition, i.e.,

$$\frac{1}{s_K^{2+\delta}} \sum_{i=1}^{K} E\left[\left|y_i - \overline{y}_i\right|^{2+\delta}\right] \leq \frac{K\left(2m\sigma_{i,\max}\right)}{K^{1+\delta/2}\sigma_{y_i,\min}^2}. \tag{63}$$

Finally, since $\sigma_i \neq 0$ requires that $\sigma_{y_i,\min}^2 \neq 0$, the above upper bound approaches zero as $K \to \infty$, hence,

$$\lim_{K\to\infty} \frac{1}{s_K^{2+\delta}} \sum_{i=1}^{K} E\left[\left|y_i - \overline{y}_i\right|^{2+\delta}\right] = 0. \tag{64}$$

■

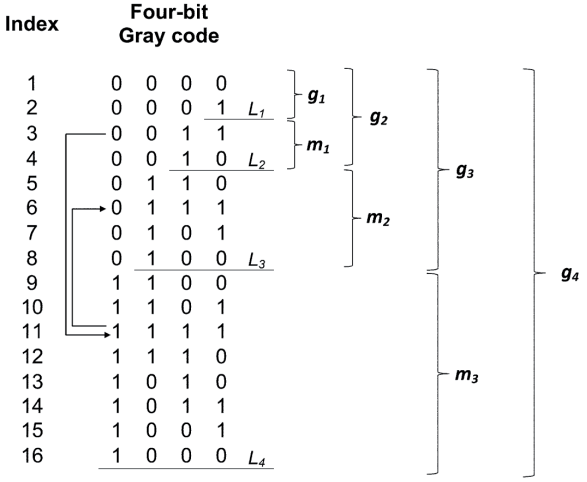

Fig. 6. Four-bit Gray code structure. The least significant bits are the rightmost ones.

APPENDIX II
PROOF OF LEMMA 1

Proof: The Gray code structure is depicted in Fig. 6, where a four-bit Gray code is decomposed by four lines L_1, L_2, L_3, and L_4 into four blocks $\mathbf{g}_1$, $\mathbf{g}_2$, $\mathbf{g}_3$, and $\mathbf{g}_4$. The vector $\mathbf{g}_k$, $k = 1, \ldots, 4$, denotes the k-bit Gray code in this format. Although only four bits are considered here, by repeating this structure we can construct Gray codes with arbitrary number of bits. According to this structure, we can see that $\mathbf{g}_{k+1}$ is generated by vertically concatenating $\mathbf{g}_k$ with $\mathbf{m}_k$, i.e., for $k \geq 1$,

$$\mathbf{g}_{k+1} = \begin{bmatrix} \mathbf{g}_k \\ \mathbf{m}_k \end{bmatrix} \tag{65}$$

where $\mathbf{m}_k$ is generated by mirroring $\mathbf{g}_k$ with respect to L_k and then flipping its $(k+1)$th bit into 1. Therefore, considering only the first k bits, $\mathbf{g}_k$ and $\mathbf{m}_k$ are symmetric with respect to L_k. The leftmost column in Fig. 6 contains the index of codewords in this structure. For $n = 1, \ldots, 2^k$, we denote the nth elements of $\mathbf{g}_k$ and $\mathbf{m}_k$ by $g_k(n)$ and $m_k(n)$, respectively.

Because of the aforementioned symmetry, for $l_e \geq 1$ and $n = 1, \ldots, 2^{l_e}$, change in the code index due to flipping the l_eth bit in $g_{l_e}(n)$ and $m_{l_e}(n)$ are the same. In other words, if flipping the l_eth bit in $g_{l_e}(n)$ converts it to $g_{l_e}(n_1)$ and flipping the same bit in $m_{l_e}(n)$ turns it into $m_{l_e}(n_2)$, then $n_1 = n_2$. That is, the change in the element index of $\mathbf{g}_{l_e}$ (i.e., $n_1 - n$) and $\mathbf{m}_{l_e}$ are equal when the l_eth bit is flipped in both $\mathbf{g}_{l_e}$ and $\mathbf{m}_{l_e}$. Moreover, since $\mathbf{g}_{l_e+1}$ is composed of $\mathbf{g}_{l_e}$ and $\mathbf{m}_{l_e}$, the same rule applies for $\mathbf{g}_{l_e+1}$. Consequently, when flipping the l_eth bit, the same jumping rule holds for all $\mathbf{g}_n$, $n \geq l_e$. Thus, in order to find how the code index is changed when flipping the l_eth bit, we only need to consider $\mathbf{g}_{l_e}$.

To maintain simplicity, we only focus on $l_e = 3$, but the general case is proved by considering the Gray code structure's

symmetry which stems from the explained mirroring process. Recall that by considering $\mathbf{g}_3$ and $l_e = 3$, we find the jumping rule when the 3rd bit is flipped in a *complete Gray code with arbitrary number of bits*. Focusing on $\mathbf{g}_3$ in Fig. 6, we see that flipping the 3rd bit is equivalent to two successive processes: *i*) increasing the code index by 2^{l_e} (which is 8 in this case), *ii*) mirroring the new codeword with respect to L_3. These two processes are shown by arrows on $g_3(3)$ in Fig. 6 as an example. $g_3(3)$ is first converted to $m_3(3)$ and then mirrored against L_3 to give $g_3(6)$.

According to the presented structure, mirroring a codeword with index $n \geq 2^{l_e}$ with respect to L_{l_e} is equivalent to decrease n by $2\mathrm{mod}(n-1, 2^{l_e})+1$. Therefore, the two mentioned processes on the code index can be indicated by the following relationship

$$k(n, l_e) = n + 2^{l_e} - 2\mathrm{mod}(n-1, 2^{l_e}) - 1 \tag{66}$$

where k denotes the new index and n denotes the old index. ■

Appendix III
Proof of Lemma 2

Proof: If k only contains a single 1 in its binary format (i.e., $n_e = 1$), then $k = 2^{k_1-1}$ and the XOR operation leads to

$$n \oplus k = \begin{cases} n + 2^{k_1-1}, & b_{k_1}(n) = 0 \\ n - 2^{k_1-1}, & b_{k_1}(n) = 1. \end{cases} \tag{67}$$

The right-hand side of this equation can be expressed in closed form by using the step function as

$$n \oplus k = n + [2u(0.5 - b_{k_1}(n)) - 1]\, 2^{k_1-1}. \tag{68}$$

For $n_e \geq 1$, we have

$$k = 2^{k_1-1} \oplus 2^{k_2-1} \oplus \ldots \oplus 2^{k_{n_e}-1}. \tag{69}$$

Hence, (34) is obtained by successively applying (68) on the first, second, ..., and n_eth bit in k. ■

References

[1] N. Jesuale, "Lights and sirens broadband," in *Proc. IEEE DySPAN*, Aachen, Germany, May 3–6, 2011, pp. 467–475.

[2] Y. Zeng, Y. Liang, S. W. O. Z. Lei, F. Chin, and S. Sun, "Worldwide regulatory and standardization activities on cognitive radio," in *Proc. IEEE DySPAN*, Washington DC, Apr. 6–9, 2010, pp. 1–9.

[3] I. F. Akyildiz, B. F. Lo, and R. Balakrishnan, "Cooperative spectrum sensing in cognitive radio networks: A survey," *Elsevier Phys. Commun.*, vol. 4, no. 1, pp. 40–62, Mar. 2011.

[4] *Unlicensed operation in the TV broadcast bands, additional spectrum for unlicensed devices below 900 MHz and in the 3 GHz band, order*, FCC Docket Nos. 04–18 and 602–380, Jan. 2011, pp. 11–131.

[5] C. Clancy, J. Hecker, E. Stuntebeck, and T. O'Shea, "Applicant. of mach. learning to cognitive radio networks," *IEEE Wireless. Commun.*, vol. 4, no. 1, pp. 47–22, Aug. 2007.

[6] G. Ganesan and Y. G. Li, "Cooperative spectrum sensing in cognitive radio—Part I: Two user networks," *IEEE Trans. Wireless Commun.*, vol. 6, no. 6, pp. 2204–2213, 2007.

[7] J. Ma, G. Zhao, and Y. Li, "Soft combination and detection for cooperative spectrum sensing in cognitive radio networks," *IEEE Trans. Wireless Commun.*, vol. 7, no. 11, pp. 28–40, Nov. 2008.

[8] Z. Quan, S. Cui, and A. H. Sayed, "Optimal linear cooperation for spectrum sensing in cognitive radio networks," *IEEE J. Sel. Topics Signal Process.*, vol. 2, no. 1, pp. 28–40, Feb. 2008.

[9] Y. Zou, Y. Yao, and B. Zheng, "A selective-relay based cooperative spectrum sensing scheme without dedicated reporting channels in cognitive radio networks," *IEEE Trans. Wireless Commun.*, vol. 10, no. 4, pp. 1188–1198, Apr. 2011.

[10] Q. Chen, M. Motani, W. Wong, and A. Nallanathan, "Cooperative spectrum sensing strategies for cognitive radio mesh networks," *IEEE J. Sel. Topics Signal Process.*, vol. 5, no. 1, pp. 56–67, Feb. 2011.

[11] K. Hossain, B. Champagne, and A. Assra, "Cooperative multiband joint detection with correlated spectral occupancy in cognitive radio networks," *IEEE Trans. Signal.Process.*, vol. 60, no. 5, pp. 2682–2687, May 2012.

[12] Z. Quan, W. Ma, S. Cui, and A. H. Sayed, "Optimal linear fusion for distributed detection via semidefinite programming," *IEEE Trans. Signal Process.*, vol. 58, no. 4, pp. 2431–2436, 2010.

[13] G. Taricco, "Optimization of linear cooperative spectrum sensing for cognitive radio networks," *IEEE J. Sel. Topics Signal Process.*, vol. 5, no. 1, pp. 77–86, Feb. 2011.

[14] Z. Quan, S. Cui, A. H. Sayed, and H. V. Poor, "Optimal multiband joint detection for spectrum sensing in cognitive radio networks," *IEEE Trans. Signal Process.*, vol. 57, no. 3, pp. 1128–1140, Mar. 2009.

[15] S. Chaudhari and V. Koivunen, "Effect of quantization and channel errors on collaborative spectrum sensing," in *Proc. 43rd Asilomar Conf. Signals, Syst., Comput.*, Nov. 2009, pp. 528–533.

[16] J. Li, Z. Li, J. Si, and Y. Zhang, "Efficient soft decision fusion rule in cooperative spectrum sensing," *IEEE Trans. Signal Process.*, vol. 61, no. 8, pp. 1931–1943, Apr. 2013.

[17] D. Oh, H. Lee, and H. Y. Lee, "Linear hard decision combining for cooperative spectrum sensing in cognitive radio systems," in *Proc. 72nd IEEE Veh. Technol. Conf.*, Sep. 6–9, 2010, pp. 1–5.

[18] T. C. Aysal, S. Kandeepan, and R. Piesiewicz, "Cooperative spectrum sensing with noisy hard decision transmissions," in *Proc. IEEE ICC*, Jun. 14–18, 2009, pp. 1–5.

[19] S. Chaudhari and V. K. J. Lunden, "BEP walls for collaborative spectrum sensing," in *Proc. IEEE Int. Conf. Acoust., Speech, Signal Process. (ICASSP)*, May 22–27, 2011, pp. 2984–2987.

[20] B. Chen and P. K. Willett, "On the optimality of the likelihood-ratio test for local sensor decision rules in the presence of nonideal channels," *IEEE Trans. Inf. Theory*, vol. 51, pp. 693–699, Feb. 2005.

[21] J. Tsitsiklis, *Decentralized detection, advances in statistical signal processing*, H. V. Poor and J. B. Thomas, Eds. Greenwich, U.K.: CT: JAI Press, 1993, vol. 2.

[22] S. Chaudhari, J. Lunden, V. Koivunen, and H. V. Poor, "Cooperative sensing with imperfect reporting channels: Hard decisions or soft decisions?," *IEEE Trans. Signal Process.*, vol. 60, no. 1, pp. 18–28, Jan. 2012.

[23] Z. Quan, S. Chui, and A. H. Sayed, "An optimal strategy for cooperative spectrum sensing in cognitive radio networks," in *Proc. IEEE GLOBECOM*, Washington DC, USA, Nov. 2007, pp. 2947–2951.

[24] Y. C. Liang, Y. Zeng, E. Peh, and A. T. Hong, "Sensing-throughput tradeoff for cognitive radio networks," *IEEE Wireless. Commun.*, vol. 7, no. 4, pp. 1326–1337, Apr. 2008.

[25] S. Chaudhari and J. Lundén, "BEP walls for cooperative sensing in cognitive radios using K-out-of-N fusion rules," *Elsevier Signal Process.*, pp. 1900–1908, Jul. 2013.

[26] H. B. Yilmaz, T. Tugcu, and F. Alagoz, "Novel quantization-based spectrum sensing scheme under imperfect reporting channel and false reports," *Int. J. Commun. Syst.*, Jul. 2012 [Online]. Available: http://onlinelibrary.wiley.com/doi/10.1002/dac.2408/abstract, doi: 10.1002/dac.2408

[27] P. Billingsley, *Probability and Measure*, 3rd ed. New York, NY, USA: Wiley, 1995.

[28] M. R. Garey and D. S. Johnson, *Computers and Intractability: A Guide to the Theory of NP-Completeness*. New York, NY, USA: Freeman, 1979.

[29] Y. Shi, Y. T. Hou, and H. Zhou, "Per-node based optimal power control for multi-hop cognitive radio networks," *IEEE Trans. Wireless Commun*, vol. 8, no. 10, pp. 5290–5299, Oct. 2009.

[30] H. D. Sheali and W. P. Admas, *A Reformulation-Linearization Technique for Solving Discrete and Continuous Nonconvex Problems*. Norwell, MA, USA: Kluwer, 1999.

[31] G. P. McCormick, *Nonlinear Programming: Theory, Algorithms, and Applications*. New York, NY, USA: Wiley, 1983.

[32] P. Belotti, J. Lee, L. Liberti, F. Margot, and A. Wachter, "Branching and bound tightening techniques for non-convex MINLP," IBM Res. Rep., 2008.
[33] J. Lundén, V. Koivunen, A. Huttunen, and H. V. Poor, "Collaborative cyclostationary spectrum sensing for cognitive radio systems," *IEEE Trans. Signal Process.*, vol. 57, no. 11, pp. 4182–4195, Nov. 2009.

Younes Abdi (S'10) received his B.Sc. degree from the University of Tabriz, Tabriz, Iran, in 2008 and his M.Sc. degree from Tarbiat Modares University, Tehran, Iran, in 2011, both in Electrical Engineering.

From October 2010 to November 2011, he was with Radio Communications Group at Iran Telecommunications Research Center (ITRC), Tehran, Iran, working on standardization and regulatory issues of cognitive radio networks. In 2012, he joined the Faculty of Information Technology at the University of Jyväskylä, Jyväskylä, Finland, where he is currently pursuing his studies towards the Ph.D. degree. He is also a member of working group 1900.1 in the IEEE Dynamic Spectrum Access Networks Standards Committee (DySPAN-SC). His research has been financially supported by Finnish National Graduate School in Electronics, Telecommunications, and Automation (GETA) and Jyväskylä Doctoral Program in Computing and Mathematical Sciences (COMAS). His current research interests are in the areas of advanced signal processing and wireless communications.

Tapani Ristaniemi (SM'11) received his M.Sc. degree in mathematics in 1995, the Ph.Lic. degree in applied mathematics in 1997, and the Ph.D. degree in wireless communications in 2000, all from the University of Jyväskylä, Jyväskylä, Finland. In 2001, he was appointed as a Professor in the Department of Mathematical Information Technology, University of Jyväskylä. In 2004, he moved to the Department of Communications Engineering, Tampere University of Technology, Tampere, Finland, where he was appointed as a Professor of wireless communications. In 2006, he moved back to the University of Jyväskylä to take up his appointment as a Professor of computer science. He is an Adjunct Professor of Tampere University of Technology. In 2013, he was a Visiting Professor in the School of Electrical and Electronic Engineering, Nanyang Technological University, Singapore. He has authored or co-authored over 150 publications in journals, conference proceedings, and invited sessions. He served as a Guest Editor of IEEE WIRELESS COMMUNICATIONS in 2011 and currently he is an Editorial Board Member of *Wireless Networks* and the *International Journal of Communication Systems*. His research interests are in the areas of brain and communication signal processing and wireless communication systems.

Besides academic activities, Professor Ristaniemi is also active in the industry. In 2005, he co-founded a start-up, Magister Solutions, Ltd., in Finland, specializing in wireless systems (R&D) for telecom and space industries in Europe. Currently, he serves as a consultant and a Member of the Board of Directors.

PII

EXTENSION OF DEFLECTION COEFFICIENT FOR LINEAR FUSION OF QUANTIZED REPORTS IN COOPERATIVE SENSING

by

Younes Abdi and Tapani Ristaniemi

Proc. IEEE 25th Annual International Symposium on Personal, Indoor, and Mobile Radio Communications (PIMRC), pp. 928-932, Washington DC, USA, Sept. 2-5, 2014

2014 IEEE 25th International Symposium on Personal, Indoor and Mobile Radio Communications

Extension of Deflection Coefficient for Linear Fusion of Quantized Reports in Cooperative Sensing

Younes Abdi and Tapani Ristaniemi
Faculty of Information Technology, University of Jyväskylä, FIN-40014 Jyväskylä, Finland
Email: younes.abdi@jyu.fi, tapani.ristaniemi@jyu.fi

***Abstract*—Maximizing the so-called *deflection coefficient* is commonly used as an effective approach to design cooperative sensing schemes with low computational complexity. In this paper, an extension to the deflection coefficient is proposed which captures the effects of the quantization processes at the sensing nodes, jointly with the impact of linear combining at the fusion center. The proposed parameter is then used to formulate a new mixed-integer nonlinear programming problem as a fast suboptimal method to design a distributed detection scenario where the nodes report their sensing outcomes to a fusion center through nonideal digital links. Numerical evaluations show that the performance of the proposed method is very close to the optimal case.**

I. Introduction

Spectrum sensing is the key element in each cognitive radio (CR) system and enables its user, commonly referred to as secondary user (SU), to find transmission opportunities in spectrum resources allocated exclusively to license holders. In this context, the license holders are called primary users (PU) and have the exclusive right of using the spectrum. The reliability of spectrum sensing is greatly enhanced through establishing certain kinds of cooperation among the sensing nodes. This cooperation is commonly coordinated by and the overall sensing outcome is generated in a special node called the fusion center (FC). Specifically, each node first performs spectrum sensing individually by using its own built-in sensing scheme. Then, the sensing nodes send their local sensing outcomes to the FC through the so-called reporting channels and finally, the FC combines the received local sensing outcomes to decide the presence or absence of the PU.

It is worth noting that, for a distributed detection problem with nonideal analogue communication channels between the distributed nodes and FC, the globally optimal structure is to perform likelihood ratio test (LRT) both at individual nodes and at the FC [1]. However, how to efficiently find the optimal LRT thresholds for individual nodes and for the fusion center is still unknown [2]. For the quantized soft decision case, i.e., when the reporting is performed through nonideal (i.e., erroneous) digital links, a solution for optimizing the local quantization levels jointly with the LRT threshold at the FC may or may not exist [3]. Even if the optimal solution exists, the threshold calculations are not trivial and complex optimization schemes are needed to solve them. These difficulties are commonly avoided by assuming a linear fusion scheme [2], [4]–[7] which is the base for our considered architecture. In particular, linear combining is shown in [2] to perform very closely to the optimal LRT method with much less computational complexity.

Maximizing the so-called *deflection coefficient* (DC) [8], [9] or its modified version, *modified deflection coefficient* (MDC) [2], [4], [6], [7] is commonly used in the literature as a fast suboptimal approach to design effective fusion schemes in distributed detection scenarios. Using this parameter, i.e., the variance-normalized distance between the centers of two conditional distributions of the global test summary, is effective in the sense that it provides very close results to the ones obtained by the optimal LRT method at low computational cost. This method is of special interest when direct formulation of the false alarm and missed detection probabilities leads to nonconvex optimization problems.

In this paper, we assume that the FC performs linear combining on the reported local test summaries which receive through nonideal digital reporting channels. We first extend our previous analysis in [6] and [7] to the case in which the CR nodes use analogue-to-digital converters (ADC) with non-integer bit resolutions. Then, we propose a new version of the deflection coefficient which captures the effects of the quantization process at the CR nodes jointly with the linear fusion at the FC. Through these extensions, we construct and solve a new mixed-integer nonlinear programming problem to optimize the linear combining process at the FC, jointly with the number of levels used by each node for quantizing the sensing outcomes before reporting them.

II. System Model

A cognitive radio network (CRN) with K sensing nodes is considered in this paper. These nodes cooperatively sense the radio spectrum to find temporal and/or spatial vacant bands for their data communication. In our adopted model, the kth sample of the received PU signal at the ith CR node is represented as

$$\begin{cases} x_i(k) = \nu_i(k), & \mathcal{H}_0 \\ x_i(k) = h_i s(k) + \nu_i(k), & \mathcal{H}_1 \end{cases} \tag{1}$$

where $\mathcal{H}_1$ and $\mathcal{H}_0$ denote the hypotheses representing the presence or absence of the PU, respectively. $s(k)$ denotes the signal transmitted by the PU and $x_i(k)$ is the received signal by the the ith SU. h_i is the listening channel block fading gain and $\nu_i(k) \sim \mathcal{CN}(0, \sigma^2_{\nu_i})$ denotes the additive white Gaussian noise (AWGN). Without loss of generality, $s(k)$ and

978-1-4799-4912-0/14/$31.00 ©2014 IEEE

$\{\nu_i(k)\}$ are assumed to be independent of each other. CR node i, $i = 1, ..., K$ performs spectrum sensing using its built-in sensor (which can be of any common types like Energy Detection (ED), Cyclostationary Detection (CSD), etc.) to derive a local test statistic u_i and then uses the following quantization rule to map it on a bit sequence of length d_i

$$\psi_i(u_i) = q_{n,i} \quad \text{if} \quad t_{n,i} \leqslant u_i < t_{n+1,i} \tag{2}$$

where $\psi_i(\cdot)$ denotes the quantization process at the ith SU, $q_{n,i}$, $n = 1, ..., 2^{d_i}$ is its nth quantization level, while $t_{n,i}$ and $t_{n+1,i}$ denote the corresponding boundaries. Given the local sensing method and the quantization processes incorporated at the ith sensing node, the probability distribution of ψ_i is obtained. We denote the number of quantization bits used in all sensing nodes by $\mathbf{d} \triangleq \left[d_1, ..., d_K\right]^T$.

The generated reporting bit sequences are then transmitted to the FC through the reporting channel in an orthogonal manner. The effect of reporting channel impairments on the transmitted bit sequences of the ith CR node is modeled as a bit error probability (BEP) denoted by $P_{\mathrm{b},i}$. The reporting channel is assumed to affect each node's transmitted reporting bit sequence independently. Moreover, errors introduced on different bits in a transmitted reporting sequence by the reporting channel are assumed to be independent and identically distributed (i.i.d). Therefore, the received quantized test statistics at the FC, y_i, $i = 1, ..., K$, are independent discrete random variables whose probability mass functions (pmf) can be represented (for $j = 0, 1$) as [3]

$$\Pr\{y_i = q_{n,i}|\mathcal{H}_j\} = \sum_{k=1}^{2^{d_i}} P_{\mathrm{b},i}^{D_{n,k}} \left(1 - P_{\mathrm{b},i}\right)^{d_i - D_{n,k}} \Pr\{\psi_i(u_i) = q_{k,i}|\mathcal{H}_j\} \tag{3}$$

where $D_{n,k}$ is the Hamming distance between bit sequences corresponding to levels $q_{n,i}$ and $q_{k,i}$.

Focusing on transmitted and received bit strings in the reporting phase, we model the effect of the reporting channel by using the Exclusive OR (XOR) operator as $r_i = s_i \oplus e_i$ where d_i-bit random variables s_i, r_i, and e_i denote the sent and received bit sequences and error caused by the reporting channel, respectively. If we denote the value of s_i associated with the nth quantization level (i.e., $q_{n,i}$) by $s_{n,i}$, the following invertible mapping describes the correspondence between the quantization levels and the bit sequences

$$\begin{cases} \Gamma : \left\{1, 2, ..., 2^{d_i}\right\} \rightarrow \left\{0, 1, ..., 2^{d_i} - 1\right\} \\ s_{n,i} = \Gamma(n) \end{cases} \tag{4}$$

In other words, $s_i = \Gamma(n)$ if and only if $\psi_i = q_{n,i}$, or equivalently, $s_i = n$ if and only if $\psi_i = q_{\Gamma^{-1}(n),i}$. Therefore, the pmf of s_i can be expressed as (for $n = 0, 1, ..., 2^{d_i} - 1$, and $j = 0, 1$)

$$P_{s_i|\mathcal{H}_j}(n) \triangleq \Pr\{s_i = n|\mathcal{H}_j\} = \Pr\left\{\psi_i = q_{\Gamma^{-1}(n),i}|\mathcal{H}_j\right\}. \tag{5}$$

Without loss of generality, we have assumed the same mapping process for all CR nodes.

Given the BEP $P_{b,i}$, each bit in the random variable e_i follows the Bernoulli distribution. Consequently, the pmf of e_i is derived as, (for $n = 0, 1, ..., 2^{d_i} - 1$)

$$P_{e_i}(n) = P_{b,i}^{w_H(n)} \left(1 - P_{b,i}\right)^{d_i - w_H(n)} \tag{6}$$

where $w_H(n)$ denotes the Hamming weight of the binary representation of n.

In order to derive the pmf of r_i, we use the fact that the assumed reporting channel contamination does not depend on the reported bit sequence s_i, nor the behavior of the PU, i.e., [7]

$$\begin{aligned} P_{r_i|\mathcal{H}_j}(n) &= \sum_{k=0}^{2^{d_i}-1} Pr\{r_i = n|e_i = k|\mathcal{H}_j\} Pr\{e_i = k\} \\ &= \sum_{k=0}^{2^{d_i}-1} Pr\{s_i = n \oplus k|e_i = k|\mathcal{H}_j\} Pr\{e_i = k\} \\ &= \sum_{k=0}^{2^{d_i}-1} Pr\{s_i = n \oplus k|\mathcal{H}_j\} Pr\{e_i = k\} \\ &= \sum_{k=0}^{2^{d_i}-1} P_{s_i|\mathcal{H}_j}(n \oplus k) P_{b,i}^{w_H(k)} \left(1 - P_{b,i}\right)^{d_i - w_H(k)} \end{aligned} \tag{7}$$

Assuming a general M-ary modulation for the reporting channel, the reporting BEP can be expressed as

$$P_{\mathrm{b},i} = c_M Q\left(\sqrt{\frac{c''_M}{d_i}}\right) \tag{8}$$

where $c''_M = \frac{c'_M |h_{r,i}|^2 E_r}{N_0 log_2 M}$, $Q(x) \triangleq \int_x^\infty \exp(-t^2/2)dt/\sqrt{2\pi}$ is the Q-function, c_M and c'_M are two constants determined by the modulation type. $h_{\mathrm{r},i}$, E_{r}, and N_0 denote the reporting channel gain, reporting signal energy, and noise power spectral density, respectively.

Linear combining is performed at the FC, meaning that, the global test statistic y_c is constructed as a weighted sum of the received quantized levels, i.e., $y_{\mathrm{c}} = \mathbf{w}^T\mathbf{y}$ where $\mathbf{w} \triangleq [w_1, ..., w_K]^T$ and $\mathbf{y} \triangleq [y_1, ..., y_K]^T$. Finally, y_c is compared against a predefined threshold ξ to decide the presence or absence of the PU, i.e.,

$$\begin{cases} \mathcal{H}_1, & y_{\mathrm{c}} \geq \xi \\ \mathcal{H}_0, & y_{\mathrm{c}} < \xi \end{cases} \tag{9}$$

The detector performance is commonly measured using two probabilities, namely the probability of false alarm $P_{\mathrm{fa}} = \Pr\{y_{\mathrm{c}} \geq \xi|\mathcal{H}_0\}$ and the probability of missed detection $P_{\mathrm{md}} = \Pr\{y_{\mathrm{c}} < \xi|\mathcal{H}_1\}$. Both false alarm and missed detection probabilities depend on the probability distribution of the global test statistics y_c which can be derived as a convolution of the pmfs of K independent random variables $\{y_i\}_{i=1}^K$.

III. Reporting-Fusion Optimization

Our goal is to jointly optimize $\mathbf{w}$ and $\mathbf{d}$ to achieve the best cooperative sensing performance. We determine the weighting vector $\mathbf{w}$ at the FC and $\mathbf{d}$ used by the sensing nodes, through

jointly considering the effects of both the listening and reporting channels.

We first formulate the optimization problem based on minimizing the missed detection probability subject to an upper bound on the false alarm probability

$$\begin{aligned} &\min_{\mathbf{w},\mathbf{d}} P_{\text{md}} \quad \text{(P1)} \\ \text{s.t.} \quad &P_{\text{fa}} \leq \alpha \end{aligned}$$

where α is the given upper limit on the false alarm probability.

According to the central limit theorem, if K is large enough, we can assume a Gaussian distribution for y_c and the false alarm and missed detection probabilities can be expressed in closed form as

$$P_{\text{fa}} = Q\left(\frac{\xi - \boldsymbol{\mu}_{\mathcal{H}_0}^T \mathbf{w}}{\sqrt{\mathbf{w}^T \boldsymbol{\Sigma}_{\mathcal{H}_0} \mathbf{w}}}\right) \tag{10}$$

$$P_{\text{md}} = 1 - Q\left(\frac{\xi - \boldsymbol{\mu}_{\mathcal{H}_1}^T \mathbf{w}}{\sqrt{\mathbf{w}^T \boldsymbol{\Sigma}_{\mathcal{H}_1} \mathbf{w}}}\right) \tag{11}$$

where (for $j = 1, 2$) $\boldsymbol{\mu}_{\mathcal{H}_j} \triangleq \mathrm{E}[\mathbf{y}|\mathcal{H}_j]$ and $\boldsymbol{\Sigma}_{\mathcal{H}_j} \triangleq \mathrm{E}[\mathbf{y}\mathbf{y}^T|\mathcal{H}_j] = diag(\sigma^2_{y_1|\mathcal{H}_j}, ..., \sigma^2_{y_K|\mathcal{H}_j})$. We have found through numerical evaluations that Gaussian distribution fits well for $K \geq 5$. Now if we eliminate ξ in Eqs. (10) and (11) by considering a target false alarm probability $P_{\text{fa}} = \alpha$, (P1) is converted to

$$\max_{\mathbf{w},\mathbf{d}} Q\left(\frac{Q^{-1}(\alpha)\sqrt{\mathbf{w}^T \boldsymbol{\Sigma}_{\mathcal{H}_0} \mathbf{w}} - \mathbf{a}^T \mathbf{w}}{\sqrt{\mathbf{w}^T \boldsymbol{\Sigma}_{\mathcal{H}_1} \mathbf{w}}}\right) \quad \text{(P2)}$$

where $Q^{-1}(\cdot)$ is the functional inverse of the Q-function, $\mathbf{a} \triangleq [a_1, ..., a_K]^T \triangleq \boldsymbol{\mu}_{\mathcal{H}_1} - \boldsymbol{\mu}_{\mathcal{H}_0}$ and for $i = 1, ..., K$ we have $a_i \triangleq \mathrm{E}[y_i|\mathcal{H}_1] - \mathrm{E}[y_i|\mathcal{H}_0]$. In our previous work [7], we have developed a Branch-and-Bound (BnB) procedure to solve (P2). Moreover, we have shown in [7] that the statistics of the reported quantized test summaries, i.e., $\mathbf{a}$, $\boldsymbol{\Sigma}_{\mathcal{H}_0}$, and $\boldsymbol{\Sigma}_{\mathcal{H}_1}$ can be obtained by the following relation

$$E[y_i^\lambda|\mathcal{H}_j] = \sum_{n=1}^{2^{d_i}} q_{n,i}^\lambda P_{r_i|\mathcal{H}_j}\left(\Gamma(n)\right), \quad \lambda = 1, 2, ... \tag{12}$$

where $P_{r_i|\mathcal{H}_j}(n)$ can be expressed as a function of d_i as

$$\begin{aligned} P_{r_i|\mathcal{H}_j}(n) &= (1 - P_{b,i})^{d_i} P_{s_i|\mathcal{H}_j}(n) \\ &+ \sum_{n_e=1}^{d_i} P_{b,i}^{n_e} (1 - P_{b,i})^{d_i - n_e} \sum_{k_1=1}^{d_i} \sum_{\substack{k_2=1 \\ k_2 \neq k_1}}^{d_i} ... \\ &\sum_{\substack{k_{n_e}=1 \\ k_{n_e} \neq k_1, ..., k_{n_e-1}}}^{d_i} P_{s_i|\mathcal{H}_j}(g(n, k_1, k_2, ..., k_{n_e})) \end{aligned} \tag{13}$$

and

$$\begin{aligned} g(n, k_1, k_2, ..., k_{n_e}) \triangleq\ & n + \left[2u(0.5 - b_{k_1}(n)) - 1\right] 2^{k_1 - 1} \\ &+ \left[2u(0.5 - b_{k_2}(n)) - 1\right] 2^{k_2 - 1} + ... \\ &+ \left[2u(0.5 - b_{k_{n_e}}(n)) - 1\right] 2^{k_{n_e} - 1} \end{aligned} \tag{14}$$

where k_i, $i = 1, ..., n_e$ denotes the location of ith 1 in k, $b_j(n)$, $j = 1, ..., d_i$ denotes the value of jth bit in n and $u(\cdot)$ is the step function which equals to 1 when its argument is positive and 0 otherwise.

For simplicity, we have considered discrete values for d_i so far. However, the number of quantization levels in ADCs is commonly characterized by their so-called bit resolution which is not necessarily an integer. For instance, one can use a 5.32-bit ADC to quantize a signal to 40 levels. Therefore, we extend the proposed analysis to account for non-integer values of d_i. We formally represent this matter by first modifying the mapping process as

$$\begin{cases} \Gamma : \left\{1, 2, ..., 2^{d_i}\right\} \rightarrow \left\{0, 1, ..., 2^{\lceil d_i \rceil} - 1\right\} \\ s_{n,i} = \Gamma(n) \end{cases} \tag{15}$$

where $\lceil d_i \rceil$ denotes the smallest integer greater that or equal to d_i. Then, the definition for the pmf has to be extended to account for the redundant bit strings. Since they are not used, their probability mass equals zero, i.e.,

$$P_{s_i|\mathcal{H}_j}(n) = 0 \quad \text{for } n \in \left\{0, ..., 2^{\lceil d_i \rceil} - 1\right\} - \mathcal{R}_\Gamma \tag{16}$$

where $\mathcal{R}_\Gamma$ denotes the range of the mapping process Γ. Finally, the pmf of the received bit strings is modified as

$$\begin{aligned} P_{r_i|\mathcal{H}_j}(n) &= (1 - P_{b,i})^{\lceil d_i \rceil} P_{s_i|\mathcal{H}_j}(n) \\ &+ \sum_{n_e=1}^{\lceil d_i \rceil} P_{b,i}^{n_e} (1 - P_{b,i})^{\lceil d_i \rceil - n_e} \sum_{k_1=1}^{\lceil d_i \rceil} \sum_{\substack{k_2=1 \\ k_2 \neq k_1}}^{\lceil d_i \rceil} ... \\ &\sum_{\substack{k_{n_e}=1 \\ k_{n_e} \neq k_1, ..., k_{n_e-1}}}^{\lceil d_i \rceil} P_{s_i|\mathcal{H}_j}(g(n, k_1, k_2, ..., k_{n_e})) \end{aligned} \tag{17}$$

The optimal linear fusion of analogue sensing outcomes can be derived through considering the Lagrange dual problem and Karush-Kuhn-Tucker (KKT) conditions [5]. Similarly, for a given $\mathbf{d}$, (P2) can be solved for optimal weighting vector as

$$\tilde{\mathbf{w}} = \boldsymbol{\Sigma}_{\mathcal{H}_0}^{-1/2} \left[Q^{-1}(\alpha)\mathbf{I}_K + \zeta \mathbf{A}\right]^{-1} \mathbf{c} \tag{18}$$

where $\mathbf{A} \triangleq \boldsymbol{\Sigma}_{\mathcal{H}_1} \boldsymbol{\Sigma}_{\mathcal{H}_0}^{-1}$ and $\mathbf{c} \triangleq \boldsymbol{\Sigma}_{\mathcal{H}_0}^{-1/2} \mathbf{a}$. ζ is the single root of the polynomial equation

$$\left\| \left[Q^{-1}(\alpha)\mathbf{I}_K + \zeta \mathbf{A}\right]^{-1} \mathbf{c} \right\| = 1 \tag{19}$$

and satisfies

$$Q^{-1}(\alpha)\mathbf{I}_K + \zeta \mathbf{A} \succ \mathbf{0} \tag{20}$$

where $\mathbf{0}$ stands for the null matrix and $\succ$ represents the element-wise inequality. Note that (19) and (20) specify ζ as a function of $\mathbf{d}$.

In order to gain insight about the major elements in (P2), we rewrite it in the following form by using (18) and through some basic algebraic manipulations,

$$\begin{aligned} &\min_{\mathbf{d},\zeta} \varphi(\mathbf{d}, \zeta) \quad \text{(P3)} \\ \text{s.t.} \quad &(19) \text{ and } (20) \end{aligned}$$

where

$$\varphi(\mathbf{d},\zeta) \triangleq \frac{Q^{-1}(\alpha) - \sum_{i=1}^{K} \frac{a_i^2}{Q^{-1}(\alpha)\sigma^2_{y_i|\mathcal{H}_0}+\zeta\sigma^2_{y_i|\mathcal{H}_1}}}{\sqrt{\sum_{i=1}^{K} \frac{a_i^2\sigma^2_{y_i|\mathcal{H}_1}}{\left(Q^{-1}(\alpha)\sigma^2_{y_i|\mathcal{H}_0}+\zeta\sigma^2_{y_i|\mathcal{H}_1}\right)^2}}}$$

Since the Q-function is strictly decreasing with respect to its argument, we have removed it from (P3) and turned the problem into a minimization.

It is worth noting that, the local sensing outcomes have greater variances when $\mathcal{H}_1$ is true (i.e., when the PU is present), compared to $\mathcal{H}_0$ case. Since the local sensing outcomes pass through the same quantization and reporting processes to reach the FC—regardless of whether the PU is active or not—the received sensing outcomes at the FC have greater variances in general when the PU signal is present. That is, $\sigma^2_{y_i|\mathcal{H}_1} \geq \sigma^2_{y_i|\mathcal{H}_0}$. Hence, we have

$$\tilde{\mathbf{w}}^T\boldsymbol{\Sigma}_{\mathcal{H}_1}\tilde{\mathbf{w}} \geq \tilde{\mathbf{w}}^T\boldsymbol{\Sigma}_{\mathcal{H}_0}\tilde{\mathbf{w}} = 1 \tag{21}$$

Applying this inequality on our cost function $\varphi(\mathbf{d},\zeta)$, we derive an upper bound, i.e.,

$$\varphi(\mathbf{d},\zeta) \leq Q^{-1}(\alpha) - \sum_{i=1}^{K} \frac{a_i^2}{Q^{-1}(\alpha)\sigma^2_{y_i|\mathcal{H}_0}+\zeta\sigma^2_{y_i|\mathcal{H}_1}} \tag{22}$$

A closer look at (22) leads to some interesting observations. In fact, the term inside the summation is the ratio of two performance metrics. Specifically, the numerator a_i^2 measures the sensor ability to discriminate between $\mathcal{H}_0$ and $\mathcal{H}_1$, whereas the denominator, measures the sensor uncertainty in declaring either $\mathcal{H}_0$ or $\mathcal{H}_1$. Note that due to (20), the denominator in (22) represents a positive linear combination of reported test summary variances $\sigma^2_{y_i|\mathcal{H}_0}$ and $\sigma^2_{y_i|\mathcal{H}_1}$. Therefore, the ratio in (22) can be interpreted as the SNR (measuring the detection quality) of the ith sensor report when received at the FC. In fact, it can be considered as an extended version of the DC and MDC which have been introduced in literature as good measures for performance optimization in cooperative spectrum sensing. We refer to the ratio in (22) as *extended deflection coefficient* (EDC).

These observations motivate us to propose a new approach for the discussed joint reporting-fusion optimization based on the EDC. We formally define EDC as

$$\Delta^2_{\text{ext}} \triangleq \frac{\left(\mathrm{E}\left[y_c|\mathcal{H}_1\right] - \mathrm{E}\left[y_c|\mathcal{H}_0\right]\right)^2}{Q^{-1}(\alpha)\mathrm{Var}\left\{y_c|\mathcal{H}_0\right\} + \zeta\mathrm{Var}\left\{y_c|\mathcal{H}_1\right\}} \tag{23}$$

Replacing y_c with its weighted sum definition, we have

$$\Delta^2_{\text{ext}} = \frac{\left(\mathbf{a}^T\mathbf{w}\right)^2}{\mathbf{w}^T\left[Q^{-1}(\alpha)\boldsymbol{\Sigma}_{\mathcal{H}_0} + \zeta\boldsymbol{\Sigma}_{\mathcal{H}_1}\right]\mathbf{w}} \tag{24}$$

We aim at finding $\mathbf{w}$ and $\mathbf{d}$ such that

$$\begin{aligned} &\max_{\mathbf{w},\mathbf{d}} \Delta^2_{\text{ext}} \quad \text{(P4)} \\ &\text{s.t.} \quad \|\mathbf{w}\| = 1 \end{aligned}$$

The constraint on the weight vector norm is necessary here to derive a unique solution since the EDC does not depend on $\|\mathbf{w}\|$. In order to derive an analytical solution for (P4) we first eliminate $\mathbf{w}$ as follows. Through the linear transformation [2]

$$\mathbf{w}' = \boldsymbol{\Sigma}_{\text{ext}}^{1/2}\mathbf{w} \tag{25}$$

the EDC is converted to

$$\Delta^2_{\text{ext}} = \frac{\mathbf{w}'^T\boldsymbol{\Sigma}_{\text{ext}}^{-T/2}\mathbf{a}\mathbf{a}^T\boldsymbol{\Sigma}_{\text{ext}}^{-1/2}\mathbf{w}'}{\mathbf{w}'^T\mathbf{w}'} \leq \left\|\boldsymbol{\Sigma}_{\text{ext}}^{-T/2}\mathbf{a}\right\|^2 \tag{26}$$

where $\boldsymbol{\Sigma}_{\text{ext}} \triangleq Q^{-1}(\alpha)\boldsymbol{\Sigma}_{\mathcal{H}_0} + \zeta\boldsymbol{\Sigma}_{\mathcal{H}_1}$ and the inequality follows the *Rayleigh-Ritz* inequality. The equality is achieved when

$$\mathbf{w}' = \boldsymbol{\Sigma}_{\text{ext}}^{-T/2}\mathbf{a} \tag{27}$$

Therefore, the optimal $\mathbf{w}$ which maximizes the EDC is derived as a function of $\mathbf{d}$ as

$$\mathbf{w}_{\text{edc}} = \frac{\boldsymbol{\Sigma}_{\text{ext}}^{-1/2}\mathbf{w}'}{\left\|\boldsymbol{\Sigma}_{\text{ext}}^{-1/2}\mathbf{w}'\right\|} \tag{28}$$

Replacing $\mathbf{w}$ with its EDC-optimal value $\mathbf{w}_{\text{edc}}$, the EDC can be rewritten as a function of $\mathbf{d}$

$$\Delta^2_{\text{ext}} = \mathbf{a}^T\boldsymbol{\Sigma}_{\text{ext}}^{-1}\mathbf{a} = \sum_{i=1}^{K} \frac{a_i^2}{Q^{-1}(\alpha)\sigma^2_{y_i|\mathcal{H}_0} + \zeta\sigma^2_{y_i|\mathcal{H}_1}} \tag{29}$$

Now, by comparing (29) with (22) we see that maximizing the variance-normalized distance between the centers of two conditional distributions of the global test summary y_c is equivalent to minimizing the upper bound in (22). Moreover, due to the existence of ζ in (29), (P4) is a MINLP problem which is NP-hard in general. A standard method for solving a MINLP is the BnB procedure. As mentioned before, we have developed a BnB algorithm in [7] for (P3) and a similar approach can be used to solve (P4) as well. Here, we develop an alternative suboptimal approach based on EDC which leads to nearly optimal performance, but at much lower computational cost. The proposed method is based on the fact that $\sigma^2_{y_i|\mathcal{H}_0}$ and $\sigma^2_{y_i|\mathcal{H}_1}$ only depend on d_i and considering a fixed value for ζ, converts (P4) from a $(K+1)$-dimensional problem into K one-dimensional integer programs. In other words, the computational complexity of the optimization is drastically decreased by considering a fixed ζ. Therefore, we decompose the optimization procedure into two consecutive processes in an iteration loop. Specifically, starting with an initial point for $\mathbf{d}$ denoted by $\mathbf{d}^{(0)}$, at kth iteration, we seek the best $\mathbf{d}^{(k)}$ based on $\zeta^{(k-1)}$ by solving the following set of optimizations,

For $i = 1, ..., K$,

$$d_i^{(k)} = \underset{d_i}{\operatorname{argmax}} \frac{a_i^2}{Q^{-1}(\alpha)\sigma^2_{y_i|\mathcal{H}_0} + \zeta^{(k-1)}\sigma^2_{y_i|\mathcal{H}_1}} \quad \text{(P5)}$$

where $d_i^{(k)}$ and $\zeta^{(k)}$ denote the values of d_i and ζ at kth iteration, respectively. Then, through considering (19) and (20) we find $\zeta^{(k)}$ for $\mathbf{d}^{(k)}$. Consequently, at each iteration we are dealing with K one-dimensional nonlinear integer programs. Therefore, the computational complexity of this approach increases linearly with the number of sensing nodes K.

TABLE I
LOW-COMPLEXITY LINEAR FUSION OF QUANTIZED REPORTS IN COOPERATIVE SENSING

Input:	ε
Output:	Suboptimal $\mathbf{d}$, $\mathbf{w}$
1.	Initialize $\mathbf{d}$ as $\mathbf{d}^{(0)}$;
2.	Solve (19) and (20) for $\zeta^{(0)}$;
3.	$k \leftarrow 0$;
4.	$\varphi^{(0)} \leftarrow \varphi(\mathbf{d}^{(0)}, \zeta^{(0)})$;
5.	**do**
6.	$k \leftarrow k + 1$;
7.	Solve (P5) for $\mathbf{d}^{(k)}$;
8.	Plug $\mathbf{d}^{(k)}$ into (19) and (20) and solve them for $\zeta^{(k)}$;
9.	$\varphi^{(k)} \leftarrow \varphi(\mathbf{d}^{(k)}, \zeta^{(k)})$;
10.	**while** $\left\|\varphi^{(k)} - \varphi^{(k-1)}\right\| \geq \varepsilon$;
11.	**return** $\mathbf{d}^{(k)}$ and $\zeta^{(k)}$;

Numerical evaluations indicate that the desired performance is achieved by only a few iterations. A pseudocode of the proposed algorithm is presented in Table I.

IV. NUMERICAL RESULTS

The ED and uniform quantization have been adopted as local sensing and test summary quantization methods at the CR nodes, respectively. In all simulations, there are $K = 5$ cooperating nodes which transmit their sensing outcomes over the reporting channels using the BPSK modulation. The PU signal is modeled as a direct-sequence spread-spectrum BPSK signal using Walsh-Hadamard code with length 16, i.e., processing gain of 16 are considered in all simulation results. The maximum number of quantization bits in each node is 7.

Fig. 1 depicts the results derived as Complementary Receiver Operational Characteristics (CROC) curves. Specifically, three cases have been considered as: *Case#1*) Depicts the performance of uniform linear combining at the fusion center and maximum number of quantization bits at the sensing nodes, *Case#2*) Depicts the performance of optimal linear combining at the fusion center and maximum number of quantization bits at the sensing nodes, *Case#3*) Depicts the performance of the proposed joint optimization, i.e., optimal linear combining at the fusion center and optimal number of quantization bits at the sensing nodes.

It is worth noting that, *Case#1*, *Case#2*, and *Case#3* represent the detector design without any optimization, only with optimal weighting, and with joint reporting-fusion optimization respectively. The plots clearly illustrate the effectiveness of our proposed detector in terms of lower false alarm and missed detection probabilities which are shown as CROC curves closer to the origin. Moreover, it can be observed that the achieved optimization results based on both the Gaussian approximation and EDC are in close agreement with each other. Note that the optimal linear combining based on the Gaussian approximation is known to provide nearly-optimal performance [2].

V. CONCLUSION

In this paper, an extension to the deflection coefficient has been proposed which captures the effects of the quantization processes at the sensing nodes, jointly with the impact of the linear combining at the fusion center. The proposed parameter has been used to formulate a new MINLP problem as a fast suboptimal method to design a distributed detection scenario where the nodes report their sensing outcomes to a fusion center through nonideal digital links. Numerical results demonstrate the effectiveness of the proposed design approach.

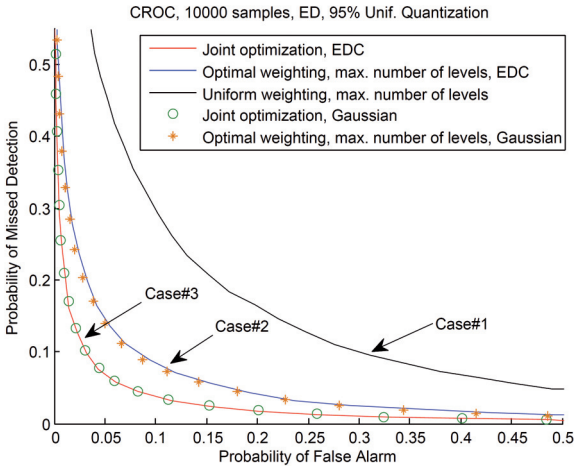

Fig. 1. CROC curves for the energy detection using 20 samples of the PU signal and uniform quantization with Chebyshev probability (see [7]) of 95%. The listening channel SNR levels at sensor inputs are {0, -2.7, -3.1, -1.4, -6.9} in dB. The reporting channel SNR levels are {10, 13, 12, 14, 11} in dB. The results are obtained using 10,000 noise realizations.

REFERENCES

[1] B. Chen and P. K. Willett, "On the optimality of the likelihood-ratio test for local sensor decision rules in the presence of nonideal channels," *IEEE Trans. Inform. Theory*, vol. 51, pp. 693–699, Feb. 2005.

[2] Z. Quan, S. Cui, and A. H. Sayed, "Optimal linear cooperation for spectrum sensing in cognitive radio networks," *IEEE J. Sel. Topics Signal Process.*, vol. 2, no. 1, pp. 28–40, Feb. 2008.

[3] S. Chaudhari, J. Lunden, V. Koivunen, and H. V. Poor, "Cooperative sensing with imperfect reporting channels: Hard decisions or soft decisions?" *IEEE Trans. Signal Process.*, vol. 60, no. 1, pp. 18–28, Jan. 2012.

[4] Z. Quan, S. Cui, A. H. Sayed, and H. V. Poor, "Optimal multiband joint detection for spectrum sensing in cognitive radio networks," *IEEE Trans. Signal Process.*, vol. 57, no. 3, pp. 1128–1140, March 2009.

[5] G. Taricco, "Optimization of linear cooperative spectrum sensing for cognitive radio networks," *IEEE J. Sel. Topics Signal Process.*, vol. 5, no. 1, pp. 77–86, Feb. 2011.

[6] Y. Abdi and T. Ristaniemi, "Joint reporting and linear fusion optimization in collaborative spectrum sensing for cognitive radio networks,," in *Proc. 9th Intl. Conf. Inform., Commun., and Signal Process. (ICICS)*, Tainan, Taiwan, Dec. 2013, pp. 1–5.

[7] ——, "Joint local quantization and linear cooperation in spectrum sensing for cognitive radio networks," *IEEE Trans. Signal. Process., doi: 10.1109/TSP.2014.2330803.*

[8] H. V. Poor, *An introduction to signal detection and estimation.* Berlin Heidelberg: Springer-Verlag, 1994.

[9] M. Derakhshani, T. Le-Ngoc, and M. Nasiri-Kenari, "Efficient cooperative cyclostationary spectrum sensing in cognitive radios at low SNR regimes," *IEEE Trans. Wireless Commun.*, vol. 10, no. 11, pp. 3754–3764, Nov. 2011.

PIII

JOINT REPORTING AND LINEAR FUSION OPTIMIZATION IN COLLABORATIVE SPECTRUM SENSING FOR COGNITIVE RADIO NETWORKS

by

Younes Abdi and Tapani Ristaniemi

Proc. 9th International Conference on Information, Communications and Signal Processing (ICICS), pp.1-5, Tanian, Taiwan, Dec. 10-13, 2013

Joint Reporting and Linear Fusion Optimization in Collaborative Spectrum Sensing for Cognitive Radio Networks

Younes Abdi, and Tapani Ristaniemi
Faculty of Information Technology, University of Jyväskylä, 40014 Jyväskylä, Finland
Email: younes.abdi@jyu.fi, tapani.ristaniemi@jyu.fi

(*Invited Paper*)

***Abstract*—In this paper, the cooperative spectrum sensing in centralized cognitive radio networks is studied as a three-phase process, composed of local sensing, reporting, and decision/data fusion and a novel approach is proposed to optimize the linear soft combining scheme at the fusion phase jointly with two elements of the reporting phase: *i*) the number of bits used by each node to quantize the local sensing outcomes, and *ii*) the power level by which each node reports its sensing outcome to the fusion center. The proposed optimization problem is represented using the conventional false alarm and missed detection probabilities and two straightforward solutions are also provided. Finally, the performance improvement associated with the proposed joint optimization scheme is demonstrated by a set of illustrative simulation results.**

I. Introduction

For more than a decade, Cognitive Radio (CR) as the best implementation candidate for the emerging dynamic spectrum management procedures, has been the core of numerous technical discussions and interactions among various academic, industrial, and regulatory groups specialized in wireless communications all over the world, see [1], [2], and the references therein.

As a matter of fact, spectrum sensing is the key element in each CR system which enables its user, commonly referred to as Secondary User (SU), to find transmission opportunities in spectrum resources allocated exclusively to the license holders which are called Primary Users (PUs). Through establishing certain kinds of cooperation among the sensing nodes, significant enhancements in sensing reliability is usually achieved in wireless environments, leading to the concept of cooperative spectrum sensing. As a common design strategy (in centralized CRNs), the cooperative sensing is coordinated by and the overall sensing outcome is generated in a special node called the Fusion Center (FC) which might be considered as a more powerful node, like a base station or an access point. This cooperation is generally performed as a three-phase process. In the first phase which we call Local Sensing, each node performs spectrum sensing individually, using its own built-in sensing scheme. In other words, they listen to their environment to detect the PU signal. Accordingly, the wireless channels between the PU and the sensing nodes are called Listening Channels. In the second phase, called Reporting, the sensing nodes send their local sensing outcomes to the FC through dedicated, or non-dedicated, Reporting Channels. Finally, in the third phase, i.e., Fusion, the FC combines the received local sensing outcomes to decide the presence or absence of the PU.

In general, there exist various options for each phase in designing an effective cooperative sensing scheme. Local sensing can be realized using well-known methods like Energy Detection (ED), Cyclostationary Detection (CSD), Covariance-Based Detection, etc. In designing the reporting phase, the effect of reporting channel impairments on the overall sensing performance must be taken into account. This effect is captured into the system model by reporting Bit Error Probability (BEP) [3]. The BEP depends in general on transmission power and bandwidth used in reporting, as well as the number of bits used in sensing nodes for quantizing the local sensing outcomes just before reporting. At the FC, the combination of the sensing outcomes can be realized in different ways among which the linear combining [4] is one of the simplest, yet most effective ones, motivating us to adopt it as the fusion method in our system model.

Optimal linear combining is a nonconvex problem studied in several papers like [4] and [5]. Besides optimal solution, the authors in [4] have proposed a suboptimal method using the so-called Modified Deflection Coefficient (MDC) and showed that this approach provides very close results to the ones obtained by the optimal method, with much lower complexity. The MDC approach is also used in several other works, see e.g., [6], to optimize the detection performance where direct formulation of optimal linear combing leads to a nonconvex problem. The effect of reporting channel impairments on the overall sensing performance has been investigated in [3] and [7] where the reporting channels are modeled as binary symmetric channels that cause errors with a certain BEP.

In this paper we jointly optimize the reporting and fusion phases of the cooperative spectrum sensing. More specifically, we formulate and solve a problem to jointly optimize the weighting vector at the FC, the number of bits used by the sensing nodes to quantize their test summaries just before

978-1-4799-0434-1/13/$31.00 ©2013 IEEE

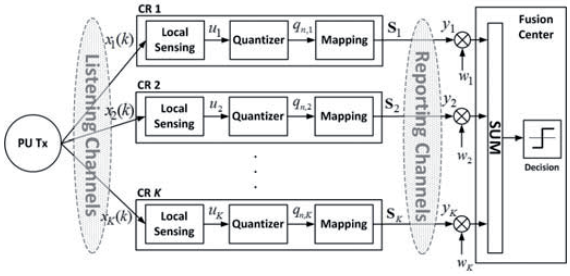

Fig. 1. Basic configuration of cooperative spectrum sensing including the listening and reporting channels, PU, SUs and FC.

reporting, and the power levels by which they transmit their sensing outcomes to the FC. In other words, we formulate and solve a new optimization problem which jointly takes into account the three major mechanisms at the reporting and fusion phases of the cooperative spectrum sensing. Therefore, the spatial/user diversities regarding the listening and reporting channels are considered in a comprehensive optimization approach, promising a better overall sensing performance.

The rest of the paper is organized as follows. In Section II the system model is described. In Section III, mathematical formulations of our proposed joint optimization are presented along with two solutions. The effectiveness of the proposed joint optimization is demonstrated through simulation results in section IV followed by concluding remarks provided in section V.

II. System Model

A CRN with K sensing nodes has been considered. These nodes cooperatively sense the radio spectrum to find temporal and/or spatial vacant bands for their data communication. Fig. 1 shows the basic configuration and major elements in a CRN exploiting cooperative spectrum sensing.

In our adopted model, the kth sample of the received PU signal at the ith CR node is represented as

$$\begin{cases} x_i(k) = \nu_i(k), & \mathcal{H}_0 \\ x_i(k) = h_i s(k) + \nu_i(k), & \mathcal{H}_1 \end{cases} \tag{1}$$

where $\mathcal{H}_1$ and $\mathcal{H}_0$ denote the hypotheses representing the presence or absence of the PU, respectively. $s(k)$ denotes the signal transmitted by the PU and $x_i(k)$ is the received signal by the the ith SU. h_i is the listening channel block fading gain. Listening channel gains are assumed to be independent circularly-symmetric Gaussian random variables. $\nu_i(k)$ denotes the circularly-symmetric zero-mean Additive White Gaussian Noise (AWGN) at the CR sensor receiver. Without loss of generality, $s(k)$ and $\{\nu_i(k)\}$ are assumed to be independent of each other.

CR node i, $i = 1, ..., K$ performs spectrum sensing using its built-in sensor (which can be of any common types like ED, CSD, etc.) to derive a local test statistic u_i and then uses the following quantization rule to map it on a bit sequence of length d_i

$$\psi_i(u_i) = q_{n,i} \quad \text{if} \quad t_{n,i} \leqslant u_i < t_{n+1,i} \tag{2}$$

where $\psi_i(\cdot)$ denotes the quantization process at the ith SU, $q_{n,i}$, $n = 1, ..., 2^{d_i}$ is its nth quantization level, and $t_{n,i}$ and $t_{n+1,i}$ denote the corresponding boundaries.

Let $\mathbf{d} \triangleq \left[d_1, ..., d_K\right]^T$ denote the number of quantization bits used in all sensing nodes. As described in [7] several quantization methods for signal detectors can be considered here like Maximum Output Entropy (MOE) quantization or Minimum Average Error (MAE) quantization. Without loss of generality, we have considered uniform and MOE quantization methods in this paper.

In the uniform quantization incorporated in the ith sensing node, the range covered by the quantization levels is $(\mu_i - m\sigma_i, \mu_i + m\sigma_i)$ where μ_i and σ_i are the mean and standard deviation of u_i respectively and m is determined by the Chebyshev inequality such that $\Pr\{|u_i - \mu_i| \geq m\sigma_i\} \leq \frac{1}{m^2}$. This coverage range is then divided into 2^{d_i} equally-spaced levels whose boundaries are denoted by

$$t_{n,i} = \mu_i + m\sigma_i \left(\frac{2(n-1)}{2^{d_i} - 1} - 1 \right) \tag{3}$$

And the conditional probability of having level $q_{n,i}$ at the ith quantizer output is

$$\Pr\{\psi_i(u_i) = q_{n,i} | \mathcal{H}_j\} = \int_{t_{n-1,i}}^{t_{n,i}} f_{u_i}(x|\mathcal{H}_j) dx \tag{4}$$

where $f_{u_i}(\cdot|\mathcal{H}_j)$ denotes the probability density function (pdf) of u_i conditioned on $\mathcal{H}_j$, $j = 0, 1$. MOE quantization is described in [7].

The generated reporting bit sequences are then transmitted to the FC through the reporting channel in an orthogonal manner. The effect of reporting channel impairments on the transmitted bit sequences of the ith CR node is modeled as a BEP denoted by $P_{\mathrm{b},i}$. The reporting channel is assumed to affect each nodes transmitted reporting bit sequence independently. Moreover, errors introduced on different bits by the reporting channel in a transmitted reporting sequence are assumed to be independent and identically distributed (i.i.d). Therefore, the received quantized test statistics at the FC, y_i, $i = 1, ..., K$ are independent discrete random variables whose probability mass functions (pmf) can be represented (for $j = 0, 1$) as [7]

$$\Pr\{y_i = q_{n,i} | \mathcal{H}_j\} = \sum_{k=1}^{2^{d_i}} P_{\mathrm{b},i}^{D_{n,k}} \left(1 - P_{\mathrm{b},i}\right)^{d_i - D_{n,k}} \Pr\{\psi_i(u_i) = q_{k,i} | \mathcal{H}_j\} \tag{5}$$

where $D_{n,k}$ is the Hamming distance between bit sequences corresponding to levels q_n and q_k.

Assuming a general M-ary modulation for the reporting channel, the reporting BEP can be expressed as

$$P_{\mathrm{b},i} = c_M Q\left(\sqrt{c'_M \gamma_{\mathrm{r},i}}\right) \tag{6}$$

where $Q(x) \triangleq \int_x^\infty \exp(-t^2/2)dt/\sqrt{2\pi}$ is the Q-function, c_M and c'_M are two constants determined by the modulation type and $\gamma_{r,i}$ is the reporting link signal-to-noise ratio (SNR).

In order to take into account the power allocation mechanism of the reporting phase, we consider a different energy level for each node. Specifically, in this model, the ith CR node transmits its sensing outcome with energy $E_{r,i} = \eta_i E_r$, where E_r denotes the total energy used by the whole CRN for transmission of the sensing outcomes to the FC, and η_i denotes the share of energy dedicated to the ith node. We collect the reporting energy ratios of all K nodes in $\boldsymbol{\eta} \triangleq [\eta_1, ..., \eta_K]^T$. With these definitions, it is clear that $0 \leqslant \eta_i \leqslant 1$ for $i = 1, ..., K$ and the elements of $\boldsymbol{\eta}$ sum to unity.

Hence, the reporting SNR associated with the ith sensing node depends on the number of bits used in its reporting bit sequence d_i as well as its normalized energy level η_i, i.e.,

$$\gamma_{\mathrm{r},i} = \frac{|h_{r,i}|^2 \eta_i E_\mathrm{r}}{N_0 d_i log_2 M} \tag{7}$$

where $h_{\mathrm{r},i}$, and N_0 denote the reporting channel gain, and noise power spectral density, respectively. Consequently, the reporting BEP of the ith CR node is a continuous function of η_i/d_i

$$P_{\mathrm{b},i} = c_M Q\left(\sqrt{c''_M \frac{\eta_i}{d_i}}\right) \tag{8}$$

where $c''_M = \frac{c'_M |h_{r,i}|^2 E_r}{N_0 log_2 M}$.

Linear combining is performed at the FC, meaning that, the global test statistic y_c is constructed as a weighted sum of the received quantized levels, i.e.,

$$y_\mathrm{c} = \sum_{i=1}^{K} w_i y_i = \mathbf{w}^T \mathbf{y} \tag{9}$$

where $\mathbf{w} \triangleq [w_1, ..., w_K]^T$ and $\mathbf{y} \triangleq [y_1, ..., y_K]^T$.

Finally, y_c is compared against a predefined threshold th to decide the presence or absence of the PU, i.e.,

$$\begin{cases} \mathcal{H}_1, & y_\mathrm{c} \geq th \\ \mathcal{H}_0, & y_\mathrm{c} < th \end{cases} \tag{10}$$

The detector performance is commonly measured using two probabilities, namely probability of false alarm

$$P_\mathrm{fa} = \Pr\{y_\mathrm{c} \geq th | \mathcal{H}_0\} \tag{11}$$

and probability of missed detection

$$P_\mathrm{md} = \Pr\{y_\mathrm{c} < th | \mathcal{H}_1\} \tag{12}$$

Both false alarm and missed detection probabilities depend on the probability distribution of the global test statistics y_c which can be derived as a convolution of the pmfs of K independent random variables $\{y_i\}_{i=1}^K$, i.e.,

$$p(y_\mathrm{c}) = p(y_1) * ... * p(y_K) \tag{13}$$

where $p(\cdot)$ and $*$ stand for pmf and convolution respectively.

These definitions now enable us to develop our proposed optimization approach in the next section.

III. Reporting-Fusion Optimization

Our problem is to jointly optimize $\mathbf{w}$, $\boldsymbol{\eta}$ and $\mathbf{d}$ to achieve the best cooperative sensing performance. We determine the weighting vector $\mathbf{w}$ at the FC, and $\boldsymbol{\eta}$ and $\mathbf{d}$ used by the sensing nodes, through jointly considering the effects of both the listening channels, and reporting channels.

We formulate our proposed optimization based on minimizing the missed detection probability subject to an upper bound on the false alarm probability

$$\begin{aligned} &\min_{\mathbf{w},\boldsymbol{\eta},\mathbf{d}} \ P_\mathrm{md} \quad \text{(P1)} \\ \text{s.t.} \ \ &P_\mathrm{fa} \leq \alpha \\ &\boldsymbol{\eta}^T \cdot \mathbf{1}_K = 1 \end{aligned}$$

where α is the given upper limit on the false alarm probability and $\mathbf{1}_K$ denotes a $K \times 1$ vector whose elements are all one.

According to the Central Limit Theorem, if K is large enough, we can assume a Gaussian distribution for y_c, and the false alarm and missed detection probabilities can be expressed in closed form as

$$P_\mathrm{fa} = Q\left(\frac{th - \boldsymbol{\mu}_{\mathcal{H}_0}^T \mathbf{w}}{\sqrt{\mathbf{w}^T \boldsymbol{\Sigma}_{\mathcal{H}_0} \mathbf{w}}}\right) \tag{14}$$

$$P_\mathrm{md} = 1 - Q\left(\frac{th - \boldsymbol{\mu}_{\mathcal{H}_1}^T \mathbf{w}}{\sqrt{\mathbf{w}^T \boldsymbol{\Sigma}_{\mathcal{H}_1} \mathbf{w}}}\right) \tag{15}$$

where (for $j = 1, 2$) $\boldsymbol{\mu}_{\mathcal{H}_j} \triangleq \mathrm{E}[\mathbf{y}|\mathcal{H}_j]$ and $\boldsymbol{\Sigma}_{\mathcal{H}_j} \triangleq \mathrm{E}\left[\mathbf{y}^T\mathbf{y}|\mathcal{H}_j\right] = diag(\sigma^2_{y_1|\mathcal{H}_j}, ..., \sigma^2_{y_K|\mathcal{H}_j})$. We have found through numerical evaluations that Gaussian distribution fits well for $K \geq 5$.

Now if we eliminate th in Eqs. (14) and (15) by considering a target false alarm probability $P_\mathrm{fa} = \alpha$, (P1) is converted to

$$\max_{\mathbf{w},\boldsymbol{\eta},\mathbf{d}} Q\left(\frac{Q^{-1}(\alpha)\sqrt{\mathbf{w}^T \boldsymbol{\Sigma}_{\mathcal{H}_0} \mathbf{w}} - \mathbf{a}^T \mathbf{w}}{\sqrt{\mathbf{w}^T \boldsymbol{\Sigma}_{\mathcal{H}_1} \mathbf{w}}}\right) \quad \text{(P2)}$$

where $Q^{-1}(\cdot)$ is the functional inverse of the Q-function, $\mathbf{a} \triangleq [a_1, ..., a_K]^T \triangleq \boldsymbol{\mu}_{\mathcal{H}_1} - \boldsymbol{\mu}_{\mathcal{H}_0}$ and for $i = 1, ..., K$ we have $a_i \triangleq \mathrm{E}[y_i|\mathcal{H}_1] - \mathrm{E}[y_i|\mathcal{H}_0]$. a_i and $\sigma_{y_i|\mathcal{H}_j}$ are related to the number of quantization bits d_i and the normalized reporting energy η_i as

$$\begin{aligned} a_i = &\sum_{n=1}^{2^{d_i}} q_{n,i} \sum_{k=1}^{2^{d_i}} P_{\mathrm{b},i}^{D_{n,k}} (1 - P_{\mathrm{b},i})^{d_i - D_{n,k}} \\ &\times [\Pr(\psi_i(u_i) = q_{k,i}|\mathcal{H}_1) - \Pr(\psi_i(u_i) = q_{k,i}|\mathcal{H}_0)] \end{aligned} \tag{16}$$

$$\begin{aligned} &\sigma^2_{y_i|\mathcal{H}_j} = \\ &\sum_{n=1}^{2^{d_i}} q^2_{n,i} \sum_{k=1}^{2^{d_i}} P_{\mathrm{b},i}^{D_{n,k}} (1 - P_{\mathrm{b},i})^{d_i - D_{n,k}} \Pr(\psi_i(u_i) = q_{k,i}|\mathcal{H}_j) - \\ &\left[\sum_{n=1}^{2^{d_i}} q_{n,i} \sum_{k=1}^{2^{d_i}} P_{\mathrm{b},i}^{D_{n,k}} (1 - P_{\mathrm{b},i})^{d_i - D_{n,k}} \Pr(\psi_i(u_i) = q_{k,i}|\mathcal{H}_j)\right]^2 \end{aligned} \tag{17}$$

For a given pair of $\mathbf{d}$ and $\boldsymbol{\eta}$ (P2) can be solved for optimal weighting vector $\tilde{\mathbf{w}}$ [5, Theorem 2]

$$\tilde{\mathbf{w}} = \boldsymbol{\Sigma}_{\mathcal{H}_0}^{-1/2} \left[(Q^{-1}(\alpha)\mathbf{I}_K + \zeta \mathbf{A} \right]^{-1} \mathbf{c} \tag{18}$$

where $\mathbf{A} \triangleq \boldsymbol{\Sigma}_{\mathcal{H}_1} \boldsymbol{\Sigma}_{\mathcal{H}_0}^{-1}$, $\mathbf{c} \triangleq \boldsymbol{\Sigma}_{\mathcal{H}_0}^{-1/2} \mathbf{a}$ and ζ is the single root of the polynomial equation

$$\left\| \left[(Q^{-1}(\alpha)\mathbf{I}_K + \zeta \mathbf{A} \right]^{-1} \mathbf{c} \right\| = 1 \tag{19}$$

Now using Eqs. (18) and (19), we remove $\mathbf{w}$ from (P3) and convert the problem to the following optimization in $\boldsymbol{\eta}$ and $\mathbf{d}$

$$\max_{\boldsymbol{\eta}, \mathbf{d}} Q \left(\frac{Q^{-1}(\alpha)\sqrt{\tilde{\mathbf{w}}^T \boldsymbol{\Sigma}_{\mathcal{H}_0} \tilde{\mathbf{w}}} - \mathbf{a}^T \tilde{\mathbf{w}}}{\sqrt{\tilde{\mathbf{w}}^T \boldsymbol{\Sigma}_{\mathcal{H}_1} \tilde{\mathbf{w}}}} \right) \quad \text{(P3)}$$

It is worth noting that d_i attains discrete values from the set $\omega_i \triangleq \{1, ..., d_{i,max}\}$ where $d_{i,max}$ is the maximum possible number of bits used in the quantization process at the ith CR node. If we also consider a set of step-wise discrete values for η_i, we can solve (P4) in a straightforward manner, through a numerical search. For instance, the designer can consider $\eta_0 = 10\%$ and $\xi_i \triangleq \{0, \eta_0, 2\eta_0, ..., 1\}$ as a set of normalized reporting energies which can be used at the ith CR node. In this way, (P3) can be solved through an exhaustive search over $\Omega \triangleq (\omega_1, \xi_1) \times ... \times (\omega_K, \xi_K)$ where $\times$ stands for the Cartesian product.

An alternative solution for joint optimization of $\mathbf{w}$, $\boldsymbol{\eta}$, and $\mathbf{d}$ can be achieved using the MDC. It can be interpreted as the SNR of the global test statistic y_c at the FC. The definition of MDC is as follows

$$\Delta_m^2 \triangleq \frac{\left(\mathrm{E}\left[y_c | \mathcal{H}_1 \right] - \mathrm{E}\left[y_c | \mathcal{H}_0 \right] \right)^2}{\mathrm{Var}\left\{ y_c | \mathcal{H}_1 \right\}} \tag{20}$$

Replacing y_c with its weighted sum definition, we have

$$\Delta_m^2 = \frac{\left(\mathbf{a}^T \mathbf{w} \right)^2}{\mathbf{w}^T \boldsymbol{\Sigma}_{\mathcal{H}_1} \mathbf{w}} \tag{21}$$

Using the MDC approach, we aim at finding $\mathbf{w}$, $\boldsymbol{\eta}$, and $\mathbf{d}$ such that

$$\begin{aligned} & \max_{\mathbf{w}, \boldsymbol{\eta}, \mathbf{d}} \Delta_m^2 \quad \text{(P4)} \\ \text{s.t.} \quad & \|\mathbf{w}\| = 1 \\ & \boldsymbol{\eta}^T \cdot \mathbf{1}_K = 1 \end{aligned}$$

The constraint on the weight vector norm is necessary here to derive a unique solution since the MDC does not depend on $\|\mathbf{w}\|$.

Now we consider two simplifying but practical assumptions. Firstly, we assume that Gray coding is used to map the reporting bit sequences to their corresponding quantization levels. In other words, we assume that the bit sequences representing the adjacent quantization levels, differ only in one bit. Secondly, we assume a reliable reporting channel, i.e., small P_bs. Consequently, we neglect the cases in which more than one bit in a sequence arrive erroneously at the FC. These assumptions lead to the following simplified form of a_i (and $\sigma_{y_i|H_1}^2$) that is differentiable with respect to d_i

$$\begin{aligned} a_i \approx & \sum_{n=1}^{2^{d_i}} q_{n,i} \sum_{k=n-1}^{n+1} P_{\mathrm{b},i}^{1-\mathbf{1}_{\{k=n\}}} (1 - P_{\mathrm{b},i})^{d_i - 1 + \mathbf{1}_{\{k=n\}}} \\ & \times \left[\Pr(\psi_i(u_i) = q_{k,i} | \mathcal{H}_1) - \Pr(\psi_i(u_i) = q_{k,i} | \mathcal{H}_0) \right] \end{aligned} \tag{22}$$

where $\mathbf{1}_{\{k=n\}}$ is the indicator function which is equal to 1 when $k = n$ and 0 otherwise. $\sigma_{y_i|H_1}^2$ can be simplified in a similar way.

In order to derive an analytical solution for (P4) we first eliminate $\mathbf{w}$ as follows. Through the linear transformation [4]

$$\mathbf{w}' = \boldsymbol{\Sigma}_{\mathcal{H}_1}^{1/2} \mathbf{w} \tag{23}$$

the MDC is converted to

$$\Delta_m^2 = \frac{\mathbf{w}'^T \boldsymbol{\Sigma}_{\mathcal{H}_1}^{-T/2} \mathbf{a} \mathbf{a}^T \boldsymbol{\Sigma}_{\mathcal{H}_1}^{-1/2} \mathbf{w}'}{\mathbf{w}'^T \mathbf{w}'} \leq \left\| \boldsymbol{\Sigma}_{\mathcal{H}_1}^{-T/2} \mathbf{a} \right\|^2 \tag{24}$$

and the equality is achieved when

$$\mathbf{w}' = \boldsymbol{\Sigma}_{\mathcal{H}_1}^{-T/2} \mathbf{a} \tag{25}$$

Therefore, the optimal $\mathbf{w}$ which maximizes the MDC is derived as function of $\boldsymbol{\eta}$, and $\mathbf{d}$ as

$$\mathbf{w}_{\mathrm{mdc}} = \frac{\boldsymbol{\Sigma}_{\mathcal{H}_1}^{-1/2} \mathbf{w}'}{\left\| \boldsymbol{\Sigma}_{\mathcal{H}_1}^{-1/2} \mathbf{w}' \right\|} \tag{26}$$

Replacing $\mathbf{w}$ with its MDC-optimal value $\mathbf{w}_{\mathrm{mdc}}$, the MDC can be rewritten as a function of $\boldsymbol{\eta}$ and $\mathbf{d}$

$$\Delta_m^2 = \mathbf{a}^T \boldsymbol{\Sigma}_{\mathcal{H}_1}^{-1} \mathbf{a} \tag{27}$$

Now, the Lagrangian function associated with the proposed optimization can be represented as

$$L(\boldsymbol{\eta}, \mathbf{d}, \lambda) = \mathbf{a}^T \boldsymbol{\Sigma}_{\mathcal{H}_1}^{-1} \mathbf{a} + \lambda(\boldsymbol{\eta}^T \cdot \mathbf{1}_K - 1) \tag{28}$$

and the solution is derived by solving the following system of equations

$$\frac{\partial L}{\partial \boldsymbol{\eta}} = 0, \frac{\partial L}{\partial \mathbf{d}} = 0, \frac{\partial L}{\partial \lambda} = 0. \tag{29}$$

IV. Numerical Results

Two typical distributed detection scenarios have been considered to illustrate the effectiveness of the proposed optimization scheme. In the first scenario, the ED and uniform quantization have been adopted as local sensing and test summary quantization methods at the CR nodes, respectively. As the second scenario, CSD and MOE quantization have been considered. In all simulations, there are $K = 3$ cooperating nodes which transmit their sensing outcomes over the reporting channels using the BPSK modulation. The PU signal is modeled as a direct-sequence spread-spectrum BPSK signal using Walsh-Hadamard code with length 16, i.e., processing gain of 16 are considered in all simulation results. The maximum number of quantization bits in each node is 7. The number of PU signal samples used in ED is 20 and the Chebychev

probability for the uniform quantization coverage interval has been set to 95%. When CSD is considered, the cyclic autocorrelation function is estimated in each node using 100 samples of the PU signal and the estimated autocorrelation corresponds to $f = 1/T_c$ and $\tau = 0$, where f is the cycle frequency, τ is the lag used in calculating the autocorrelation, and T_c is the chip period of the PU signal.

Fig.s 2 and 3 depict the results derived as Complementary Receiver Operational Characteristics (CROC) curves for both energy and cyclostationary detectors. Specifically, for each detector three cases have been considered as

- Case#1: Depicts the performance of uniform linear combining at the fusion center, uniform reporting power allocation, and maximum number of quantization bits at the sensing nodes,
- Case#2: Depicts the performance of optimal linear combining at the fusion center, uniform reporting power allocation and maximum number of quantization bits at the sensing nodes,
- Case#3: Depicts the performance of the proposed joint optimization, i.e., optimal linear combining at the fusion center, optimal reporting power allocation, and optimal number of quantization bits at the sensing nodes.

It is worth noting that in both figures, Case#1, Case#2, and Case#3 represent the detector design without any optimization, only with optimal weighting, and with joint reporting-fusion optimization respectively. The plots clearly illustrate the effectiveness of our proposed detector in terms of lower false alarm and missed detection probabilities which are shown as CROC curves closer to the origin.

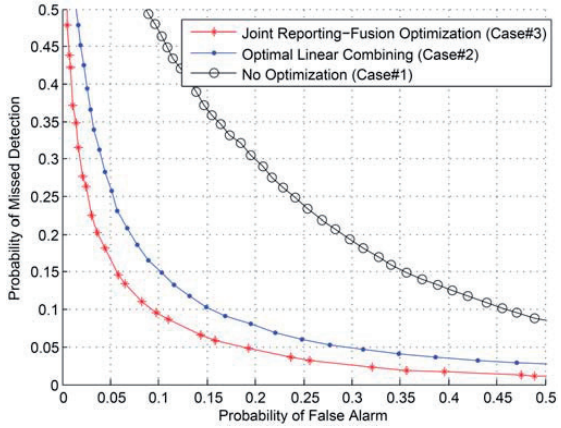

Fig. 2. CROC curves for the energy detection using 20 samples of the PU signal and uniform quantization with Cebyshev probability of 95%. The listening channel SNR levels at sensor inputs are {-6.9, 0, -2.7} in dB. The reporting channel SNR levels are {10, 13, 12} in dB. The results are obtained using 10000 noise realizations.

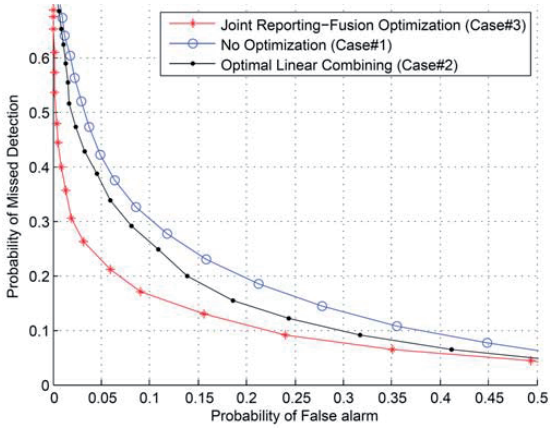

Fig. 3. CROC curves for the cyclostationary detection using 100 samples of the PU signal and MOE quantization. The local SNR levels at sensor inputs are {-1.9, 5, 2.3} in dB. The reporting channel SNR levels are {11, 14, 13} in dB. The results are obtained using 10000 noise realizations.

V. Conclusion

In this paper, the cooperative sensing in centralized cognitive radio networks has been studied as a three-phase process, composed of local sensing, reporting, and decision/data fusion and a novel approach has been proposed to optimize the linear soft combining scheme at the fusion phase jointly with two significant mechanisms at the reporting phase. The simulation results following the presented analytical formulations demonstrate that, by joint consideration of reporting and fusion phases, better detection performances can be achieved which is due to better exploitation of spatial/user diversities.

Acknowledgement

This work has been financially supported by Graduate school in Electronics, Telecommunications, and Automation (GETA) coordinated by Aalto University, Espoo, Finland.

References

[1] I. F. Akyildiz, B. F. Lo, and R. Balakrishnan, "Cooperative spectrum sensing in cognitive radio networks: A survey," *Elsevier Physical Commun.*, vol. 4, no. 1, pp. 40–62, March 2011.

[2] Y. Zeng, Y. Liang, S. W. O. Z. Lei, F. Chin, and S. Sun, "Worldwide regulatory and standardization activities on cognitive radio," in *Proc. IEEE DySPAN 2010*, Washington DC, April 6-9 2010, pp. 1–9.

[3] S. Chaudhari and V. K. J. Lunden, "BEP walls for collaborative spectrum sensing," in *Proc. IEEE International Conf. on Acoustics, Speech and Signal Processing (ICASSP)*, May 22-27 2011, pp. 2984–2987.

[4] Z. Quan, S.Cui, and A. H. Sayed, "Optimal linear cooperation for spectrum sensing in cognitive radio networks," *IEEE J. Sel. Topics Signal Process.*, vol. 2, no. 1, pp. 28–40, Feb. 2008.

[5] G. Taricco, "Optimization of linear cooperative spectrum sensing for cognitive radio networks," *IEEE J. Sel. Topics Signal Process.*, vol. 5, no. 1, pp. 77–86, Feb. 2011.

[6] K. Hossain, B. Champagne, and A. Assra, "Cooperative multiband joint detection with correlated spectral occupancy in cognitive radio networks," *IEEE Trans. Signal.Process.*, vol. 60, no. 5, pp. 2682–2687, May 2012.

[7] S. Chaudhari, J. Lundn, V. Koivunen, and H. V. Poor, "Cooperative sensing with imperfect reporting channels: Hard decisions or soft decisions?" *IEEE Trans. Signal Process.*, vol. 60, no. 1, pp. 18–28, Jan. 2012.

PIV

RANDOM INTERRUPTIONS IN COOPERATION FOR SPECTRUM SENSING IN COGNITIVE RADIO NETWORKS

by

Younes Abdi and Tapani Ristaniemi 2016

IEEE Transactions on Communications (submitted for publication)

PV

LINEAR FUSION OF INTERRUPTED REPORTS IN COOPERATIVE SPECTRUM SENSING FOR COGNITIVE RADIO NETWORKS

by

Younes Abdi and Tapani Ristaniemi

Proc. IEEE 26th Annual International Symposium on Personal, Indoor, and Mobile Radio Communications (PIMRC), pp. 365-369, Hong Kong, China, Aug. 30 - Sept. 2, 2015

2015 IEEE 26th International Symposium on Personal, Indoor and Mobile Radio Communications - (PIMRC): Fundamentals and PHY

Linear Fusion of Interrupted Reports in Cooperative Spectrum Sensing for Cognitive Radio Networks

Younes Abdi and Tapani Ristaniemi
University of Jyvaskyla, Department of Mathematical Information Technology
P.O. Box 35, FI-40014 University of Jyvaskyla, Finland
Email: younes.abdi@jyu.fi, tapani.ristaniemi@jyu.fi

***Abstract*—Interrupted reporting has recently been introduced as an effective method to increase the energy efficiency of cooperative spectrum sensing schemes in cognitive radio networks. In this paper, joint optimization of the reporting and fusion phases in a cooperative sensing with interrupted reporting is considered. This optimization aims at finding the best weights used at the fusion center to construct a linear fusion of the received interrupted reports, jointly with Bernoulli distributions governing the statistical behavior of the interruptions. The problem is formulated by using the *deflection criterion* and as a nonconvex quadratic program which is then solved for a suboptimal solution, in a computationally-affordable fashion, by a semidefinite relaxation technique. The system performance is then demonstrated by a set of numerical results which compare the performance of the system for the cases with and without the optimal linear fusion.**

***Index Terms*—Cognitive radio (CR), cooperative spectrum sensing, decision fusion, correlation, non-ideal reporting channels.**

I. Introduction

Traditional fixed spectrum assignment policy has been proved inefficient as measurements demonstrate that the radio spectrum is severely underutilized [1]. This underutilization stems from the fact that, many portions of licensed spectrum are neglected or underutilized by the licensees [2]. The scarcity in the available spectrum resources and continuous growth in demand for wireless communications necessitate developing more efficient spectrum management policies, procedures, and technologies. In consequence, cognitive radio (CR) has gained a great deal of interest as a powerful asset for realizing the dynamic spectrum access (DSA) technology. CRs aim at enabling their users, commonly referred to as secondary users (SU), to find temporarily- or spatially-available portions of the radio spectrum which are not used by the so-called primary users (PU) who are in fact the licensees. When appropriate spectral opportunities are found, the CRs adapt their own parameters to establish communication. This communication is realized by CRs while no particular spectrum band is assigned to them.

Since CRs are obliged not to compromise the integrity of the primary networks, they need to get informed about the PU activities in their surrounding radio environment. In order to accomplish this task, they are equipped with spectrum sensing facilities to inspect the radio spectrum and discover whether the PU is active. In this manner, CRs can avoid making harmful interference for the PUs.

It is well-known that, when the nodes in a CR network (CRN) cooperate in spectrum sensing, better overall detection performance is achieved. This is due to the fact that, when cooperating, spatial diversity of the sensing nodes are exploited to alleviate the effects of shadowing and multipath fading, which might prevent the individual nodes from detecting the PU signal. In this cooperation scheme which is referred to as cooperative spectrum sensing, all nodes report their local sensing outcome to a so-called fusion center (FC) [2]–[5]. Then, based on the received reports, the FC decides the presence or absence of the PU signal and informs other nodes of the decision.

Likelihood ratio test (LRT) [6] is known as the optimal fusion method when the sensing nodes report their sensing outcomes through nonideal links. However, finding the LRT thresholds is not practical due to its high computational complexity. Optimal linear combining has been proposed in [2], [4], [5] as a low-complexity suboptimal fusion method which nearly achieves the performance of the LRT. The main idea of linear combining is that the combining weight for the signal from a particular user represents its contribution to the global decision. For those SUs experiencing deep fading or shadowing, their weights are decreased in order to reduce their negative contribution to the overall decision. Therefore, this method makes a discrimination between the reports received from the reliable and unreliable sensing nodes.

In our previous work [7], we have established, analyzed, and optimized a novel energy-efficient approach for discriminating between the reliable and unreliable nodes by introducing random energy-saving interruptions in the cooperation of the sensing nodes with the FC. In this approach, instead of suppressing the contribution of nodes working under deep fading or shadowing, they are occasionally ordered not to cooperate. By optimizing this interruption process subject to an upper bound on the energy consumed at the local sensing and reporting processes, significant levels of energy efficiency is achieved.

In this paper, we optimize the interrupted reporting mechanism jointly with the commonly-used linear combining scheme at the FC. We formulate an optimization problem for finding the best weights used at the FC to linearly combine the received sensing outcomes, jointly with Bernoulli distributions based on which the random interruptions are realized. This optimization is proposed based on maximizing the *modified*

978-1-4673-6782-0/15/$31.00 ©2015 IEEE

deflection coefficient (MDC) [5], [7] of the overall detection and as a nonconvex quadratic program which can be solved for a suboptimal solution by a polynomial-complexity semidefinite relaxation technique. The system performance is then demonstrated by a set of simulation results which compare the case where the linear fusion is involved in the optimization process with the case in which the optimization only concerns the interrupted reporting.

II. System Model and Analysis

In this section, we first introduce our notation along with a set of definitions which facilitate mathematical representation of the proposed analysis. Then, the system model is introduced and the parameters needed for performance optimization are derived accordingly. Note that the notation and system model represented in this section are similar to the ones introduced in [7].

A. Notation

Matrices and column-vectors are denoted in boldface by uppercase and lowercase letters, respectively. The notation $\|\mathbf{x}\|$ denotes the Euclidean norm of the vector $\mathbf{x}$. The notation $\mathrm{diag}(\mathbf{x})$ represents a diagonal matrix whose main diagonal is $\mathbf{x}$. Matrix inequality is represented by $\succeq$, i.e., $\mathbf{A} \succeq \mathbf{B}$ means that $\mathbf{A}-\mathbf{B}$ is positive semidefinite and for a vector it denotes the element-wise inequality with $\succ$ representing the strict inequality. The identity matrix is denoted by $\mathbf{I}$ and $\mathbf{0}_n$ denotes the $n \times n$ null matrix while $\mathbf{1}$ and $\mathbf{0}$ denote all-ones and all-zeros column vectors, respectively. $\mathbf{e}_i$ denotes a column vector where all elements are zero except for the ith element which is one. $\mathrm{Tr}(\mathbf{A})$ refers to the trace of $\mathbf{A}$, i.e., sum of elements in the main diagonal of $\mathbf{A}$. The vectorization of matrix $\mathbf{A}$ is denoted by $\mathrm{vec}(\mathbf{A})$ which represents a vector obtained by stacking the columns of $\mathbf{A}$ on top of one another.

In order to account for temporal and spatial representations of signals, we use the following notation. For vector $\mathbf{x}$ in the following form

$$\mathbf{x}(m) = [x_1(m), ..., x_K(m)]^T \tag{1}$$

we consider these three notations

$$\mathbf{X}_L(m) \triangleq [\mathbf{x}(m), \mathbf{x}(m-1), ..., \mathbf{x}(m-L)]^T \tag{2}$$

$$\mathbf{x}_L(m) \triangleq \mathrm{vec}\left(\mathbf{X}_L(m)\right) \tag{3}$$

$$\tilde{\mathbf{X}}_L(m) \triangleq \mathrm{diag}\left(\mathbf{x}_L(m)\right) \tag{4}$$

Note that we represent the time index by m.

For the two hypotheses considered in this paper, i.e., the null hypothesis $\mathcal{H}_0$ corresponding to the absence of the PU signal and $\mathcal{H}_1$ representing the presence of the PU signal, the following notations are used to represent conditional second-order statistics of signals (for $h = 1, 2$)

$$\begin{aligned}\mathbf{C}_{\mathbf{x}|\mathcal{H}_h} &\triangleq E\left[(\mathbf{x}-\boldsymbol{\mu}_{\mathbf{x}|\mathcal{H}_h})(\mathbf{x}-\boldsymbol{\mu}_{\mathbf{x}|\mathcal{H}_h})^H \middle| \mathcal{H}_h\right] \\ &= \mathbf{R}_{\mathbf{x}|\mathcal{H}_h} - \boldsymbol{\mu}_{\mathbf{x}|\mathcal{H}_h}\boldsymbol{\mu}^H_{\mathbf{x}|\mathcal{H}_h}\end{aligned} \tag{5}$$

$$\begin{aligned}\mathbf{C}_{\mathbf{xy}|\mathcal{H}_h} &\triangleq E\left[(\mathbf{x}-\boldsymbol{\mu}_{\mathbf{x}|\mathcal{H}_h})(\mathbf{y}-\boldsymbol{\mu}_{\mathbf{y}|\mathcal{H}_h})^H \middle| \mathcal{H}_h\right] \\ &= \mathbf{R}_{\mathbf{xy}|\mathcal{H}_h} - \boldsymbol{\mu}_{\mathbf{x}|\mathcal{H}_h}\boldsymbol{\mu}^H_{\mathbf{y}|\mathcal{H}_h}\end{aligned} \tag{6}$$

where $\boldsymbol{\mu}_{\mathbf{x}|\mathcal{H}_h}$ and $\boldsymbol{\mu}_{\mathbf{y}|\mathcal{H}_h}$ denote mean of $\mathbf{x}$ and mean of $\mathbf{y}$, conditioned on $\mathcal{H}_h$, respectively. The main diagonal of the autocorrelation matrix $\mathbf{R}_{\mathbf{x}|\mathcal{H}_h}$ is denoted $\mathfrak{R}_{\mathbf{x}|\mathcal{H}_h}$ which is defined as

$$\left(\mathfrak{R}_{\mathbf{x}|\mathcal{H}_h}\right)_{i,j} \triangleq \delta_{i,j}\left(\mathbf{R}_{\mathbf{x}|\mathcal{H}_h}\right)_{i,j} \tag{7}$$

where $\delta_{i,j}$ is Kronecker's delta function which equals to 1 if $i = j$ and 0 otherwise.

Non-conditional statistics are related to their conditional counterparts according to the following definitions

$$\mathbf{C}_{\mathbf{x}} \triangleq \Pr\{\mathcal{H}_0\}\mathbf{C}_{\mathbf{x}|\mathcal{H}_0} + \Pr\{\mathcal{H}_1\}\mathbf{C}_{\mathbf{x}|\mathcal{H}_1} \tag{8}$$

$$\mathbf{C}_{\mathbf{xy}} \triangleq \Pr\{\mathcal{H}_0\}\mathbf{C}_{\mathbf{xy}|\mathcal{H}_0} + \Pr\{\mathcal{H}_1\}\mathbf{C}_{\mathbf{xy}|\mathcal{H}_1} \tag{9}$$

Note that other non-conditional statistics in this paper are related to their conditional counterparts in a similar fashion.

As another definition regarding the second-order statistics, we have the following $K(L+1) \times K$ matrix

$$\begin{aligned}\mathbf{C}_{\mathbf{x}_L\mathbf{y}} \triangleq\ & E\left[\mathbf{x}_L(m)y_1^\dagger(m), ..., \mathbf{x}_L(m)y_K^\dagger(m)\right] \\ & - \left[\boldsymbol{\mu}_{\mathbf{x}_L}y_1^\dagger(m), ..., \boldsymbol{\mu}_{\mathbf{x}_L}y_K^\dagger(m)\right]\end{aligned} \tag{10}$$

where $\boldsymbol{\mu}_{\mathbf{x}_L} \triangleq E[\mathbf{x}_L]$ and $\dagger$ denotes complex conjugation.

B. System Model and Problem Formulation

A CRN with K sensing nodes is considered. These nodes cooperatively sense the radio spectrum to find temporal and/or spatial vacant bands for their data communication. Each CR node is equipped with a built-in spectrum sensor which enables it to detect the PU signal through inspecting its own listening channel. Listening channels are referred to the channels between the PU and the sensing nodes. The sensing nodes have access to a dedicated but nonideal reporting channel to send their individual sensing outcomes to the FC.

In our adopted model, the mth sample of the received PU signal at the ith CR node is represented as

$$\begin{cases} x_i(m) = \nu_i(m), & \mathcal{H}_0 \\ x_i(m) = h_i s(m) + \nu_i(m), & \mathcal{H}_1 \end{cases} \tag{11}$$

where $s(m)$ denotes the signal transmitted by the PU and $x_i(m)$ is the received signal by the ith SU. h_i is the listening channel block fading coefficient, which is assumed to be constant during the detection interval. Listening channel gains are assumed to be independent circularly-symmetric Gaussian random variables. $\nu_i(m)$ denotes the circularly-symmetric zero-mean additive white Gaussian noise (AWGN) at the CR sensor receiver, i.e., $\nu_i(m) \sim \mathcal{CN}(0, \sigma^2_{\nu_i})$. $s(m)$ and $\{\nu_i(m)\}$ are assumed to be independent of each other.

In this cooperative sensing scheme, the behavior of each node is controlled by a predetermined sequence of binary random numbers generated at the FC. Whenever the cooperative sensing is performed, only the nodes whose corresponding random number is one are allowed to contribute to the overall

sensing process. Specifically, if the ith CR is among the cooperating nodes, $i \in \{1,2,...,K\}$, it performs spectrum sensing by using its built-in sensor to derive a local test statistic u_i. Without loss of generality, the local sensing process is assumed to be in the form of energy detection which can be represented as

$$u_i(m) = \sum_{k=0}^{N-1} |x_i(Nm-k)|^2 \tag{12}$$

The resulting sensing outcome is then transmitted to the FC through the reporting channel. We represent this *interrupted reporting* as

$$y_i(m) = \theta_i(m)u_i(m) + z_i(m) \tag{13}$$

where $y_i(m)$ denotes the ith received sensing outcome at the FC, $\theta_i(m) \in \{0,1\}$ denotes the random number which controls the ith sensing node, and $z_i(m) \sim \mathcal{CN}(0,\sigma_z^2)$ is the reporting channel contamination modeled as AWGN. (13) clearly demonstrates that when the generated random number θ_i is zero, nothing is transmitted to the FC. This process can be implemented in practice by using an energy-saving controller which suspends the local sensing and reporting processes when the corresponding random number is zero.

In the matrix form we can represent (13) as

$$\mathbf{y}(m) = \text{diag}(\boldsymbol{\theta}(m))\mathbf{u}(m) + \mathbf{z}(m) \tag{14}$$

where $\mathbf{y}(m) \triangleq [y_1(m),...,y_K(m)]^T$, $\boldsymbol{\theta}(m) \triangleq [\theta_1(m),...,\theta_K(m)]^T$, $\mathbf{u}(m) \triangleq [u_1(m),...,u_K(m)]^T$, and $\mathbf{z}(m) \triangleq [z_1(m),...,z_K(m)]^T$. In the proposed system the random numbers θ_i, $i=1,...,K$, are generated independently over time and space, i.e., $\theta_k(m-l)$ and $\theta_n(m-r)$ are independent if $k \neq n$ or $l \neq r$. Moreover, $\theta_i(m)$ follows the Bernoulli distribution with $p_i(m) \triangleq \Pr\{\theta_i(m)=1\}$. Note that $\boldsymbol{\theta}$, $\mathbf{u}$, and $\mathbf{z}$ are assumed to be independent of each other. We also need $\mathbf{p}(m) \triangleq [p_1(m),...,p_K(m)]^T$ and $\mathbf{b}(m) \triangleq [b_1(m),...,b_K(m)]^T$ in our formulations. $\mathbf{b}(m)$ denotes a realization of the random vector $\boldsymbol{\theta}(m)$. For simplicity, we will drop the time index m when representing vectors and matrices.

The reported sensing outcomes feed a linear estimator which uses spatial and temporal correlations of the received test summaries to estimate their actual (i.e., non-contaminated and non-interrupted) values. Specifically, the observation vector used by the estimator is $\mathbf{y}_L$ which, based on the notation provided in Section II-A, can be expressed as

$$\mathbf{y}_L = \tilde{\boldsymbol{\Theta}}_L \mathbf{u}_L + \mathbf{z}_L \tag{15}$$

Note that $\tilde{\boldsymbol{\Theta}}_L$ is a $K(L+1) \times K(L+1)$ diagonal matrix. The estimation process at the FC is represented as

$$\hat{\mathbf{u}} = \boldsymbol{\xi}^T \mathbf{y}_L + \boldsymbol{\epsilon} \tag{16}$$

where the weight vector $\boldsymbol{\xi}$ and the constant $\boldsymbol{\epsilon}$ are obtained as the minimizer of the mean-squared error (MMSE) $E\left[\|\hat{\mathbf{u}} - \mathbf{u}\|^2\right]$. Hence,

$$\boldsymbol{\xi}^* = \mathbf{C}_{\mathbf{y}_L}^{-1} \mathbf{C}_{\mathbf{y}_L \mathbf{u}} \tag{17}$$

and since $\mathbf{u}$ has nonzero mean in general, the optimum value of the bias term $\boldsymbol{\epsilon}$ is given by

$$\boldsymbol{\epsilon}^* = E[\mathbf{u}] - \boldsymbol{\xi}^{*T} E[\mathbf{y}_L]. \tag{18}$$

We have shown in [7] that,

$$\mathbf{C}_{\mathbf{y}_L \mathbf{u}} = \tilde{\mathbf{P}}_L \mathbf{C}_{\mathbf{u}_L \mathbf{u}} \tag{19}$$

$$\mathbf{C}_{\mathbf{y}_L} = \tilde{\mathbf{P}}_L \left(\mathbf{I} - \tilde{\mathbf{P}}_L\right) \mathfrak{R}_{\mathbf{u}_L} + \tilde{\mathbf{P}}_L \mathbf{C}_{\mathbf{u}_L} \tilde{\mathbf{P}}_L + \sigma_z^2 \mathbf{I}. \tag{20}$$

Where $\tilde{\mathbf{P}}_L = E[\tilde{\boldsymbol{\Theta}}_L]$. Note that, $\mathbf{C}_{\mathbf{u}_L \mathbf{u}}$, $\mathbf{C}_{\mathbf{u}_L}$, and $\mathfrak{R}_{\mathbf{u}_L}$ are obtained in terms of the second-order statistics of the channel gains between the PU and SUs as well as noise variances experienced by the sensors.

According to the central limit theorem, if the number of samples N in (12) is large enough, the local test summaries follow the Gaussian distribution. Consequently, the estimated local test summaries conditioned on a given realization of $\boldsymbol{\theta}_L$ are normal random variables, i.e., for $h=0,1$, we have $\hat{\mathbf{u}} \sim \mathcal{N}\left(\boldsymbol{\mu}_{\hat{\mathbf{u}}|\{\mathcal{H}_h,\mathbf{b}_L\}}, \mathbf{C}_{\hat{\mathbf{u}}|\{\mathcal{H}_h,\mathbf{b}_L\}}\right)$ where

$$\begin{aligned} \boldsymbol{\mu}_{\hat{\mathbf{u}}|\{\mathcal{H}_h,\mathbf{b}_L\}} &\triangleq E\left[\hat{\mathbf{u}}|\mathcal{H}_h, \boldsymbol{\theta}_L = \mathbf{b}_L\right] \\ &= \boldsymbol{\xi}^{*T} E\left[\tilde{\boldsymbol{\Theta}}_L \mathbf{u}_L + \mathbf{z}_L | \mathcal{H}_h, \boldsymbol{\theta}_L = \mathbf{b}_L\right] + \boldsymbol{\epsilon}^* \\ &= \boldsymbol{\xi}^{*T} \tilde{\mathbf{B}}_L E\left[\mathbf{u}_L|\mathcal{H}_h\right] + \boldsymbol{\epsilon}^* \end{aligned} \tag{21}$$

and $\mathbf{C}_{\hat{\mathbf{u}}|\{\mathcal{H}_h,\mathbf{b}_L\}}$ denotes the conditional covariance matrix of $\hat{\mathbf{u}}$. Note that, conditioned on $\boldsymbol{\theta}_L = \mathbf{b}_L$, the observation vector is $\mathbf{y}_L = \tilde{\mathbf{B}}_L \mathbf{u}_L + \mathbf{z}_L$ which leads to [7]

$$\mathbf{C}_{\hat{\mathbf{u}}|\{\mathcal{H}_h,\mathbf{b}_L\}} = \boldsymbol{\xi}^{*T} \left(\tilde{\mathbf{B}}_L \mathbf{C}_{\mathbf{u}_L|\mathcal{H}_h} \tilde{\mathbf{B}}_L + \sigma_z^2 \mathbf{I}\right) \boldsymbol{\xi} \tag{22}$$

In the proposed cooperative sensing, the estimated local sensing outcomes are used at the FC to make the decision. Specifically, the estimated local sensing outcomes are linearly combined to form a so-called global test summary $S(\hat{\mathbf{u}})$ which is defined as

$$S(\hat{\mathbf{u}}) \triangleq \mathbf{w}^T \hat{\mathbf{u}} \tag{23}$$

where $\mathbf{w}$ is the weighting vector. $S(\hat{\mathbf{u}})$ is compared against a predefined threshold to decide the presence or absence of the PU signal. Consequently, the system performance is characterized by the statistical behavior of $S(\hat{\mathbf{u}})$.

In the following, we use the MDC to optimize the proposed system performance. The MDC has long been used in developing distributed detection schemes and can be justified as a performance metric by various arguments [8]. In order to formulate this optimization, we need to evaluate the first- and second-order statistics of the global test summary $S(\hat{\mathbf{u}})$. More specifically, we require $\Delta\mu_S \triangleq E\left[S(\hat{\mathbf{u}})|\mathcal{H}_1\right] - E\left[S(\hat{\mathbf{u}})|\mathcal{H}_0\right]$ and $\sigma^2_{S|\mathcal{H}_h} \triangleq \text{Var}\left\{S(\hat{\mathbf{u}})|\mathcal{H}_1\right\}$.

The MDC is defined as the variance-normalized distance between the centers of two conditional pdfs of the global test summary, i.e.,

$$\Delta_m^2 \triangleq \frac{\left(E\left[S(\hat{\mathbf{u}})|\mathcal{H}_1\right] - E\left[S(\hat{\mathbf{u}})|\mathcal{H}_0\right]\right)^2}{\text{Var}[S(\hat{\mathbf{u}})|\mathcal{H}_1]} = \frac{(\Delta\mu_S)^2}{\sigma^2_{S|\mathcal{H}_1}} \tag{24}$$

By considering the fact that the elements of $\tilde{\mathbf{P}}_L$ lie between zero and one, and by using Taylor series expansions, we have shown in [7] that

$$\Delta\mu_S \approx \mathbf{w}^T \mathbf{C}_{\mathbf{u}_L\mathbf{u}}^T \tilde{\mathbf{P}}_L^2 \left(E\left[\mathbf{u}_L|\mathcal{H}_1\right] - E\left[\mathbf{u}_L|\mathcal{H}_0\right]\right) \tag{25}$$

$$\mathbf{\Sigma}_{\mathcal{H}_h} \approx \mathbf{C}_{\mathbf{u}_L\mathbf{u}}^T \tilde{\mathbf{P}}_L^2 \mathbf{C}_{\mathbf{u}_L\mathbf{u}} \tag{26}$$

For simplicity, we have assumed $\sigma_z^2 = 1$.

Now, we formally represent the joint optimization of the reporting and fusion schemes in the proposed cooperative sensing as

$$(\mathbf{w}^*, \mathbf{p}_L^*) = \underset{\mathbf{w},\mathbf{p}_L}{\operatorname{argmax}} \Delta_m^2 \tag{P1}$$
$$\text{s.t.} \begin{cases} \mathbf{0} \preceq \mathbf{p}_L \preceq \mathbf{1} \\ \mathbf{1}^T \cdot \mathbf{p}_L \leq (1-\eta)n \end{cases}$$

where η denotes the power-efficiency constraint we consider in designing the proposed interrupted reporting scheme. Note that for $0 < \eta \leq 1$ some elements of $\mathbf{p}_L$ have to be less than 1, which means we are forcing some sensing nodes to occasionally go to the sleeping mode (i.e., avoid cooperation). Moreover, it is clear that in general, the higher η we chose, the higher is the number of nodes which are forced to sleep, or the more likely any node is to go to the sleeping mode. In fact, η is the parameter by which we control the energy consumption of the proposed interrupted reporting scheme.

III. Joint Interruption-Fusion Optimization

In this section, we develop our proposed approach for solving the optimization problem. Note that the optimization problem in (P1) is a fractional program. By change of variables, we first turn this fractional program into a quadratic optimization and then use standard quadratic programming techniques to solve the problem.

By using (25) and (26) and based on the following definitions,

$$\mathbf{w}_p \triangleq \tilde{\mathbf{P}}_L^2 \mathbf{C}_{\mathbf{u}_L\mathbf{u}} \mathbf{w} \tag{27}$$

$$\mathbf{a} \triangleq E\left[\mathbf{u}_L|\mathcal{H}_1\right] - E\left[\mathbf{u}_L|\mathcal{H}_0\right] \tag{28}$$

we can approximate our objective function as

$$\Delta_m^2 \approx \frac{\left(\mathbf{w}_p^T \mathbf{a}\right)^2}{\mathbf{w}_p^T \tilde{\mathbf{P}}_L^{-2} \mathbf{w}_p} \tag{29}$$

This objective function is homogeneous with respect to $\mathbf{w}_p$, so we can limit $\mathbf{w}_p$ to be on the unit ball. In addition, the MDC in (29) can be expressed as a *Rayleigh quotient* by which we can maximize the objective function for a given $\mathbf{p}_L$. To this end, we use the following linear transformation

$$\mathbf{w'}_p \triangleq \tilde{\mathbf{P}}_L^{-1} \mathbf{w}_p \tag{30}$$

which leads to

$$\Delta_m^2 \approx \frac{\mathbf{w'}_p^T \tilde{\mathbf{P}}_L \mathbf{a}\mathbf{a}^T \tilde{\mathbf{P}}_L \mathbf{w'}_p}{\mathbf{w'}_p^T \mathbf{w'}_p} \tag{31}$$

Therefore, the objective function can be maximized, by using the Lagrange multipliers, for a given $\mathbf{p}_L$ by

$$\mathbf{w'}_p^* = \tilde{\mathbf{P}}_L \mathbf{a} \tag{32}$$

which is the eigenvector of the positive semi-definite matrix $\tilde{\mathbf{P}}_L \mathbf{a}\mathbf{a}^T \tilde{\mathbf{P}}_L$ corresponding to the maximum eigenvalue (the nonzero eigenvalue). Consequently, $\mathbf{w}_p^*$, which maximizes the objective function for a given $\mathbf{p}_L$, is derived as

$$\mathbf{w}_p^* = \frac{\tilde{\mathbf{P}}_L^2 \mathbf{a}}{\left\| \tilde{\mathbf{P}}_L^2 \mathbf{a} \right\|_2} \tag{33}$$

and $\mathbf{w}^* = \mathbf{C}_{\mathbf{u}_L\mathbf{u}}^{-1} \tilde{\mathbf{P}}_L^{-2} \mathbf{w}_p^*$. Now we can eliminate $\mathbf{w}$ from our objective function and convert it to

$$\Delta_m^2 \approx \mathbf{a}^T \tilde{\mathbf{P}}_L^2 \mathbf{a} = \mathbf{p}_L^T \mathbf{D} \mathbf{p}_L \tag{34}$$

where $\mathbf{D} \triangleq \left[\operatorname{diag}(\mathbf{a})\right]^2$. Consequently, (P1) can be reformulated as

$$\mathbf{p}_L^* = \underset{\mathbf{p}_L}{\operatorname{argmax}} \mathbf{p}_L^T \mathbf{D} \mathbf{p}_L \tag{P2}$$
$$\text{s.t.} \begin{cases} \mathbf{0} \preceq \mathbf{p}_L \preceq \mathbf{1} \\ \mathbf{1}^T \mathbf{p}_L \leq (1-\eta)n \end{cases}$$

It is worth noting that, solving (P2) requires maximizing a convex quadratic objective function over a convex set, which is NP-hard in general. Fortunately, there exist numerous relaxation techniques in literature for solving nonconvex quadratic programs in a computationally-efficient manner. A variety of these relaxations can be formulated as semidefinite programs (SDPs) and it is shown in [9] that very good results are achieved when the so-called reformulation linearization technique (RLT) [10] is jointly used with SDP relaxation. Accordingly, we first reformulate (P2) by introducing a new variable as $\mathbf{V} = \mathbf{p}_L \mathbf{p}_L^T$ which leads to

$$\max_{\mathbf{V},\mathbf{p}_L} \operatorname{Tr}(\mathbf{D}\mathbf{V}) \tag{P3-a}$$
$$\text{s.t.} \begin{cases} \mathbf{0} \preceq \mathbf{p}_L \preceq \mathbf{1} \\ \mathbf{1}^T \mathbf{p}_L \leq (1-\eta)n \\ \mathbf{V} = \mathbf{p}_L \mathbf{p}_L^T \end{cases}$$

The SDP relaxation is then realized by replacing the last constraint in (P3-a) by $\mathbf{V} \succeq \mathbf{p}_L \mathbf{p}_L^T$, while the RLT is constructed based on using products of upper and lower bound constraints on the original variables to obtain valid linear inequality constraints on the new variable $\mathbf{V}$. Consequently, the resulting optimization is

$$\max_{\mathbf{V},\mathbf{p}_L} \operatorname{Tr}(\mathbf{D}\mathbf{V}) \tag{P3-b}$$
$$\text{s.t.} \begin{cases} \mathbf{1}^T \mathbf{p}_L \leq (1-\eta)n \\ \mathbf{V} - \mathbf{p}_L \mathbf{1}^T - \mathbf{1}\mathbf{p}_L^T + \mathbf{1}\mathbf{1}^T \geq 0 \\ \mathbf{V} - \mathbf{p}_L \mathbf{1}^T \leq 0 \\ \mathbf{V} \geq 0 \\ \mathbf{V} \succeq \mathbf{p}_L \mathbf{p}_L^T \end{cases}$$

Note that the last constraint in this problem is equivalent to

$$\begin{pmatrix} 1 & \mathbf{p}_L^T \\ \mathbf{p}_L & \mathbf{V} \end{pmatrix} \succeq 0 \tag{35}$$

Therefore, (P3-b) is a convex optimization problem which can be solved, to any arbitrary accuracy, in a numerically-reliable and efficient fashion.

In the following section, we demonstrate the proposed system performance considering the cases with and without the optimal linear combining.

IV. Simulation Results

In this section, we report simulation results demonstrating the performance of the proposed joint optimization scheme. We use the optimal linear combining scheme in [2], [4], [5] as the benchmark. In performance evaluation of the proposed detector, we consider two cases as (i) the system performance with equal-gain combining (ECG) (i.e., when equal weights are used for all sensors) and optimal distributions for interrupted reports and (ii) the system performance when the linear fusion is jointly optimized by the interrupted reporting scheme.

Three sensing nodes are considered, i.e., $K = 3$, operating at different SNR regimes. The listening channels are characterized by SNRs equal to $\{12, 5, 8\}$ in dB. The reporting channel noise variance is $\sigma_z^2 = 10$. The correlation coefficient ρ between the local sensing outcomes when $\mathcal{H}_1$ is true is 0.1 and the number of samples N used by each sensing node for energy detection is 20. All simulations are conducted by 100,000 sample realizations. When comparing the proposed system performance with the optimal linear fusion, the energy efficiency levels considered are 30%, 50%, 70%, and 90%. We have set $L = 0$ to demonstrate that, compared to the optimal linear fusion, no more information is required about the PU signal in the proposed system.

Fig. 1 depicts the complementary receiver operational characteristics (CROC) curves demonstrating the performance of the proposed detector operating with different levels of energy efficiency, along with a CROC curve corresponding to the performance of the optimal linear combiner. The curves corresponding to the joint optimization are designated as "Joint wp opt." whereas the curves corresponding to optimal interruptions and uniform weighting (EGC) are denoted by "Opt. p".

In this figure, we observe that for all the different levels of energy efficiency, the system performance does not change significantly by involving the linear fusion in the optimization process. These results clearly illustrate that the propose random-interruptions-based cooperative sensing is capable of discriminating between the reliable and unreliable sensing nodes on its own and achieves the best performance even when the linear combining is realized by EGC. More specifically, we have established that, when interrupted reporting scheme is incorporated in cooperation, EGC at the FC is nearly the optimal fusion rule. Recall that the optimal linear combining [5] closely achieves the optimal performance of LRT in existing cooperative sensing schemes for CRNs.

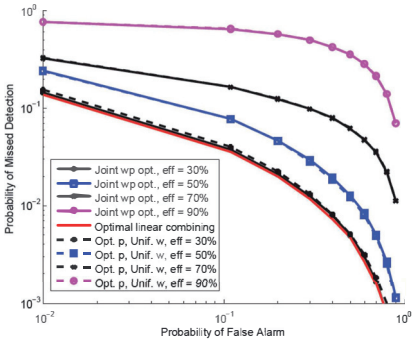

Fig. 1. CROC curves demonstrating the performance of the proposed cooperative sensing scheme working under different energy-efficiency levels and the performance of the optimal linear combining. The CRN considered has three sensing nodes experiencing SNR levels as $\{12, 5, 8\}$ in dB at the listening channels. The reporting channel noise variance is $\sigma_z^2 = 10$ and the correlation coefficient between the local sensing outcomes when $\mathcal{H}_1$ is true is $\rho = 0.1$.

V. Conclusion

In this paper, we have jointly optimized the reporting and fusion phases of cooperative spectrum sensing scheme with linear fusion at the FC and random interruptions in cooperation of the sensing nodes with the FC. The results achieved based on maximizing the MDC in this system demonstrate that, when random interruptions are employed, there is no more need for discriminating between the reliable and unreliable nodes by the fusion process, and the EGC scheme at the FC is enough to nearly have the optimal overall detection performance.

References

[1] I. F. Akyildiz, B. F. Lo, and R. Balakrishnan, "Cooperative spectrum sensing in cognitive radio networks: A survey," *Elsevier Physical Commun.*, vol. 4, no. 1, pp. 40–62, March 2011.

[2] G. Taricco, "Optimization of linear cooperative spectrum sensing for cognitive radio networks," *IEEE J. Sel. Topics Signal Process.*, vol. 5, no. 1, pp. 77–86, Feb. 2011.

[3] S. Chaudhari, J. Lundén, V. Koivunen, and H. V. Poor, "BEP walls for cooperative sensing in cognitive radios using K-out-of-N fusion rules," *Elsevier Signal Process*, vol. 93, no. 7, pp. 1900–1908, July 2013.

[4] Z. Quan, W. Ma, S. Cui, and A. H. Sayed, "Optimal linear fusion for distributed detection via semidefinite programming," *IEEE Trans. Signal Process.*, vol. 58, no. 4, pp. 2431–2436, 2010.

[5] Z. Quan, S. Cui, and A. H. Sayed, "Optimal linear cooperation for spectrum sensing in cognitive radio networks," *IEEE J. Sel. Topics Signal Process.*, vol. 2, no. 1, pp. 28–40, Feb. 2008.

[6] H. V. Poor, *An introduction to signal detection and estimation.* Berlin Heidelberg: Springer-Verlag, 1994.

[7] Y. Abdi and T. Ristaniemi, "Random interruptions in cooperation for spectrum sensing in cognitive radio networks," *IEEE Trans. Signal. Process.*, (submitted for publication, available on arxiv.org).

[8] B. Picinbono, "On deflection as a performance criterion in detection," *Aerospace and Electronic Systems, IEEE Transactions on*, vol. 31, no. 3, pp. 1072–1081, Jul 1995.

[9] X. Bao, N. Sahinidis, and M. Tawarmalani, "Semidefinite relaxations for quadratically constrained quadratic programming: A review and comparisons," *Mathematical Programming*, vol. 129, no. 1, pp. 129–157, 2011.

[10] K. Anstreicher, "Semidefinite programming versus the reformulation-linearization technique for nonconvex quadratically constrained quadratic programming," *Journal of Global Optimization*, vol. 43, no. 2-3, pp. 471–484, 2009.

PVI

ANALYTICAL AND LEARNING-BASED SPECTRUM SENSING TIME OPTIMISATION IN COGNITIVE RADIO SYSTEMS

by

Hossein Shokri-Ghadikolaei, Younes Abdi, and Masoumeh Nasiri-Kenari

IET Communications, vol. 7, no. 5, pp. 480 - 489, 2013 (**IET Premium Paper Award 2014**)

www.ietdl.org

Published in IET Communications
Received on 29th May 2012
Revised on 24th November 2012
Accepted on 12th December 2012
doi: 10.1049/iet-com.2012.0302

ISSN 1751-8628

Analytical and learning-based spectrum sensing time optimisation in cognitive radio systems

Hossein Shokri-Ghadikolaei, Younes Abdi, Masoumeh Nasiri-Kenari

Wireless Research Laboratory, Electrical Engineering Department, Sharif University of Technology, Tehran, Iran
E-mail: mnasiri@sharif.edu

Abstract: In this study, the average throughput maximisation of a secondary user (SU) by optimising its spectrum sensing time is formulated, assuming that a priori knowledge of the presence and absence probabilities of the primary users (PUs) is available. The energy consumed to find a transmission opportunity is evaluated, and a discussion on the impacts of the number of PUs on SU throughput and consumed energy are presented. To avoid the challenges associated with the analytical method, as a second solution, a systematic adaptive neural network-based sensing time optimisation approach is also proposed. The proposed scheme is able to find the optimum value of the channel sensing time without any prior knowledge or assumption about the wireless environment. The structure, performance and cooperation of the artificial neural networks used in the proposed method are explained in detail, and a set of illustrative simulation results is presented to validate the analytical results as well as the performance of the proposed learning-based optimisation scheme.

1 Introduction

Intense public interest in new wireless technologies has motivated communication system designers and policy makers worldwide to revolutionise traditional inefficient spectrum management mechanisms and develop advanced flexible scenarios for better spectrum utilisation, see [1]. These efforts have revealed that the old strategy of giving the exclusive right of using particular spectrum bands to some specific users (licensees) makes this valuable resource severely under-utilised. Fortunately, the concept of cognitive radio (CR) has emerged to mitigate this issue. In fact, CRs are intended to find transmission opportunities in wireless environment when no particular spectrum has been assigned to them. To protect primary users (PUs) from harmful interference, CRs have to be capable of sensing the radio spectrum, learning and adapting to the wireless environment [2].

Spectrum sensing schemes are of major importance in designing superior CR systems. The average throughput of the secondary users (SUs), their consumed energy and the amount of interference experienced by PUs are directly related to the effectiveness of the sensing schemes incorporated in CRs. Slotted CRs usually divide their time-slots into two parts; one for sensing and the other for data transmission [3, 4]. Sensing time refers to the portion of time-slots used for sensing the radio spectrum. Generally speaking, increasing the sensing time leads to higher sensing accuracy but decreases the average CR throughput [4, 5]. Hence, it is certainly a challenge to find an optimal value for the spectrum sensing time to have the maximum possible throughput while protecting PUs from harmful interference [3]. On the other hand, because of the dynamic behaviour of the PUs, the number and location of the temporarily-available transmission opportunities in the radio spectrum change occasionally. This behaviour is modelled as spectrum mobility and when it is taken into account, the aforementioned sensing time optimisation problem becomes even more challenging. Since the distribution of white spaces changes because of spectrum mobility, CRs have to handoff spectrums in order to maintain a predefined quality-of-service level. In other words, the SU must leave its current spectrum and continue its transmission on another spectrum when the corresponding PU arrives. This process is called spectrum hand-over or simply hand-over (HO).

In recent years, throughput maximisation by optimising spectrum sensing time has gained a lot of interest. In [5], the impact of spectrum sensing time on the overall throughput of an SU is investigated, and the optimum value of the sensing time has been found numerically. In [6], two distributed Q-learning algorithms have been proposed to determine the optimum value of sensing time. Joint optimisations of sensing time and decision threshold have been addressed in [7] for wideband OFDM-based cognitive radio networks (CRNs). However, none of these works have considered the effect of spectrum mobility and consequent HOs in their utilised CR system models. In [8–10], the problem of sequential channel sensing for an SU has been evaluated. Sequential channel sensing means that the SU starts sensing the channels from top of a list (called sensing sequence), and if the considered channel is sensed as occupied, the SU senses the next one and this process is continued until an idle spectrum is found. Based on this assumption, an optimisation problem is formulated in [8] in order to minimise the average sensing time. The false

detection and spectrum HO effects on sensing time have been investigated in [8]; however the adverse effect of the HO (the sensing time effect) on SU throughput has not been considered. The impact of sensing time on the average achievable throughput in sequential sensing scheme has been partially studied in [9, 10].

In this paper, two independent solutions are proposed for this problem. In the first proposed method, spectrum sensing time optimisation of a CR system is investigated analytically. Specifically, the throughput of an SU is clearly formulated in terms of sensing time when the spectrum mobility and consequent HOs are taken into account. Moreover, the energy cost of HOs is considered in the proposed modelling in order to address the energy-throughput tradeoff encountered in designing portable and/or green CR systems. In other words, the tradeoff between the maximum achievable throughput and the sensing energy consumption is explained and a design parameter is introduced to modify the optimisation problem to address the consumed energy.

The optimum value of sensing time derived through conventional analytical optimisation procedures depends directly on the models adopted for the channel, the users' traffic and the PUs' behaviour. Despite the increased analytical complexity associated with using more complete modellings, these models are not necessarily consistent with the actual environments in which the CRs work; and therefore the derived values cannot be considered as the perfect optimum ones. Moreover, if any changes occur in the parameters describing the wireless environment and traffic conditions experienced by the SUs, it is required to estimate the new parameters, repeat the analysis and recalculate the optimum values of sensing time. To deal with these issues appropriately, we propose a second method which is based on systematic configuration of two kinds of well-known artificial neural networks. Specifically, a multilayer feed-forward (MFF) neural network [11] is used to replace the mathematical modelling, which learns the actual behaviour of the secondary link, that is, the effect of spectrum sensing time on average throughput of the SU. Based on the actual (non-analytical) model of the link which is learned by the MFF network, a Kennedy-Chua (KC) neural network [12] is used to find the optimum value of spectrum sensing time. This learning-based optimisation scheme has several advantages over the analytical method. First, no prior knowledge about link behaviour, such as the presence or absence probabilities of PUs are required. Second, the limited consistency of the mathematical models with the real wireless environment does not affect the optimality of the derived spectrum sensing time. Third, using this learning-based optimisation scheme, an adaptive system is proposed which is capable of effectively following the variations in the link and keeping the average throughput at the maximum level in non-stationary conditions.

The main reason for selecting the MFF and the KC networks in our proposed scheme is that these networks can efficiently learn unknown mappings and optimise general non-linear programming problems. More specifically, Hornik *et al*. [13, 14] have shown that an MFF neural network with as few as a single hidden layer and an appropriately smooth hidden layer activation function is capable of providing arbitrarily accurate approximation of almost any given function and its derivatives, which enables the proposed scheme to learn the effect of spectrum sensing time on average throughput of the SU. On the other hand, the KC neural network, which is an advanced version of the classical Hopfield neural network [15], is capable of effectively solving general non-linear programming problems in a very short period of time, without any need of computationally demanding iterative procedures [12]. This neural network is entirely made of simple electronic devices such as capacitors, resistors and operational amplifiers, and is also suitable for implementation in a very large scale integration technology [16]. Furthermore, the stability of its solution is analytically guaranteed [12]. Owing to these benefits, it has been widely used in high-performance low-complexity adaptive communication systems, see [16–18] and references therein.

The rest of this paper is organised as follows. In Section 2, we describe the considered CR system model and derive the related optimisation problem. In Section 3, the utilised neural networks as well as the proposed learning-based sensing time optimisation scheme are introduced. Numerical results are then presented in Section 4, followed by concluding remarks in Section 5.

2 System model and the related optimisation problem

2.1 System model

We assume a primary network with N_p users, each of them with a dedicated channel, and also a single SU. The SU utilises narrow-band spectrum sensing, that is, it senses only one spectrum (out of N_p spectrums) at a time. Hence, the maximum possible transmission opportunities obtained after each sensing phase are one. We assume that the SU always has packets to transmit, that is, the SU starts its transmission when an opportunity is found. The SU senses the channels in an order determined by its sensing sequence. If the sensed channel is busy, the SU reconfigures its sensing circuitry in order to sense the next spectrum indicated in its sensing sequence. Assume that it takes a constant time τ_{ho} for the SU to do an HO. τ_{ho} does not depend on the amount of frequency shift required by the reconfiguration. The state of channel k is denoted by s_k

$$s_k = \begin{cases} 1: & \text{if channel } k \text{ is occupied, or } \mathcal{H}_1 \\ 0: & \text{if channel } k \text{ is idle, or } \mathcal{H}_0 \end{cases} \quad (1)$$

where $\mathcal{H}_0$ and $\mathcal{H}_1$ represent the absence and presence hypotheses of the kth PU, respectively. Spectrum sensing can be formulated as a binary hypothesis testing problem [5]

$$\begin{cases} \mathcal{H}_0: & y(n) = z(n) \text{:channel is idle} \\ \mathcal{H}_1: & y(n) = u(n) + z(n) \text{:channel is occupied} \end{cases} \quad (2)$$

where $z(n)$s denote samples of zero mean complex-valued Gaussian noise with independent and identical distributions (i.i.d.), $u(n)$ denotes the PUs signal which is independent of $z(n)$ and $y(n)$ is the nth sample of the received signal.

We consider the energy detector (ED) method for PU detection in which the energy of the received signal is computed during a sensing time τ, and then the result is compared with a predefined threshold to take the decision [3]. Let N denote the number of samples of the received signal, that is, $N = \tau f_s$, where τ is the sensing time and f_s is the sampling frequency. By defining X as a decision metric

for the ED scheme, we have

$$X = \sum_{n=1}^{N} |y(n)|^2 \tag{3}$$

Let λ denote the threshold of the ED decision rule. Then

$$\begin{cases} X < \lambda \equiv \mathcal{H}_0 \\ X \geq \lambda \equiv \mathcal{H}_1 \end{cases} \tag{4}$$

If N is large enough, X can be described by a Gaussian distribution [5]. Assume that P_{fa}, P_{d} and $P_{\text{d}}^{\min}$ denote the false alarm probability, detection probability and minimum allowable detection probability (i.e. we must have $P_{\text{d}} \geq P_{\text{d}}^{\min}$), respectively. Then [5]

$$P_{\text{fa}} = Q\left[\left(\frac{\lambda}{\sigma_u^2} - 1\right)\sqrt{\tau f_{\text{s}}}\right] \tag{5}$$

$$P_{\text{d}} = Q\left[\left(\frac{\lambda}{\sigma_u^2} - 1 - \gamma\right)\sqrt{\frac{\tau f_{\text{s}}}{1+2\gamma}}\right] \tag{6}$$

where σ_u^2 is the received energy of the PU signal and σ_z^2 is the noise variance. The received signal-to-noise ratio because of PU activity is $\gamma = (\sigma_u^2/\sigma_z^2)$.

Taking (5) and (6) into account, for $P_{\text{d}} = P_{\text{d}}^{\min}$ we have

$$P_{\text{fa}} = Q\left[\beta + \gamma\sqrt{\tau f_{\text{s}}}\right] \tag{7}$$

where $\beta = Q^{-1}(P_{\text{d}}^{\min})\sqrt{1+2\gamma}$.

2.2 Sensing time optimisation problem

We consider a sequential HO method [8] as described in the Introduction. Based on the energy detection scheme assumed, the ith channel is sensed as occupied with probability

$$\begin{aligned} q_i &= \Pr\{\text{ED}_i = 1 | s_i = 0\} P_{i,0} + \Pr\{\text{ED}_i = 1 | s_i = 1\} \\ P_{i,1} &= P_{\text{fa}} P_{i,0} + P_{\text{d}} P_{i,1} \end{aligned} \tag{8}$$

where ED_i is the output of the ED because of sensing of the ith channel. $\text{ED}_i = 1$ means that the CR has detected a PU on the ith channel whereas $\text{ED}_i = 0$ means that no PU has been detected. $P_{i,0}$ and $P_{i,1}$ are the absence and presence probabilities of the ith PU, respectively.

Let α denote the maximum number of allowed HOs. α is limited by two constraints. First, the number of sensed channels which cannot exceed the number of PUs. Second, the elapsed time for both sensing and HO procedures that cannot exceed the time-slot duration, T. Therefore

$$\alpha = \min\left(\left\lfloor \frac{T-\tau}{\tau+\tau_{\text{ho}}} \right\rfloor, N_{\text{P}} - 1\right) \tag{9}$$

Using the sequential spectrum sensing scheme, the SU transmits on channel i when i–1 consecutive handoff events occur, that is, when $\text{ED}_k = 1$ for all $k < i$ and $\text{ED}_i = 0$. Clearly, because of possible sensing errors, the SU might mistakenly decide to transmit on a channel which has already been occupied by a PU. Therefore two maximum throughput levels are expected for an SU depending on the presence or absence of a PU on the adopted channel. We denote these two maximum throughput levels by C_1 and C_0 for the occupied and free channels, respectively. Using these definitions, the contribution of the ith channel on the overall maximum achievable throughput of the SU can be expressed as

$$\begin{aligned} \overline{R}_i = {} & C_0 T_i \Pr\{\text{ED}_i = 0 \text{ and } \text{ED}_k = 1 \text{ for } k < i \text{ and } s_i = 0\} \\ & + C_1 T_i \Pr\{\text{ED}_i = 0 \text{ and } \text{ED}_k = 1 \text{ for } k < i \text{ and } s_i = 1\} \end{aligned} \tag{10}$$

where

$$C_0 = \log_2(1+\gamma_{\text{s}}) \quad \text{and} \quad C_1 = \log_2\left(1 + \frac{P_{\text{s}}}{N_0 + P_{\text{p}}}\right) = \log_2\left(1 + \frac{\gamma_{\text{s}}}{1+\gamma_{\text{p}}}\right),$$

respectively, are the SUs capacities under the hypotheses $\mathcal{H}_0$ and $\mathcal{H}_1$. γ_{s} and γ_{p} are the received SNRs because of the secondary and PUs' signals at the SU receiver, respectively. T_i is the fraction of time-slots remaining for data transmission after sensing i–1 channels occupied and is calculated as

$$\begin{aligned} T_i &= T - \tau - (i-1)(\tau + \tau_{\text{ho}}) \quad \text{for} \\ & i = 1, 2, \ldots, N_{\text{p}} \end{aligned} \tag{11}$$

Although the random variables ED_i, $i = 1, 2, \ldots, N_{\text{p}}$, are mutually independent, each pair ED_i and s_i (the state of channel i) are related to each other based on the incorporated spectrum sensing algorithm which is characterised by P_{fa} and P_{d}. Hence, (10) can be restated as

$$\begin{aligned} \overline{R}_i &= \big(C_0 T_i \Pr\{\text{ED}_i = 0 \text{ and } s_i = 0\} \\ &\quad + C_1 T_i \Pr\{\text{ED}_i = 0 \text{ and } s_i = 1\}\big) \prod_{k=1}^{i-1} \Pr\{\text{ED}_k = 1\} \\ &= \big(C_0 T_i \Pr\{\text{ED}_i = 0 | s_i = 0\} + \\ &\quad C_1 T_i \Pr\{\text{ED}_i = 0 | s_i = 1\}\big) \prod_{k=1}^{i-1} \Pr\{\text{ED}_k = 1\} \\ &= \big(C_0 T_i (1 - P_{\text{fa}}) P_{i,0} + C_1 T_i (1 - P_{\text{d}}) P_{i,1}\big) \prod_{k=1}^{i-1} q_k \end{aligned} \tag{12}$$

where q_i, $P_{i,0}$ and $P_{i,1}$ are defined in (8). Finally, the aggregate maximum achievable throughput of the SU is derived by summing over all $\overline{R}_i$, that is, for $i = 1, 2, \ldots, \alpha$. Hence, the following proposition has been proved.

Proposition 1: The overall average throughput of a CR system which incorporates the energy detection and sequential spectrum sensing schemes to find transmission opportunities among N_{p} primary channels is

$$\begin{aligned} R = \sum_{i=0}^{\alpha} & q_0 q_1 \cdots q_i \big(C_1 P_{i+1,1}(1 - P_{\text{d}}) + C_0 P_{i+1,0}(1 - P_{\text{fa}})\big) \\ & \left(1 - \frac{\tau + i(\tau + \tau_{\text{ho}})}{T}\right) \end{aligned} \tag{13}$$

where $q_0 \triangleq 1$.

doi: 10.1049/iet-com.2012.0302

Considering (13), the optimum throughput can be obtained by solving the following optimisation problem $P1$

$$P1: \max_{\tau,\lambda} \quad R \quad \text{s.t.} \begin{cases} P_{\text{fa}} \le P_{\text{fa}}^{\max} \\ P_{\text{d}} \ge P_{\text{d}}^{\min} \\ 0 < \tau < T \end{cases} \tag{14}$$

The derived optimisation problem cannot be simplified to a one-dimensional (1D) one, as [5], without any preassumptions on P_{fa} or P_{d}. However, we can convert our 2D optimisation problem to a 1D one by using an acceptable value for the detection probability imposed by standards like 'IEEE 802.22'. Supposing $P_{\text{d}} = P_{\text{d}}^{\min}$, the optimisation problem is converted to

$$P2: \max_{\tau,\lambda} R \quad \text{s.t.} \begin{cases} P_{\text{fa}} \le P_{\text{fa}}^{\max} \\ P_{\text{d}} = P_{\text{d}}^{\min} \\ 0 < \tau < T \end{cases} \tag{15}$$

Note that, under the assumption $P_{\text{d}} = P_{\text{d}}^{\min}$ and using (6), λ can be expressed in terms of τ and as a result, the throughput of the SU derived in (13) only depends on τ. Moreover, based on the first constraint of (15) and from (7), we have $Q\left[\beta + \gamma\sqrt{\tau f_{\text{s}}}\right] \le P_{\text{fa}}^{\max}$ which in turn leads to

$$\tau \ge \frac{1}{f_{\text{s}}}\left(\frac{Q^{-1}\left(P_{\text{fa}}^{\max}\right) - \beta}{\gamma}\right)^2$$

Therefore $P2$ can be simplified as

$$P3: \max_{\tau} \quad R \quad \text{s.t.} \quad \tau_{\min} < \tau < T \tag{16}$$

where

$$\tau_{\min} = \frac{1}{f_{\text{s}}}\left(\frac{Q^{-1}\left(P_{\text{fa}}^{\max}\right) - \beta}{\gamma}\right)^2$$

2.3 Energy-throughput tradeoff

Recall that as defined in (8), q_i denotes the probability that the channel i is sensed busy. Thus, the probability of only one HO occurring in the system equals to $q_1(1 - q_2)$. In the same way, the probability of performing exactly two HOs by the system equals to $q_1q_2(1 - q_3)$ and so on. In other words, for the sequential HO method described, the probability of having i consecutive HOs and transmitting on the $(i+1)$th channel is equal to $\left(1 - q_{i+1}\right)\prod_{k=1}^{i} q_k$. Hence, if we denote the average number of HOs required for finding a free transmission opportunity by $\overline{g}$, we have

$$\overline{g} = q_1\left(1 - q_2\right) + 2q_1q_2\left(1 - q_3\right) + \cdots + (\alpha - 1)\left(1 - q_\alpha\right)\prod_{j=1}^{\alpha-1} q_j + \alpha\prod_{j=1}^{\alpha} q_j \tag{17}$$

where α is defined in (9). Clearly, the average number of sensed channels equals to $1 + \overline{g}$.

Assume that $E_{\text{c}}(\tau)$ and $E_{\text{c}}(\tau_{\text{ho}})$ denote the consumed energies for sensing of each primary channel and for each HO, respectively. Hence, the average consumed energy for finding a transmission opportunity is computed

$$E = \left(1 + \overline{g}\right)E_{\text{c}}(\tau) + \overline{g}E_{\text{c}}\left(\tau_{\text{ho}}\right) \tag{18}$$

The processes of channel sensing and signal transmission consume more energy compared with the HO [19]. Therefore it is reasonable to ignore the second term $\overline{g}E_{\text{c}}\left(\tau_{\text{ho}}\right)$ in (18) compared with the first one.

When the number of PUs increases, α in (9) increases, and thus R and $\left(1 + \overline{g}\right)$ in (13) and (17) rise, consequently. Therefore increasing the number of PUs increases both the maximum achievable throughput and the number of sensed channels (equivalently the consumed energy). However, among these two metrics, the consumed energy increases more rapidly than the maximum throughput. To illustrate this phenomenon, in the following we consider a numerical example.

Fig. 1 shows the plot of the normalised energy consumed for finding a transmission opportunity [i.e. $(E/(E_c))$] which is equal to the number of sensed channels] against the maximum achievable throughput assuming $P_{\text{fa}}^{\max} = 0.1$, $P_{\text{d}}^{\min} = 0.9$, $T = 100$ ms, $\tau_{\text{ho}} = 0.1$ ms and $f_{\text{s}} = 6$ MHz. The simulation setup procedure is described in Section 4. As illustrated, for high throughput values, increasing the consumed energy cannot improve the data rate significantly. In fact, since increasing the number of HOs reduces the time duration left for the transmission, the achievable data rate is not substantially improved. For instance, for $N_{\text{p}} = 4$ with the average number of sensed channels equal to 1.8757, the maximum data rate is 0.8544, whereas for $N_{\text{p}} = 15$ with the average sensed channels equal to 3.398, the maximum data rate is 0.8809. As a result, increasing the average number of sensed channels by 81% only leads to a near 3% increase in the maximum data rate. Therefore at the cost of a small reduction of the maximum throughput, the consumed energy can be substantially decreased. To take into account the energy consumption, in the following, we reformulate the optimisation problem.

At first, we show that R in (13) does not depend on the number of PUs for sufficiently large N_{p}. If we rewrite R, from (13) we have

$$R\left(\tau, \lambda, N_{\text{p}}\right) = \sum_{m=0}^{\alpha\left(\tau, N_{\text{p}}\right)} A_m(\tau, \lambda)B_m(\tau, \lambda)$$

$$\text{where} \quad \begin{cases} A_m(\tau, \lambda) = C_1P_{m+1,1}\left(1 - P_{\text{d}}\right) + C_0P_{m+1,0}\left(1 - P_{\text{fa}}\right) \\ B_m(\tau, \lambda) = q_0q_1 \cdots q_m\left(1 - \dfrac{\tau + m\left(\tau + \tau_{\text{ho}}\right)}{T}\right) \\ \alpha(\tau, N_{\text{p}}) = \min\left(\left\lfloor \dfrac{T - \tau}{\tau + \tau_{\text{ho}}} \right\rfloor, N_{\text{p}} - 1\right) \end{cases} \tag{19}$$

$R(\tau, \lambda, N_{\text{p}})$ is the throughput as a function of τ, λ and N_{p}. Considering the constraint of the derived optimisation problem imposed by sensing time, that is, $\tau_{\min} < \tau < T$, if $N_{\text{p}} \ge \lfloor((T - \tau_{\min})/\tau_{\min} + \tau_{\text{ho}})\rfloor + 1$, we have

$$\alpha(\tau, N_{\text{p}}) = \left\lfloor \frac{T - \tau}{\tau + \tau_{\text{ho}}} \right\rfloor = \alpha(\tau) \tag{20}$$

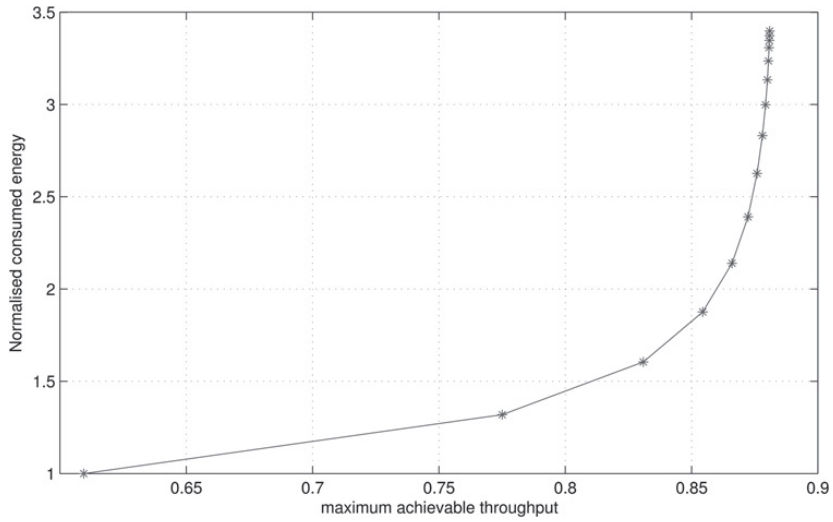

Fig. 1 *Relationship between the normalised consumed energy of an SU and its maximum achievable throughput*

so

$$R(\tau, \lambda, N_{\mathrm{p}})_{|N_{\mathrm{p}} \geq \lfloor (T-\tau_{\min})/(\tau_{\min}+\tau_{\mathrm{ho}}) \rfloor + 1} = R(\tau, \lambda) \tag{21}$$

If we indicate the maximum achievable throughput of the SU by L, from (21) we have

$$L = \max_{\tau} R\left(\tau, \lambda, N_{\mathrm{P}} = \left\lfloor \frac{T-\tau_{\min}}{\tau_{\min}+\tau_{\mathrm{ho}}} \right\rfloor + 1\right) = R(\tau, \lambda) \quad \text{s.t.} \quad \tau_{\min} < \tau < T \tag{22}$$

To take into account the energy consumption, we define

$$\tau_{\mathrm{opt}} = \arg\max_{\tau} R\left(\tau, \lambda, N_{\mathrm{P}} = \left\lfloor \frac{T-\tau_{\min}}{\tau_{\min}+\tau_{\mathrm{ho}}} \right\rfloor + 1\right) \quad \text{s.t.} \quad \tau_{\min} < \tau < T \tag{23}$$

and the corresponding optimum number of HO is

$$\alpha_{\mathrm{opt}} = \alpha_{|\tau=\tau_{\mathrm{opt}}} \tag{24}$$

As stated above, at the throughput close to the maximum achievable one, that is, L, defined in (22), by a small reduction of the throughput, the average energy consumption is substantially reduced. Now, let us define TF ($0 \leq \mathrm{TF} \leq 1$) as a Tradeoff factor indicating the amount of throughput reduction considered. That is the target throughput is set as $R_{\mathrm{TF}} = \mathrm{TF} \times L$. Then, from (22), the maximum number of HOs $\overline{\alpha}\left(\overline{\alpha} \leq \alpha_{\mathrm{opt}}\right)$ considering the energy consumption concern (reflected in the parameter TF) are obtained by solving the following equation:

$$\mathrm{TF} = \frac{\sum_{m=0}^{\overline{\alpha}} A_m(\tau, \lambda) B_m(\tau, \lambda)}{L} \tag{25}$$

That is from (22), L is calculated and by choosing a value for TF, $\overline{\alpha}$ is obtained from (25). Finally, a new optimisation problem considering the consumed energy is formulated as

$$\max_{\tau} R_{\mathrm{TF}} = \sum_{m=0}^{\bar{\alpha}} \left(\begin{array}{c} \left(C_1 P_{m+1,1}\left(1-P_{\mathrm{d}}\right) + C_0 P_{m+1,0}\left(1-P_{\mathrm{fa}}\right)\right) \\ \times q_0 q_1 \cdots q_m \left(1 - \dfrac{\tau + m\left(\tau+\tau_{\mathrm{ho}}\right)}{T}\right) \end{array} \right) \quad \text{s.t.} \quad \tau_{\min} < \tau < T \tag{26}$$

This new derived optimisation problem enables the SU to have control over the consumed energy and the achieved average throughput by the parameter TF.

3 Neural network-based optimisation scheme

3.1 Learning and optimisation

To recast the aforementioned optimisation problem in a suitable form for the learning-based optimisation scheme, first note that the proposed optimisation problem can be divided into two distinct parts. First, obtaining the mappings between τ and R described by (13). Second, from (16), finding the optimum value for τ using the derived mapping. In the proposed learning-based optimisation scheme, both of these parts are performed effectively using KC and MFF neural networks.

To restate the spectrum sensing time optimisation problem suitable for the KC neural network, we define our adaptable parameter x, the cost function φ and the constraint functions f_1 and f_2 as

$$\begin{array}{c} x \triangleq \tau \\ \varphi(x) \triangleq 1/R(x) \\ f_1(x) \triangleq T - x \\ f_2(x) \triangleq x - \tau_{\min} \end{array} \tag{27}$$

Hence, from (16) and (27), the optimisation problem can be

doi: 10.1049/iet-com.2012.0302

rewritten as

$$x^{\text{opt}} = \arg\min_{x} \varphi(x) \tag{28}$$

$$\text{s.t.} \quad f_1(x) \geq 0 \tag{29}$$

$$f_2(x) \geq 0 \tag{30}$$

We collect the constraint functions and their derivatives in a matrix named $\boldsymbol{F}$ defined as

$$\boldsymbol{F} = \begin{bmatrix} f_1(x) & f_2(x) \\ f_1'(x) & f_2'(x) \end{bmatrix} \tag{31}$$

The exploited MFF network has three layers, that is, one input layer, one hidden layer and one output layer. There is one neuron at the input layer, K neurons at the hidden layer and one neuron at the output layer. The proper value of K will be discussed in Section 4. The network input and output are x and the learned version of $\phi(x)$ defined in (27), respectively. There is also one extra output corresponding to the sensitivity of the cost function, that is, $\partial\phi/\partial x$ [20].

The output of the ith neuron at the lth layer is described as

$$u_i(l) = \sum_{j=1}^{N_{l-1}} w_{ij}(l) a_j(l-1) + b_i(l) \tag{32}$$

$$a_i(l) = h_l(u_i(l)), \quad 1 \leq i \leq N_l, \quad l = 1, 2 \tag{33}$$

where N_l is the number of neurons at the lth layer; and $u_i(l)$ and $a_i(l)$ are the activation and output values of the ith neuron at the lth layer. $w_{ij}(l)$ refers to the weight connecting the output from the jth neuron at the $(l-1)$th layer to the input of the ith neuron at the lth layer. $b_i(l)$ refers to the bias associated with the ith neuron at the lth layer. The utilised transferring function $h_l(\cdot)$ in (33) is logistic sigmoid at hidden layer ($l=1$) and is hyperbolic tangent sigmoid at output layer ($l=2$), that is

$$h_l(x) = \begin{cases} (1+\mathrm{e}^{-x})^{-1}, & l = 1 \\ 2(1+\mathrm{e}^{-2x})^{-1} - 1, & l = 2 \end{cases} \tag{34}$$

The input unit is demonstrated by $a_i(0)$ and the output unit by $a_i(2)$, so we have

$$\begin{aligned} x &= a_1(0) \\ \hat{\varphi}(x) &\triangleq a_1(2) \end{aligned} \tag{35}$$

where $\hat{\varphi}$ is the learned version of the cost function. We denote the set of weights and biases by the matrix $\boldsymbol{w}$. The MFF network can be trained to model the function φ, by recursively adjusting $w_{ij}(l)$ and $b_i(l)$ to minimise the mean-squared error between the MFF network output $\hat{\varphi}$ and our cost function φ

$$d = \frac{1}{2}\sum_{m=1}^{M} \left|\hat{\varphi}_m - \varphi_m\right|^2 \tag{36}$$

where M is the number of teacher patterns.

The first-order output derivative of the MMF networks, that is, $\partial a_1(2)/\partial a_1(0)$, can be calculated by applying a backward chaining partial differentiation rule that is described in detail in [20]

$$\begin{aligned} \frac{\partial a_j(2)}{\partial a_i(0)} &= \sum_{k=1}^{N_1} \frac{\partial a_j(2)}{\partial a_k(1)} a_k(1)\left[1 - a_k(1)\right] w_{ki}(1) \\ &= \sum_{k=1}^{N_1} \frac{\partial a_j(2)}{\partial u_j(2)} \frac{\partial u_j(2)}{\partial a_k(1)} a_k(1)\left[1 - a_k(1)\right] w_{ki}(1) \\ &= \left[1 - a_j(2)^2\right] \sum_{k=1}^{N_1} w_{jk}(2)\, a_k(1)\left[1 - a_k(1)\right] w_{ki}(1) \end{aligned} \tag{37}$$

The KC neural network has one output voltage corresponding to the adaptable parameter x. This network calculates the optimum sensing time based on the cost function learned by the MFF network. Now, if there exists a training process to adjust the weight and bias values of the MFF network appropriately and if the learned mapping approximates the actual cost function closely, then the KC network output is equal to the optimum value of x (i.e. the sensing time).

The dynamic equation implemented by the KC neural network is [12, 21]

$$C\frac{\mathrm{d}x}{\mathrm{d}t} = -\frac{\partial\hat{\varphi}}{\partial x} - \sum_{j=1}^{2} i_j \frac{\partial f_j}{\partial x} - Gx \tag{38}$$

where $i_j = g_j(f_j(x))$, and C and G are the output capacitor and the parasitic conductance of the KC network, respectively, and $g_j(.)$ is defined as [12]

$$g_j(v) = \begin{cases} 0, & v \geq 0 \\ \dfrac{1}{R}v, & v \leq 0 \end{cases}, \quad R \to 0 \tag{39}$$

The proper values for C and G will be discussed later in Section 4.

3.2 Proposed scheme

Fig. 2 demonstrates the proposed neural network-based optimisation scheme. It consists of a KC neural network cooperating with an MFF neural network in a feedback loop, a training process which calculates and updates the weight and bias values of the MFF network, and a throughput estimator (TE).

The TE estimates the SU throughput and calculates the value of $\varphi(x)$. This estimation can be performed by inspecting the packets and their acknowledgments (ACKs) at the secondary transmitter for a period of time equal to T_{ep} (estimation period) [22]. T_{ep}, as a design parameter, depends on the PUs activity and link behaviour.

As mentioned before, the KC neural network has one output corresponding to $x = \tau$. It calculates the optimum value for τ based on the cost function provided by the MFF network $\hat{\varphi}(x)$. Its output, even though not necessarily optimal at first, is always used by the ED as the channel sensing time. The learned mapping of the MFF network is considered as the cost function by the KC network. Specifically, this learned function, that is, $\hat{\varphi}(x)$, and its derivative are used by the KC network to establish (38). Thus, the KC network output x will be sufficiently close to the optimum value provided that the function learned by the MFF network can model the link behaviour sufficiently accurately, that is, $\hat{\varphi}(x) \simeq \varphi(x)$. Once the KC network

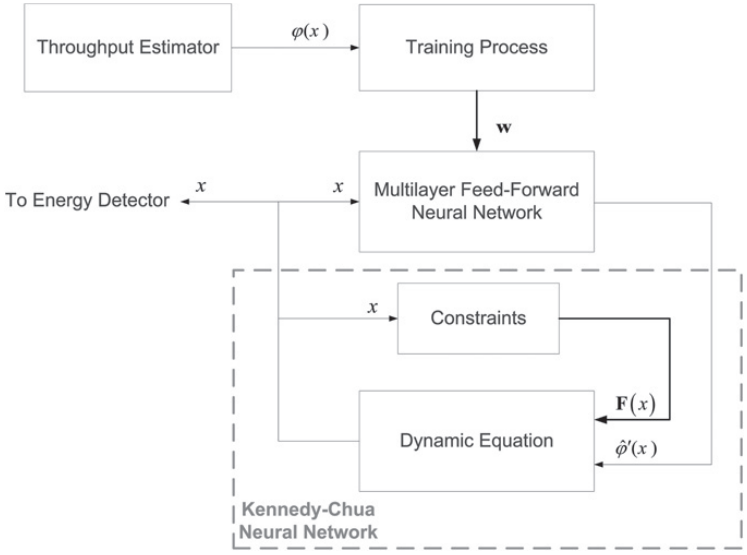

Fig. 2 *Block diagram of the proposed neural network-based sensing time optimisation scheme*

output x is applied to set the spectrum sensing time of the ED, the TE estimates the throughput obtained by this setting and calculates $\varphi(x)$ within T_{ep} seconds. Then, the training process uses x as the input and the estimated $\phi(x)$ as the target to adjust the weight and bias values of the MFF network by the well-known backpropagation algorithm [11]. Having its weight and bias values modified, the MFF network models the link more accurately, and therefore the KC network output takes a new value closer to the optimal point x^{opt}. By iterating this learning and optimisation cycle, we observe a joint convergence in the weight and bias values $\boldsymbol{w}$ and more importantly in the KC network output x. That is, $\boldsymbol{w}$ converges to $\boldsymbol{w}^{\text{opt}}$ by which the learned mapping fits the cost function $\varphi(x)$ appropriately and x converges to x^{opt} which denotes the optimum value for τ, thanks to the universal approximation theorem [14].

To sum up, the proposed adaptive system works according to the following three-steps algorithm:

Step 1: Setting: The KC network output x is applied to the ED to set its sensing time-duration.
Step 2: Throughput estimation: The average throughput is estimated by inspecting the packets and their ACKs for T_{ep} seconds, and accordingly $\varphi(x)$ is calculated.
Step 3: Training: The KC network output x and the TE outputs $\varphi(x)$ are used as an input-target pair to adjust the weights and biases of the MFF network, and then the process returns to Step 1).
Computational complexity of the proposed system is due to the backpropagation algorithm, whose order is $\mathcal{O}(N)$, where N is the number of weights and biases of the MFF network [11]. For the examples considered in the numerical results section, nine hidden neurons were enough to well model the relationship between sensing time and SUs throughput. The MFF network with nine hidden neurons can be considered equivalently as an adaptive filter with $N = 1 \times 9 + 1 \times 9 + 10 = 28$ weights which are being updated by the LMS algorithm.

It is worth noting that the proposed learning-based optimisation scheme adapts the sensing time of spectrum sensing according to the variations in the statistics associated with the wireless environment. More specifically, the optimisation is based on the link throughput estimated by the TE, which according to the presented analysis is directly related to the average SNR, experienced by the CR nodes [see (5)–(8) and (13)], instead of instantaneous variations of the wireless media. That is, in the proposed scheme, the weights change according to variations of (a) average channel SNRs, which change far more slowly than the instantaneous values of the SNRs, and (b) PUs' presence probabilities, which do not change or changes slowly. Therefore considering its considerably low update rate, even though the proposed system is designed for links with a non-stationary behaviour, the computational complexity of the backpropagation algorithm, that is, $\mathcal{O}(N)$, overall is not very substantial .

4 Numerical results

In this section, we evaluate the performance of the proposed schemes considering various parameters introduced throughout the paper. To this end, first an SU performing sequential channel sensing is simulated, and then by implementation of the MFF and KC networks, the performance of the proposed learning-based approach is evaluated. For numerical evaluations, the parameters are set

Table 1 Simulation parameters

Parameter	Description	Value
$P_{\text{d}}^{\min}$	minimum allowable detection probability	0.9
$P_{\text{fa}}^{\max}$	maximum allowable false alarm probability	0.1
f_{s}	receiver sampling frequency	6 MHz
T	time-slot duration	100 ms
τ_{ho}	required time for HO	0.1 ms
N_{p}	number of PUs	15
K	number of hidden neurons	9
C	capacitances of KC network	10 nF
G	conductances of KC network	0.001 Ω^{-1}

doi: 10.1049/iet-com.2012.0302

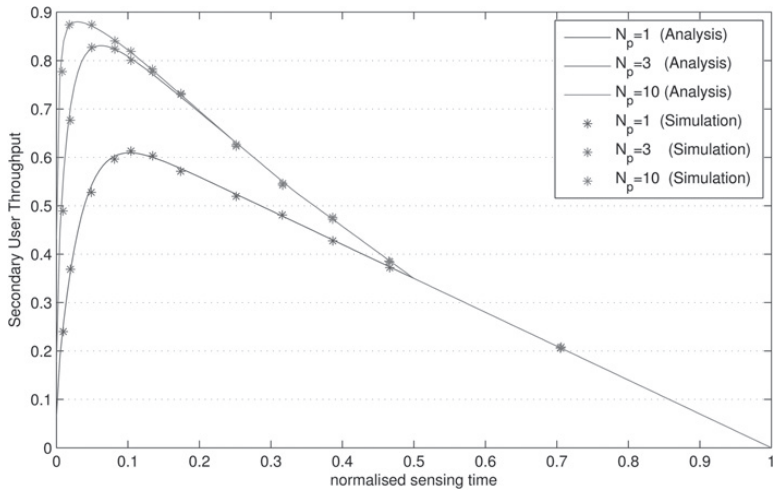

Fig. 3 *SU throughput against normalised sensing time*

according to Table 1. The values of SNR and sampling frequency are adopted from [5], and $P_{\mathrm{d}}^{\min}$ and $P_{\mathrm{fa}}^{\max}$ are chosen according to the 'IEEE 802.22' standard [23]. In simulation evaluations, the average throughput has been computed after simulating the scenario for 100 time slots.

As stated previously, the MFF network, exploited in the learning-based scheme, has three layers with one neuron at the input layer, K neurons at the hidden layer and one neuron at the output layer. As shown in [24], increasing the number of hidden neurons in an MFF network promotes its learning capability, and once satisfactory performance is obtained, further increasing the number of hidden neurons does not degrade the performance. Therefore as in [24, 25], the value of K ($=9$) is chosen in our simulations as the minimum value which leads to a satisfactory performance (see Figs. 4–6). Moreover, to build a KC network, first, it must be noted that the values of C (capacitances) and G (conductances) do not prevent KC network outputs from the convergence to the optimum point [From the analyses provided in [12], it can be concluded that the values of C and G only affect the convergence speed of the KC network, which is negligible compared with the throughput estimation period and MMF training phases (see Fig. 6). Therefore those values have no considerable effects on the performance of the proposed system.], provided that C is strictly positive and G is very small. In practice, those very small conductances are realised using op-amps based active elements with high input impedances [12]. In the following numerical evaluations, the values of C and G are adopted from [16].

Fig. 3 verifies our analysis and depicts the achievable data rate versus the normalised sensing time [i.e. (τ/T)] for various values of N_{p} assuming that the presence probabilities of all the PUs are equal to 0.65. As observed, for large normalised sensing time, the plots for different values of N_{p} coincide. This behaviour is expected because of our previous discussions on the constraints which affect the number of possible HOs for an SU. As stated previously in Section 2,

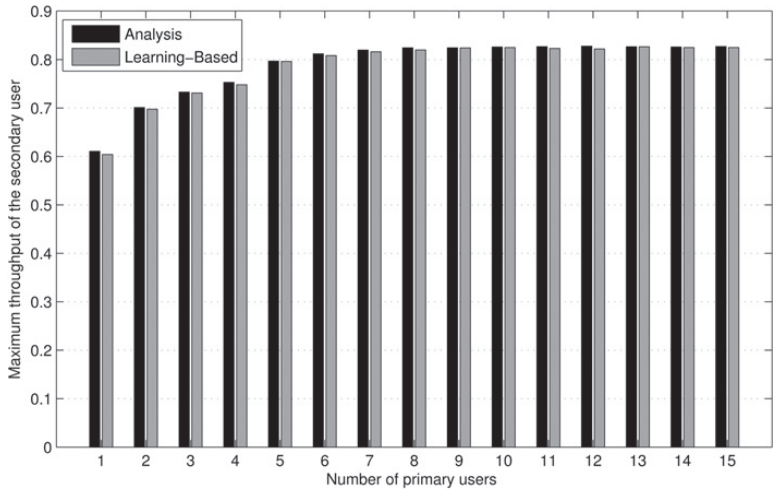

Fig. 4 *Maximum normalised throughput of the SU against the number of channels*

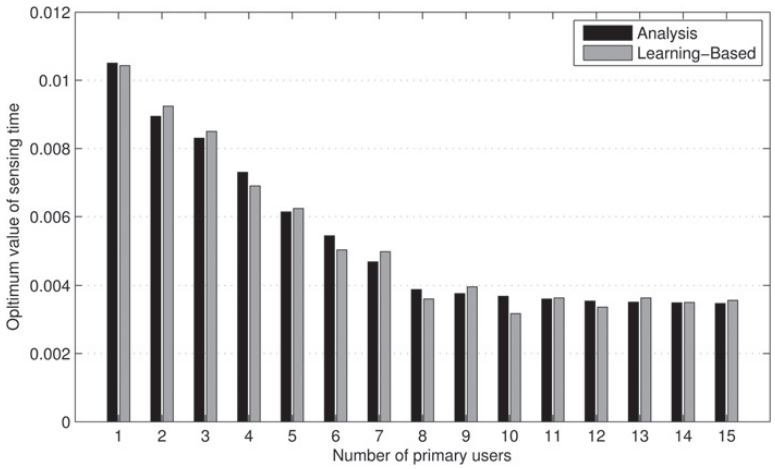

Fig. 5 *Optimal value of the sensing time obtained by the two methods*

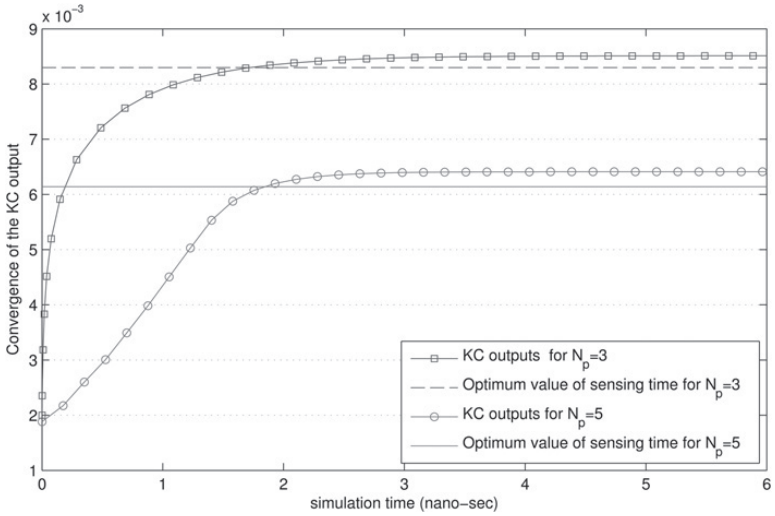

Fig. 6 *Convergence of the output of the KC neural network to optimal sensing time using a learned model for secondary links with $N_p = 3$ and $N_p = 5$ primary channels*

the number of possible HOs is dictated by two factors; namely, N_p, and the ratio $(T - \tau)/(\tau + \tau_{ho})$. Therefore as τ increases, we observe that the second factor dominates and regardless of the number of available primary channels N_p, the achieved throughput becomes limited to a value corresponding to a lower N_p. The throughput of the SU where there are 10 primary channels equals the throughput of the SU with 3 primary channels for approximately $\tau > 1/4T$. Other important observations can be made through Fig. 3. First, there exists an optimum value for the spectrum sensing time. Second, as the number of primary channels increases, the SU throughput increases as well, but in a saturating manner. This is due to the fact that as the number of primary channels increases, although the average number of obtained transmission opportunities increases, the average time-duration in which the SU transmits data reduces. Third, the importance and efficiency of having multiple HOs can be observed; the improvement in the throughput when using multiple HOs, that is, $N_p \geq ((T - \tau_{min})/(\tau_{min} + \tau_{ho})) + 1$, is about 44.5% compared with the case of $N_p = 1$, with no HO capability.

The effectiveness of the discussed energy-throughput tradeoff on the proposed sensing time optimisation scheme is demonstrated by Table 2. In this table, two design sets are presented namely *Design 1* and *Design 2*. *Design 1* is referred to the analytical optimisation that does not consider

Table 2 SUs average throughput and normalised consumed energy (NCE) for TF = 1 in *Design 1* (without considering energy-throughput tradeoff) and TF = 0.98 in *Design 2*

	Design 1		Design 2	
	Throughput	NCE	Throughput	NCE
$N_p = 2$	0.775	1.3186	0.775	1.3186
$N_p = 6$	0.8723	2.3909	0.8660	2.1397
$N_p = 12$	0.8807	3.3080	0.8660	2.1397

doi: 10.1049/iet-com.2012.0302

Table 3 Primary free probabilities

k	1	2	3	4	5	6	7	8	9	10	11	12	13	14	15
$P_{k,0}$	0.71	0.46	0.34	0.72	0.66	0.72	0.76	0.35	0.25	0.70	0.37	0.23	0.72	0.24	0.43

the energy consumed by the SU, whereas in *Design 2*, the sensing time is optimised using the TF to obtain an energy-efficient sensing scheme. This table illustrates that considering energy-throughput tradeoff provides near maximum throughput for each N_p with much lower consumed energy (compared with *Design 1*). It is worth noting that the SU consumed energy can be very high when N_p is large. From Table 2, the proposed energy-efficient sensing time optimisation procedure reduces the consumed energy dramatically when the consumed energy concern is more serious, that is, when the number of primary channels is large. See the 65% reduction in consumed energy for *Design 2* compared with *Design 1* at the expense of only 2% reduction in the throughput when $N_p = 12$.

Figs. 4 and 5 demonstrate the performance of the proposed learning-based optimisation scheme. They compare the maximum normalised throughputs and the optimum sensing times of the learning-based optimisation scheme and analytical modelling. This comparison is performed for various numbers of primary channels, for the presence probabilities of the PUs given in Table 3. Results labeled as 'Analysis' depict the maximum normalised throughput and optimum sensing time obtained by the analytical modelling; and results labeled as 'Learning-based' are the ones obtained through the neural network-based optimisation. As can be realised from Fig. 4, the average throughput values obtained by the proposed neural network-based optimisation method are very close to those obtained through mathematical analysis. Moreover, Fig. 5 shows that optimum sensing times calculated through our learning-based optimisation method are very close to the results obtained by the analysis.

Fig. 6 depicts the KC network output convergence to the optimal sensing time corresponding to secondary links with $N_p = 3$ and $N_p = 5$ primary channels. As shown in this figure, using the learned cost function provided by the MFF network, the KC output converges to the optimal sensing time very fast. Therefore we observe that if the learned function well-approximates the actual link model, the KC output represents the optimal value of the sensing time.

5 Conclusion

In this paper, we considered the problem of channel sensing time optimisation for a SU which senses the primary channels sequentially. Maximising the average throughput of the SU by optimising the spectrum sensing time was formulated assuming that a priori knowledge of the presence and absence probabilities of the PUs are available. Then, the energy-throughput tradeoff of a CR system was discussed using the derived expressions. Moreover, a learning-based sensing time optimisation approach was proposed using a novel and effective combination of two powerful and well-organised artificial neural networks. Finally, the validity of the analytical results as well as the capability of the proposed adaptive system in finding the optimal spectrum sensing time were demonstrated by a set of illustrative simulation results.

6 References

1 Wang, B., Liu, K.J.R.: 'Advances in cognitive radio networks: a survey', *IEEE J. Sel. Topics Signal Process*., 2011, **5**, (1), pp. 5–23
2 He, A., Bae, K.K., Newman, T.R., *et al*.: 'A survey of artificial intelligence for cognitive radios', *IEEE Trans. Veh. Technol.*, 2010, **59**, (4), pp. 1578–1592
3 Akyildiz, I.F., Lo, B.F., Balakrishnan, R.: 'Cooperative spectrum sensing in cognitive radio networks: a survey', *Phys. Commun.*, 2001, **4**, (1), pp. 40–62
4 Shokri-Ghadikolaei, H., Nasiri-Kenari, M.: 'Sensing matrix setting schemes for cognitive networks and their performance analysis', *IET Commun.*, **6**, (7), pp. 3026–3035
5 Liang, Y.C., Zeng, Y., Peh, E.C.Y., Hoang, A.T.: 'Sensing-throughput tradeoff for cognitive radio networks', *IEEE Trans. Wirel. Commun.*, 2008, **7**, (4), pp. 1326–1337
6 van den Biggelaar, O., Dricot, J.M., Doncker, P.D., Horlin, F.: 'Sensing time and power allocation for cognitive radios using distributed q-learning', *EURASIP J. Wirel. Commun. Netw.*, 2012, **2012**, pp. 1–40
7 He, J., Xu, C., Li, L.: 'Joint optimization of sensing time and decision thresholds for wideband cognitive ofdm radio networks'. *IET ICWMNN*, September 2010, pp. 230–233
8 Lee, D.J., Jang, M.S.: 'Optimal spectrum sensing time considering spectrum handoff due to false alarm in cognitive radio networks', *IEEE Commun. Lett.*, 2009, **13**, (12), pp. 899–901
9 Shokri-Ghadikolaei, H., Sheikholeslami, F., Nasiri-Kenari, M.: 'Distributed multiuser sequential channel sensing schemes in multichannel cognitive radio networks', accepted in IEEE Trans. on Wireless Commun. (to appear), Feb 2013.
10 Shokri-Ghadikolaei, H., Fallahi, R.: 'Intelligent sensing matrix setting scheme in cognitive networks', *IEEE Commun. Letter*, 2012, **16**, (11), pp. 1824–1827
11 Fine, T.L.: 'Feedforward neural network methodology' (Springer, New York, 1999, 1st edn.)
12 Kennedy, M.P., Chua, L.O.: 'Neural networks for nonlinear programming', *IEEE Trans. Circuits Syst.*, 1988, **35**, (5), pp. 554–562
13 Hornik, K., Stochcombe, M., White, H.: 'Multilayer feedforward networks are universal approximators', *Neural Netw.*, 1989, **2**, pp. 359–366
14 Hornik, K., Stochcombe, M., White, H.: 'Universal approximation of an unknown mapping and its derivatives using multilayer feedforward networks', *Neural Netw.*, 1990, **3**, pp. 551–560
15 Dayhoff, J.E.: 'Neural network architectures' (Van Nostrand Reinhold, New York, 1990)
16 Fantacci, R., Tarch, D., Marini, M., Rabbini, A.: 'A neural network approach to MMSE receivers in a DS-CDMA multipath fading environment', *IEEE Trans. Commun.*, 2006, **54**, (5), pp. 778–782
17 Zurada, J.M.: 'Introduction to artificial neural systems' (Van Nostrand Reinhold, Boston, MA, 1995)
18 Maa, C., Shanblatt, M.: 'Linear and quadratic programming neural network analysis', *IEEE Trans. Neural Netw.*, 1992, **3**, (4), pp. 580–594
19 Monica, M.S., Sharma, A.K.: 'Comparative study of energy consumption for wireless sensor networks based on random and grid deployment strategies', *Int. J. Comput. Appl. IJCA*, 2010, **6**, (1), pp. 28–35
20 Hashem, S.: 'Sensitivity analysis of feedforward artificial neural networks with differentiable activation functions'. Proc. IEEE IJCNN, Baltimore, MD, June 1992, vol. 1, pp. 419–424
21 Abdi, A., Azmi, P.: 'Intelligent cross-layer adaptation scheme for wireless links with QoS-guranteed traffic'. Proc. Fifth Int. Symp. Telecommunications (IST), Tehran, December 2010, vol. 1, pp. 419–424
22 Park, S.H., Yoon, H., Kim, J.W.: 'A cross-layered network cadaptive HD video steaming in digital A/V home network: hannel monitoring and video rate adaptation', *IEEE Trans. Consum. Electron.*, 2006, **52**, (4), pp. 1245–1252
23 Stevenson, C.R., Chouinard, G., Lei, W.H.Z., Shellhammer, S.J.: 'IEEE 802.22: the first cognitive radio wireless regional area network standard', *IEEE Commun. Mag.*, 2009, **47**, (1), pp. 130–138
24 Caruana, R., Lawrence, S., Giles, L.: 'Overfitting in neural nets: Backpropagation, conjugate gradient, and early stopping'. Proc. Neural Inf. Process. Syst., Dec. 2001, pp. 402–408
25 Jiao, L., Bo, L., Wang, L.: 'Fast sparse approximation for least square support vector machine', *IEEE Trans. Neural Netw.*, 2007, **18**, (3), pp. 685–697